

MARCH 1937.

FINAL REPORT

RECOVERY OF SPINNING SATELLITES

(NASA-CR-150245) RECOVERY OF SPINNING
SATELLITES Final Report (Northrop Services,
Inc., Huntsville, Ala.) 105 p HC A06/MF A01
CSCI 22A

N77-22159

Unclas

G3/15 25121

Submitted To:

NATIONAL AERONAUTICS AND SPACE ADMINISTRATION
GEORGE C. MARSHALL SPACE FLIGHT CENTER
Science and Engineering Directorate

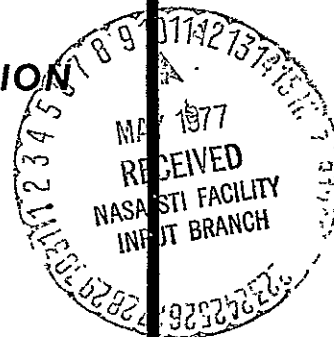
Under Contract NAS8-29627

Submitted By:

NORTHROP SERVICES, INC.

P. O. BOX 1484 Huntsville, Alabama 35807 (205) 837-0580

NSi



RECOVERY OF SPINNING SATELLITES

March 1977

by


J. M. Coppey
W. R. Mahaffey

PREPARED FOR.

NATIONAL AERONAUTICS AND SPACE ADMINISTRATION
GEORGE C. MARSHALL SPACE FLIGHT CENTER
SCIENCE AND ENGINEERING DIRECTORATE

Under Contract NAS8-29627

REVIEWED AND APPROVED BY:


M. A. Sloan, Manager
Systems Dynamics

NORTHROP SERVICES, INC.
HUNTSVILLE, ALABAMA

FOREWORD

This report presents the results of work performed by Northrop Services, Inc., Huntsville, Alabama, under Contract NAS8-29627 for the Systems Dynamics Laboratory of the George C. Marshall Space Flight Center, Huntsville, Alabama.

This final report documents and summarizes the results of the entire contract effort, including recommendations and conclusions based on the experience and results obtained.

Technical contact was maintained through Mr. D. P. Vallely and Ms. Alberta W. King of the Servomechanisms and Systems Stability Branch, ED-14.

ABSTRACT

Investigation of the recovery of spinning satellites began in August 1973 under Contract NAS8-29627. An initial study was performed to analyze the behavior of the system made up of a Space Tug and a spinning satellite in a coupled configuration.

As interest developed in the capture of spinning targets of various sizes and shapes, a docking concept was developed to investigate the requirements pertaining to the design of a docking interface.

A study of sensing techniques and control requirements for the chase vehicle was performed to assess the feasibility of an automatic docking. Also, the effects of nutation dampers and liquid propellant slosh motion upon the docking transient were investigated.

This report is an executive summary of the work that was performed under Phases A and B, and a detailed discussion of the results of Phase C is presented.

A digital 12-DOF simulation was developed for the purpose of the study, and is referenced in this document (Reference 5, Section VIII). The simulation can be used to solve problems involving the motion of any two bodies, in both independent and coupled configuration.

TABLE OF CONTENTS

<u>Section</u>	<u>Title</u>	<u>Page</u>
	FOREWORD.	ii
	ABSTRACT.	iii
	LIST OF ILLUSTRATIONS	vi
	LIST OF TABLES.	ix
I	INTRODUCTION.	1-1
II	PHASE A: POST-DOCKING STUDY.	2-1
	2.1 METHODOLOGY.	2-1
	2.2 RESULTS.	2-1
	2.3 CONCLUSIONS.	2-5
III	PHASE B: SOFT-DOCKING STUDY.	3-1
	3.1 METHODOLOGY.	3-1
	3.2 RESULTS.	3-1
	3.3 DESCRIPTION OF CANDIDATES.	3-4
	3.4 CANDIDATE EVALUATION	3-6
	3.5 SIMULATION	3-7
	3.6 ROTATING FACEPLATE	3-9
	3.7 CONCLUSIONS.	3-9
IV	PHASE C: PREDOCKING STUDY.	4-1
	4.1 METHODOLOGY.	4-1
	4.2 NUTATION DAMPING.	4-2
	4.3 RESPONSE TO MISSED DOCKING	4-2
	4.4 CONCLUSIONS.	4-7
	4.5 LIQUID PROPELLANT SLOSH.	4-7
V	SENSING REQUIREMENTS.	5-1
	5.1 METHODOLOGY.	5-1
	5.2 RESULTS.	5-1
	5.3 SENSING CONCEPTS	5-2
VI	CONTROL REQUIREMENTS.	6-1
	6.1 METHODOLOGY.	6-1
	6.2 RESULTS.	6-1
	6.3 BASIC CONTROL COMMANDS	6-4

TABLE OF CONTENTS (Concluded)

<u>Section</u>	<u>Title</u>	<u>Page</u>
VII	CONCLUSIONS	7-1
	7.1 POST-DOCK STUDY.	7-1
	7.2 SOFT-DOCK STUDY.	7-1
	7.3 PREDOCK STUDY.	7-1
	7.4 RECOMMENDED CONCEPT.	7-4
VIII	REFERENCES.	8-1
	Appendix A -- BODY EQUATIONS OF MOTION	A-1
	Appendix B -- ALIGNMENT TORQUER CONCEPT.	B-1
	Appendix C -- ROTATING FACEPLATE EQUATIONS	C-1
	Appendix D -- PRECESSION DAMPER EQUATIONS.	D-1
	Appendix E -- PROPELLANT SLOSH MODEL	E-1
	Appendix F -- FEEDBACK CONTROL SYSTEM.	F-1
	Appendix G -- TRAJECTORY APPROACH.	G-1
	Appendix H -- INTERCEPT CONTROL.	H-1
	Appendix I -- COMPUTATION OF RANGE ERROR	I-1

LIST OF ILLUSTRATIONS

<u>Figure</u>	<u>Title</u>	<u>Page</u>
1	TWO-BODY BEHAVIOR FOR UNCONTROLLED CHASE VEHICLE	2-3
2	TWO-BODY BEHAVIOR 3 AXIS-ATTITUDE CONTROL ON CHASE VEHICLE . .	2-4
3a	DAMPING EFFECT	2-6
3b	ALIGNMENT NEUTRAL FREQUENCY EFFECT	2-7
4a	VALUES OF MISALIGNMENT ANGLE VERSUS RING GEOMETRY FOR CONVER- GENCE	3-3
4b	MINIMUM VELOCITY REQUIREMENTS FOR TWO TARGETS	3-3
5	CAPTURE-CENTER CONCEPT	3-5
6	DOCKING INTERFACES ON SPINNING FACEPLATES	3-10
7	DAMPER CONFIGURATION	4-3
8a	SATELLITE CONING ANGLE VERSUS TIME WITH ACTIVE NUTATION DAMPER	4-4
8b	MISALIGNMENT ANGLE VERSUS TIME FOR MISSED DOCKING ATTEMPT WITHOUT NUTATION DAMPER.	4-5
8c	MISALIGNMENT ANGLE VERSUS TIME FOR MISSED DOCKING ATTEMPT WITH NUTATION DAMPER	4-6
9a	PROPELLANT SLOSH MASS MODEL	4-8
9b	PROPELLANT MOTION	4-9
9c	SLOSH FORCE IN LOX TANK WALL, (X-AXIS) VERSUS TIME	4-10
9d	SLOSH FORCE ON LOX TANK WALL, (Y-AXIS) VERSUS TIME	4-11
9e	SLOSH MOMENT ALONG Z-AXIS VERSUS TIME	4-12
9f	MISALIGNMENT ANGLE OF CHASER DUE TO MOTION OF LOX PROPELLANT .	4-13
10	LASER BEAM SENSING CONCEPT	5-6
11a	ERROR ON RANGE ESTIMATION VERSUS RANGE FOR OPTICAL AND RADAR SENSORS	5-7

LIST OF ILLUSTRATIONS (Continued)

<u>Figure</u>	<u>Title</u>	<u>Page</u>
11b	REFLECTIVE STRIP CONFIGURATION	5-9
11c	REFLECTED SIGNAL VERSUS INCIDENCE ANGLE	5-9
11d	DEFINITION OF INCIDENCE ANGLE γ	5-10
12	FEEDBACK CONTROL APPROACH	6-2
13	TRAJECTORY APPROACH	6-5
14	INTERCEPT CONTROL	6-6
15	CIRCLING MANEUVERS	6-8
16a	FEEDBACK CONTROL COMMAND	6-10
16b	MISALIGNMENT ANGLE VERSUS TIME	6-11
16c	LATERAL DISPLACEMENT VERSUS TIME	6-12
16d	NUTATION DAMPER DISPLACEMENT VERSUS TIME	6-13
16e	ALIGNMENT RATE VERSUS TIME	6-14
17a	SLOSH FORCE VERSUS TIME	6-15
17b	SLOSH MOTION	6-16
17c	FACEPLATE ANGLE RATE VERSUS TIME	6-17
17d	FORCE ON CHASER VERSUS TIME	6-18
18a	MISALIGNMENT VERSUS TIME	6-20
18b	AXIAL DISPLACEMENT VERSUS TIME	6-21
18c	RELATIVE RADIAL MOTION OF DOCKING PORTS	6-22
18d	FACEPLATE ANGLE RATE VERSUS TIME	6-23
19a	ALIGNMENT RATE VERSUS TIME	6-24
19b	CONTROL TORQUE ON CHASER VERSUS TIME	6-25

LIST OF ILLUSTRATIONS (Concluded)

<u>Figure</u>	<u>Title</u>	<u>Page</u>
19c	CONTROL TORQUE ON CHASER VERSUS TIME	6-26
19d	CONTROL TORQUE ON CHASER VERSUS TIME	6-27
C-1	FACEPLATE SIMULATION MODEL	C-2
E-1	PROPELLANT SLOSH MODEL COORDINATES	E-2

LIST OF TABLES

<u>Table</u>	<u>Title</u>	<u>Page</u>
1	ANALYTICAL STABILITY STUDY RESULTS	2-2
2	COMPARISON OF THREE BASIC CONCEPTS	3-6
3a	DATA FOR SELECTED SPINNING TARGET	3-7
3b	DATA FOR SELECTED CHASE VEHICLE	3-8
4	DATA FOR SLOSH MODEL	4-14
5	SPECIFIC REQUIREMENTS FOR TARGET SENSING	5-12
6	REQUIREMENTS FOR RECOMMENDED CONCEPT	7-3

Section I

INTRODUCTION

This is the final report of a study of techniques and concepts for recovery of spinning satellites. Previous reports submitted under this contract give detailed analyses of various phases of the work. Documentation of a digital simulation for post-docking response is presented in Reference 1. A study of the stability and response for a coupled two-body system is presented in Reference 2. The results of a study of the capture of cooperative spinning satellites is presented in Reference 3. Reference 4 documents a digital simulation designed for the study of docking with a spinning satellite. Reference 5 is a users manual for a digital 12-DOF simulation that was developed for the purpose of this study on the recovery of spinning satellites.

Initially, a study was performed to analyze the behavior of a system made up of a Space Tug and a spinning satellite in a coupled configuration. The study then evolved into an analysis of techniques for the capture of spinning targets of various sizes and shapes. In accomplishing this phase of the study, a docking concept was developed to investigate the requirements pertaining to the design of a docking interface. A study of sensing techniques and control requirements on the chase vehicle was performed to assess the feasibility of automatic docking. The effects on the docking transient behavior of nutation dampers and liquid propellant slosh motion were investigated.

This report is an executive summary of (1) the initial study of an analysis of a system made up of a Space Tug and a spinning satellite in a coupled configuration and (2) the study of docking concepts to investigate the requirements pertaining to the design of a docking interface.

A detailed presentation of the results of the study of sensing techniques and control requirements for the chase vehicle is presented in the report.

For presentation purposes, this report breaks the docking maneuver into three phases. These three phases were investigated in the study.

Phase A - A post-docking phase was performed to analyze the stability and response of a system of coupled bodies.

Phase B - A study of a soft-docking phase was made to facilitate the design of a candidate docking mechanism adaptable to the capture of spinning targets.

Phase C - A study of the predocking phase was performed to establish sensing techniques and recognize the control requirements necessary to perform the docking maneuver.

Phases A and B are covered in detail in References 1 and 2, respectively. The presentation of these phases in this report will be of a summary nature. The Phase C study has not previously been reported, and is presented in detail in this report. A number of appendixes are included, presenting detailed mathematical derivation of some of the equation and concepts.

Section II describes Phase A, the post-docking study. Section III presents the results of the Phase B study on soft-docking. The predocking study is covered in Section IV, and Section V includes descriptions of the numerous sensing requirements. The various control requirements are explained in Section VI. The conclusions reached from the three studies along with a recommended concept are given in Section VII. Related reports that have been prepared in the course of this work are referenced in Section VIII. This report contains nine appendixes which contain pertinent equations, concepts, models, and approaches.

Section II

PHASE A: POST-DOCKING STUDY

2.1 METHODOLOGY

The two coupled bodies were modeled as separate bodies connected by a massless joint or hinge featuring the docking port. Angular motion was allowed between the vehicles. The target vehicle was free to spin about the docking port axis. The purpose of the effort was to design a system that could drive the relative scissoring-type angular motion to zero while despinning the target. The equations of motion of the bodies were derived as shown in Appendix A. Alignment of the bodies was provided through an alignment torquer of springs and dampers. Target despin was achieved through a despin torquer. Equations are shown in Appendix B.

A linearization of the model was performed in order to investigate the stability of the system near the aligned configuration. Parametric variations of despin torque, moment of inertia, and spring damper characteristics were performed to determine the stability conditions in the frequency domain for various conditions of attitude controlled and free chase vehicles.

A two-body digital simulation was developed and used to verify the results in the time domain.

2.2 RESULTS

The results of the analytical stability study of the linearized model with an ideal attitude control system for the chase vehicle are summarized in Table 1 for the various combinations of alignment and despin torques.

In the foregoing studies, it was found that the results derived from a nonlinear simulation agreed well with those predicted by the linear analytical stability analysis.

Figures 1 and 2 show the overall results of these studies for an uncontrolled Tug and for one with perfect attitude control, respectively. Three target inertias are considered: a disk, and end dock cylinder, and a side dock

Table 1. ANALYTICAL STABILITY STUDY RESULTS

ALIGNMENT TORQUE	DESPIN. TORQUE	CHASER ATTITUDE CONTROL		
		NONE	X-AXIS ONLY	3-AXIS
NO	NO	NO CONCLUSION (FOR NONLINEAR MODEL)	UNSTABLE	NO CONCLUSION (FOR NONLINEAR MODEL)
YES	NO	ABSOLUTELY STABLE	ABSOLUTELY STABLE	ABSOLUTELY STABLE
NO	YES	UNSTABLE	UNSTABLE	UNSTABLE
YES	YES	ASYMPTOTICALLY STABLE	ASYMPTOTICALLY STABLE	ASYMPTOTICALLY STABLE

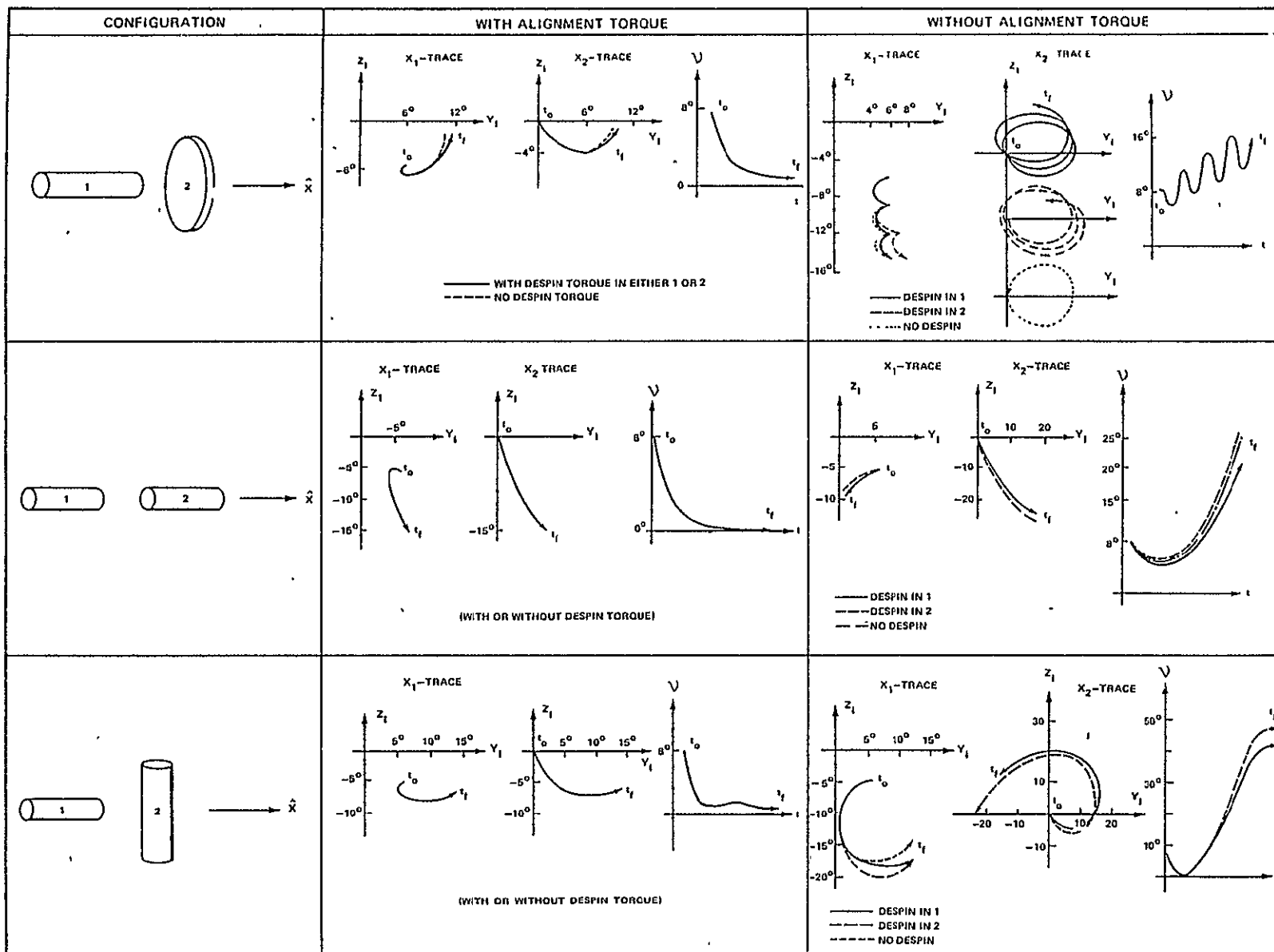


Figure 1. TWO-BODY BEHAVIOR FOR UNCONTROLLED CHASE VEHICLE

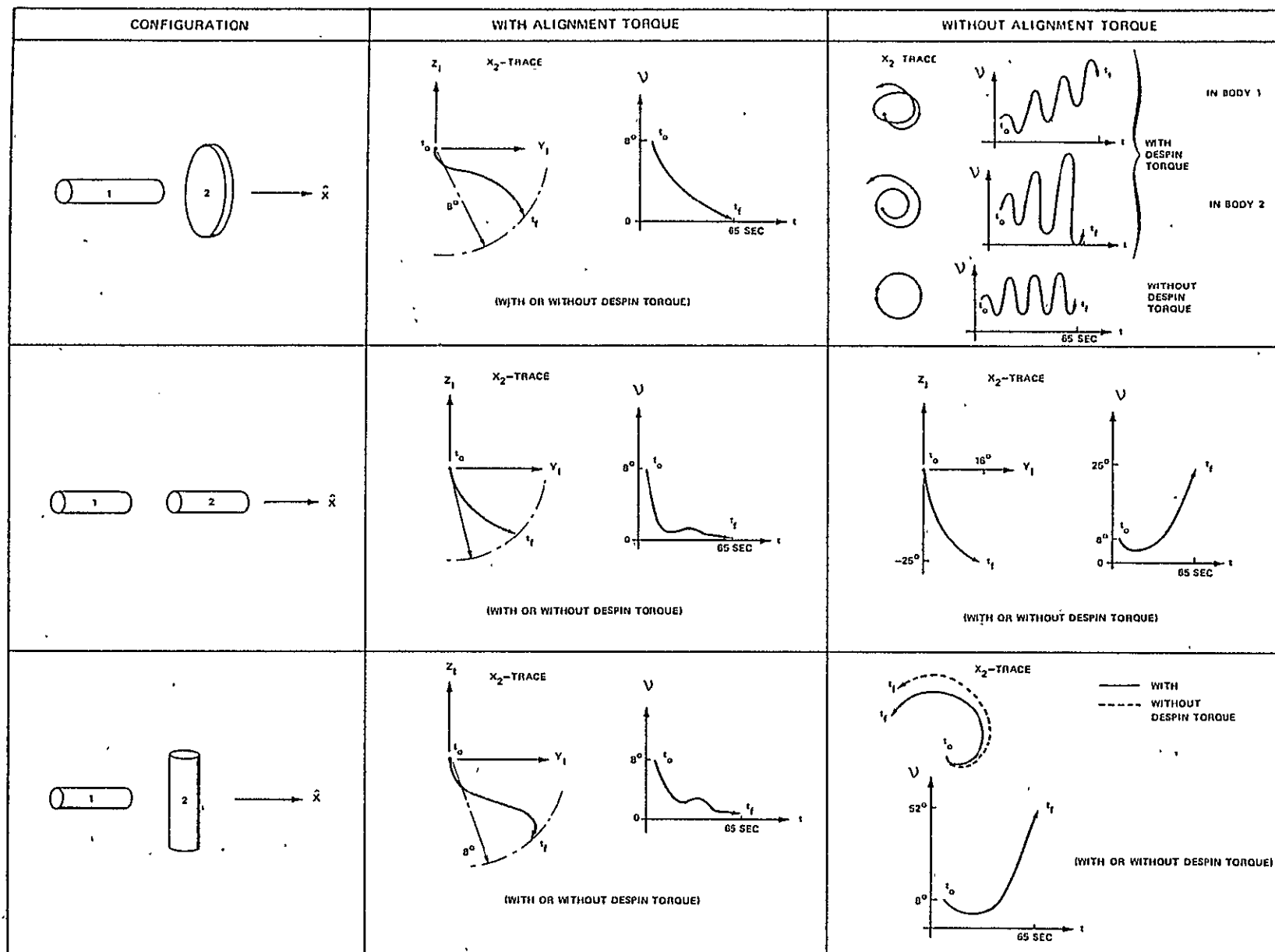


Figure 2. TWO-BODY BEHAVIOR FOR 3-AXIS ATTITUDE CONTROL ON CHASE VEHICLE

ORIGINAL PAGE IS
OF POOR QUALITY

2-4

cylinder. In each case the target is assumed to be initially at a constant angular rate about the docking port centerline with some misalignment and wobble. The response curves show qualitatively the parametric angular motion of the target centerline in inertial space and the time response of the angle ψ between the Tug and target vehicle centerlines, with and without alignment springs and dampers.

The results in Figure 1 show that the uncontrolled post-dock configuration is stable for all three types of targets, provided alignment springs and dampers are present. The motion of both centerlines is well behaved, and the alignment angle tends toward zero in all cases. The right-hand column in Figure 1 illustrates the fact that the post-dock configuration tends to be unstable without alignment springs and dampers. The angle between the two centerlines diverges indicating the tendency of the two vehicles to pitch and yaw into each other. Figure 2 shows that alignment springs and dampers are still necessary even when the Tug has ideal attitude control.

Alignment damping and natural frequency were parameterized as was despin torque to determine appropriate settings. Figure 3a shows the behavior of the misalignment angle ψ for several damping ratios with all other conditions held constant. The conclusion is that critical damping ($\xi = 1.0$) is best in driving misalignment quickly to zero with a minimum of oscillation. Natural frequency should be as high as possible for fast settling time, as shown in Figure 3b, but will be limited by the weight of the springs in relation to vehicle weights.

2.3 CONCLUSIONS

Results from both analytical and numerical studies show that:

- An alignment torque damping factor in the proximity of critical damping is best for reducing misalignment between the docking port axes to zero with a minimum of oscillation.
- An alignment torque natural frequency should be as high as possible for fast settling time, but will obviously be limited by structural weight considerations.

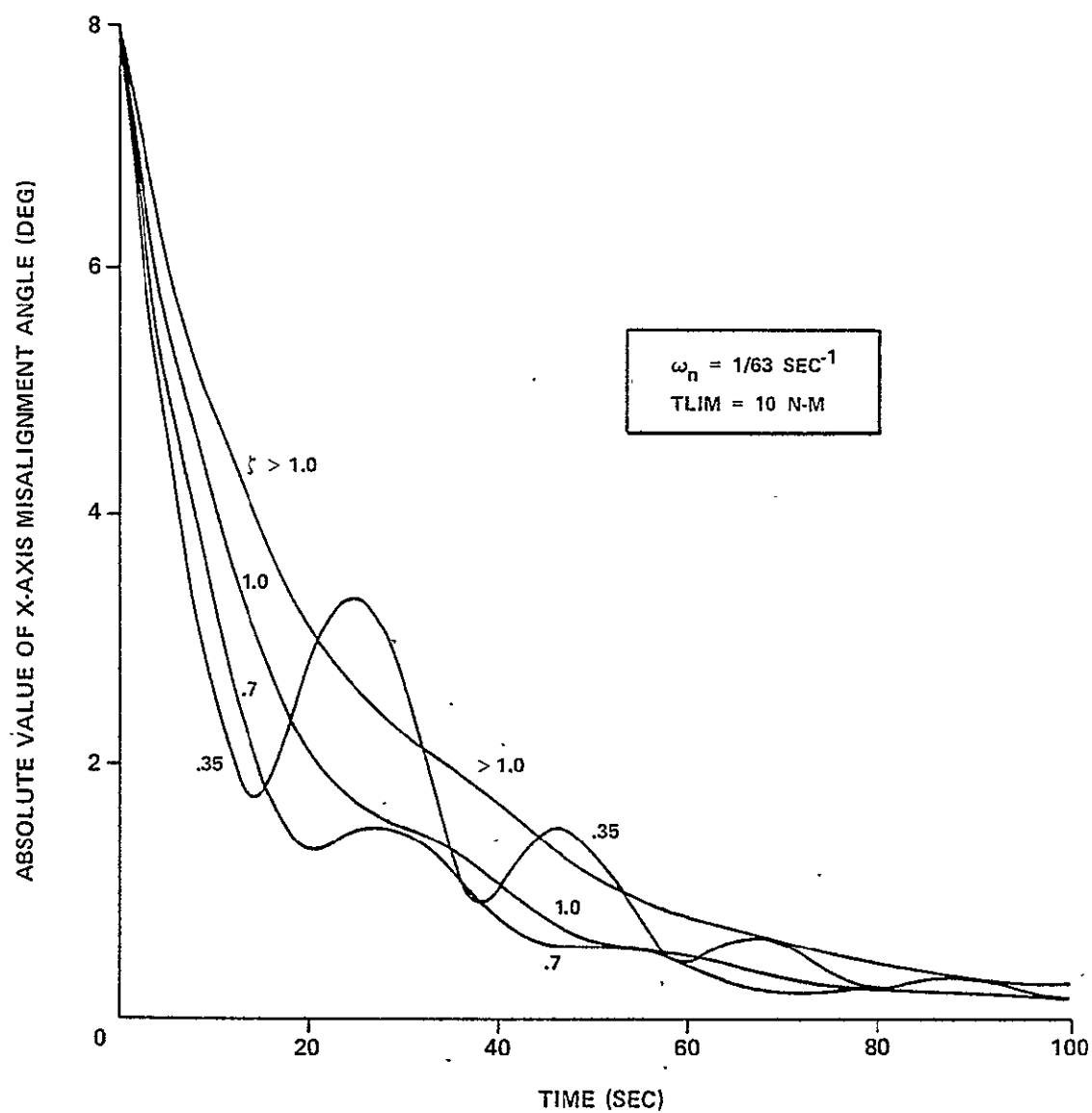


Figure 3a. DAMPING EFFECT

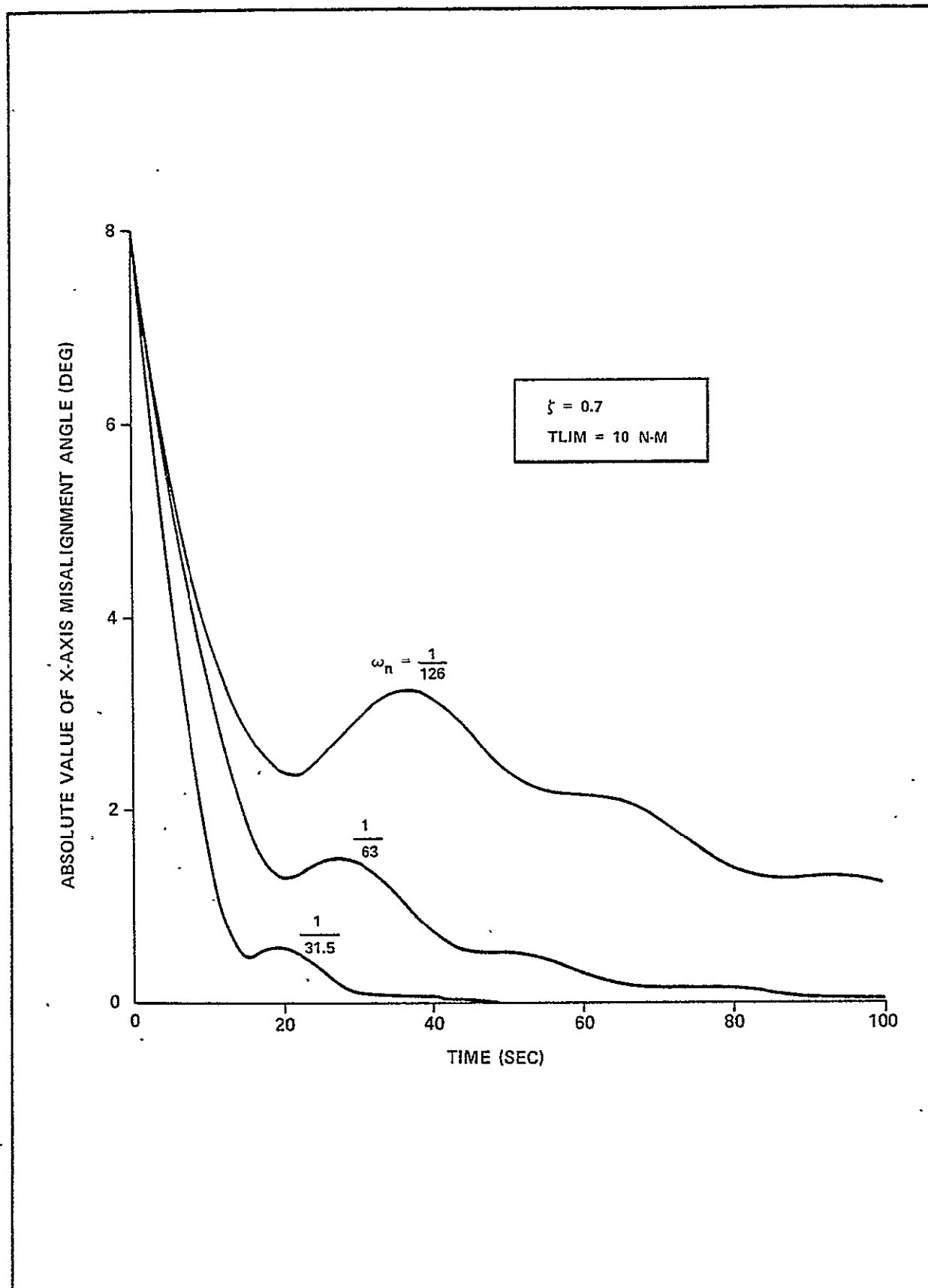


Figure 3b. ALIGNMENT NATURAL FREQUENCY EFFECT

- The despin time is linearly proportional to the despin torque (for a reasonable range of values) with a smaller torque requiring a longer despin time.
- The two body coupled system is stable as long as some dissipative and energy storage (spring and damper) alignment torque exists.
- No system instabilities were encountered for reasonable values of the despin torque.

Section III

PHASE B: SOFT-DOCKING STUDY

3.1 METHODOLOGY

The development of a docking mechanism capable of capturing a spinning target is subject to specific performance requirements. Identification of the expected performance requirement was made by defining a docking system criteria that could be used as a tool in the selection of an adequate concept from a variety of proposed docking systems. Considerations such as cost and weight burden, compatability with different shapes and sizes of targets, reliability, reset conditions, and stability were analyzed.

A preliminary docking concept was then selected according to the developed criteria. The concept was subsequently defined and simulated for performance evaluation. Deficiencies in its functionality (friction) led to the search of an alternate concept with implied improvements. Again, the new concept (rotating face plate) was simulated and its performance compared to the first concept.

3.2 RESULTS

Selection from a variety of proposed docking systems candidates is made possible using a rationale of criteria applicable to the specific problems raised. These criteria are listed below in the order of their importance.

The weight, volume, and cost penalties inflicted on the target by the recovery system should be minimal. System complexities should be supported to the maximum extent possible by the chase vehicle rather than the target.

The effect of a missed docking attempt will be most severe if prominent parts on one body impact the surface of the other body. The probability of such an event should be minimized by the selected configuration.

Once both bodies have impacted, the relative alignment angle (ψ) between their docking axes should gradually converge to zero. Design values for the

size of the docking interface (ring) can be chosen to satisfy this requirement. Figure 4a shows these domains of convergence as functions of a ring diameter (D) and location of that ring along the longitudinal axis (L). The velocity vector of the target center of mass was selected to be normal to the chaser's docking plate.

If a planar interface is chosen, a minimum velocity is required for the axial closure to permit the full contact of both interfaces before the bodies repel each other. This is shown on Figure 4b for an initial misalignment ($\nu = 10$ degrees). The lines represented show the minimum velocity requirements as functions of the diameter of the interface ring. It can also be seen that a larger misalignment angle will call for a larger closing velocity.

Regardless of the technique used to capture the spinning satellite, it must be brought to the final state of zero spin relative to the chaser. This reduction of momentum can be achieved in many ways, and this requirement must be met by the docking system.

The compatibility of a docking system with the international docking port would certainly enhance the value of the system by making possible the recovery of manned spacecraft and space station modules with common hardware. Such a configuration would call for a free space at the center of the docking port, therefore ruling out the use of a probe-drogue approach wherein some of the docking hardware must be mechanically removed for boarding purpose.

A feature that in all probability will be mandatory is the capability to rotate the target (once it is captured and despun) to a final roll alignment relative to the chaser and lock it in that position for the remainder of the mission.

The size of a docking port can be cumbersome to a small satellite or can require too much space in the launch rocket. Provision should be made for the chaser to adapt to various diameters of docking ports. Hopefully, the chaser port diameter could be adjusted automatically in flight to allow, for example, a mission requiring deployment of a large satellite and retrieval of a small one.

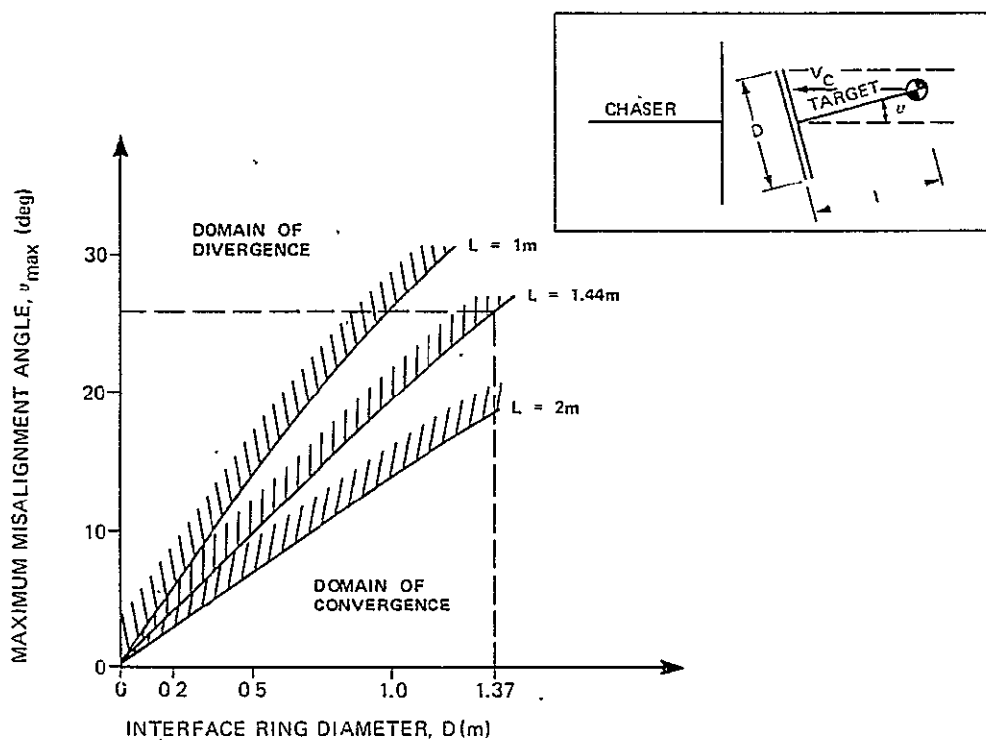


Figure 4a. VALUES OF MISALIGNMENT ANGLE VERSUS RING GEOMETRY FOR CONVERGENCE

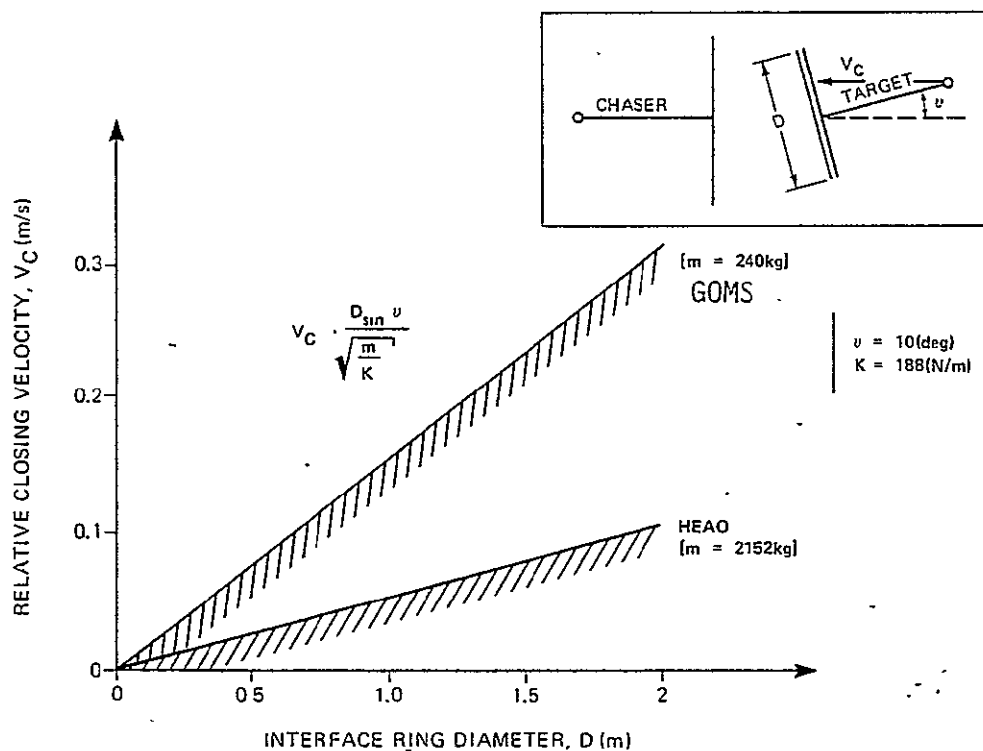


Figure 4b. MINIMUM VELOCITY REQUIREMENTS FOR TWO TARGETS

The docking system, after a missed docking attempt, should have the capability to make repeated attempts. A missed docking attempt is characterized by the failure of the latches to close properly on the target.

In the concept introduced in this study, for example, three cases of missed docking are recognized: (1) the impact fails to trigger the latches and the target is repelled; (2) the latches fasten improperly, thus causing asymmetric loads; or (3) in the case of an overload, the latches are released to avoid structural damage.

To enable a repeated attempt, the latches previously triggered must first be reset to their original positions. This requirement is certainly of appreciable consideration in the mechanical design of the docking interface. The second requirement to be met before the recapture phase can begin is the condition of the target wobble. If wobbling motion is too large for an immediate docking, a delay will be needed to give time for the motion to settle down. Nutation dampers should be considered to accelerate the process if necessary.

On the basis of the criteria discussed, a docking concept was developed and compared with alternate approaches. The following is a discussion of the concepts and alternate approaches.

3.3 DESCRIPTION OF CANDIDATES

• Probe-Drogue

The concept of the probe-drogue has been used in previous docking systems and could be used for spinning targets without major changes in its configuration.

• Center-Capture Concept

This interface is made up of a ring on the target and a square frame on the chaser with finger-like supports to guide the impacting bodies to a desired latching position.

• Capture-Center Concept

The proposed interface, as shown on Figure 5, is made up of a plate mounted on the chase vehicle, supported by a pattern of shock absorbers. Four latches are embedded in the plate and set up to close on the matching ring on the target when individual contacts occur. These latches, once fastened, permit the target ring to slide through and, being allowed to rotate on themselves and move radially, are then individually forced to a desired centered position.

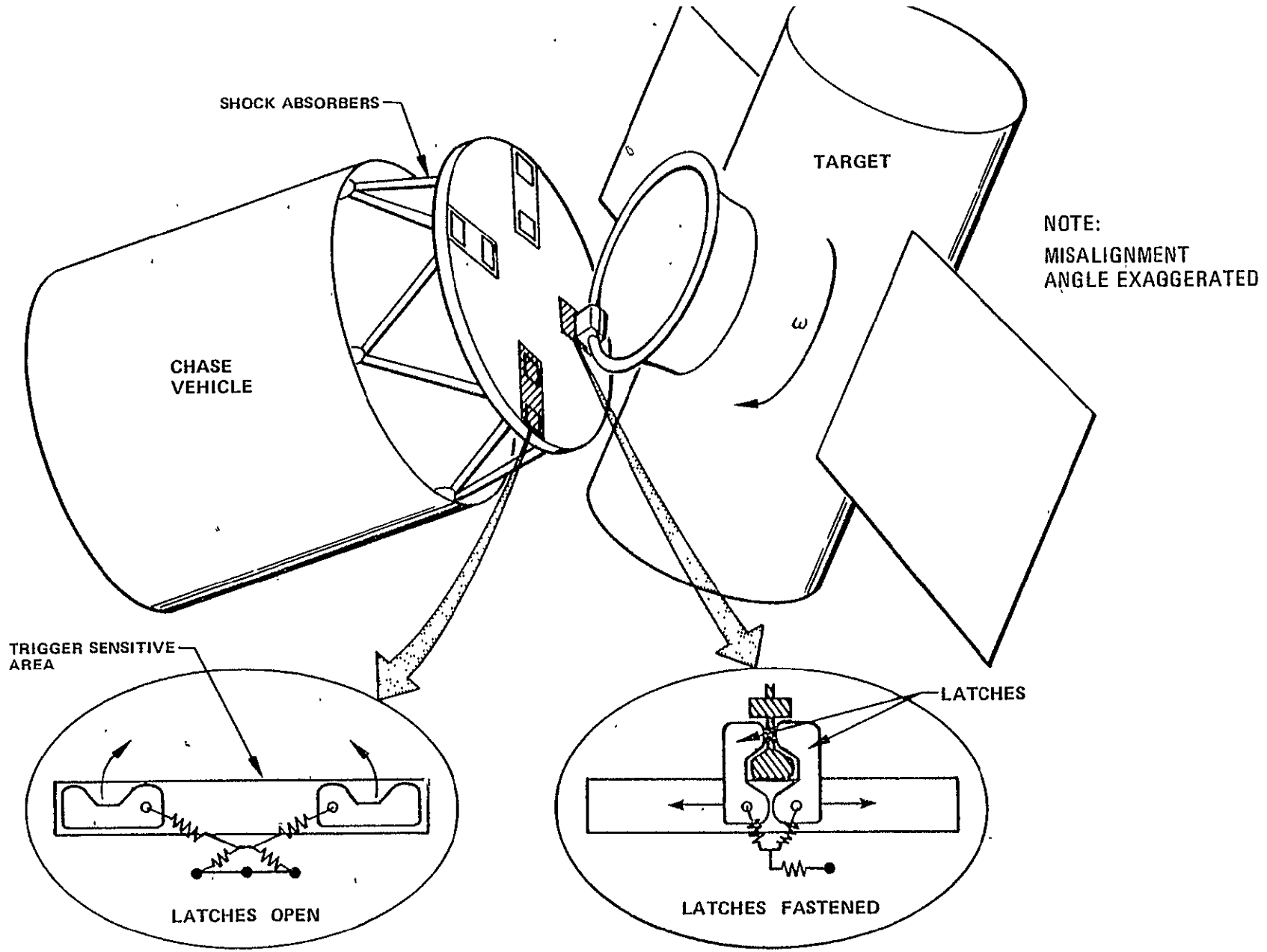


Figure 5. CAPTURE-CENTER CONCEPT

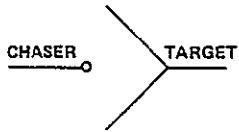
The main feature of such a mechanism is the emphasis of the first step in docking to be the capture of the target, rather than its centering as seen in other concepts.

3.4 CANDIDATE EVALUATION

A comparison of the three concepts is shown in Table 2. The ranking was made according to a relative scale of values from not suitable (0) to very good (3). The total score shows the superiority of the capture-center concept, where the major difference in it and the center-capture concept lies in the construction of the docking interface with no prominent hardware features hindering the capture.

The capture-center docking concept is adaptable to various sizes of satellites and is believed to satisfy the requirements of minimum cost to the target vehicle and still provide a system giving maximum capturability.

Table 2. COMPARISON OF THREE BASIC CONCEPTS

CONCEPT CRITERIA			
	PROBE	CENTER - CAPTURE	CAPTURE - CENTER
WT/VOL/S ON TARGET	1	2	2
DETERIORATIVE IMPACTS	1	1	3
CONVERGENCE MISAL.	0	1	3
CONVERGENCE RADIAL	3	1	3
PROB. FULL CAPTURE.	2	1	3
REPEATED ATTEMPTS	3	2	1
KEYING IN ROLL	3	2	2
INTERNATIONAL D. PORT	0	3	2
DIFFERENT SIZE	3	0	2
SPIN UP	0	1	2
LEGEND	16	14	23
0 NOT SUITABLE			
1 POOR			
2 GOOD			
3 VERY GOOD			

3.5 SIMULATION

Two distinct targets were chosen for the simulation tests with the selected docking interface. The two spacecraft chosen are believed to be representative of the range of spinning payloads to be recovered. These are: (1) the HEAO — a heavy satellite with a relatively low spin rate (2 rpm) that could be induced when disabled by loss of control, and (2) the GOMS — a small spin stabilized satellite with a relatively high spin rate (100 rpm). Data for these targets and the chaser are given in Tables 3a and 3b. The characteristics of the interface were investigated for each target, aided by simulated variation of the design parameters. After analytical trade-offs, a mechanism compatible with both kinds of targets was eventually defined. An attitude and attitude rate control system was active on the chaser vehicle, and a despin torque was initiated at predetermined times.

Table 3a. DATA FOR SELECTED SPINNING TARGET

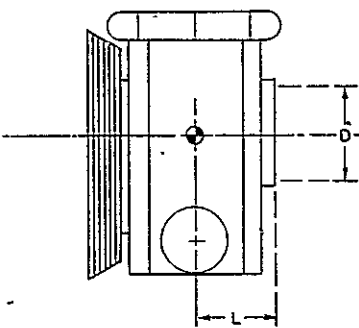
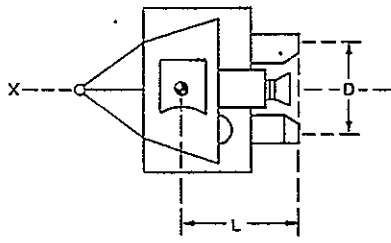
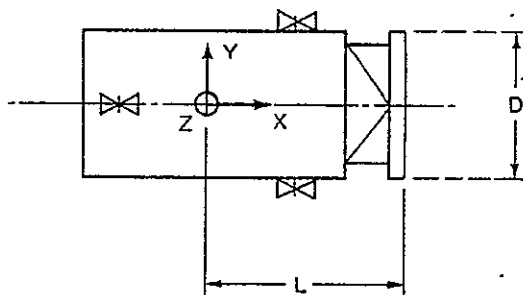
SATELLITES USED IN DOCKING	HEAO	GOMS ORBITING
NOT SCALED		
MASS	3003 [KG]	240.9 [KG]
M.O. INERTIA	5477 [KG-M ²] 5070 [KG-M ²] 2318 [KG-M ²]	88.5 [KG-M ²] 80.3 [KG-M ²] 81.5 [KG-M ²]
SPIN RATE, ω_x	2 [RPM]	100 [RPM]
RING DIAMETER, D	1.37 [M]	1.37 [M]
RING DIST, L	1.44 [M]	1.44 [M]

Table 3b. DATA FOR SELECTED CHASE VEHICLE



MASS	[KG]	7667
I_{XX}	[KG-M ²]	7149
I_{YY}	[KG-M ²]	38383
I_{ZZ}	[KG-M ²]	37312
L	[M]	5.52
$Y_{CG} - \bar{Q}$	[M]	0
$Z_{CG} - \bar{Q}$	[M]	0
D	[M]	1.8
ω_X	[RPM]	0

A domain of docking conditions was derived from considerations of physical boundaries of the docking interface.

The hypothetical capture boundaries tested for latching at closing velocities of 0.1 and 0.2 m/s are as follows:

- Radial miss distance, $0 \rightarrow 0.2$ m.
- Angular misalignment, $0 \rightarrow 10$ deg.
- Angular closing rate, $0 \rightarrow 7$ deg/s.
- Coning motion, $0 \rightarrow 5$ deg.

All capture attempts made within these boundaries using the docking mechanism earlier described resulted in a successful capture of both investigated targets.

Time responses of the docking transient are shown in the last part of this study.

3.6 ROTATING FACEPLATE

As discussed earlier, the transient behavior during the recovery of spinning satellites with high spin rates is very sensitive to the friction between the two contacting bodies. Since it is most impractical to spin up the chaser to synchronize with the target, an accommodation is made to permit the docking interface to spin relative to the chaser's docking axis (Figure 6).

Two possible docking configurations are introduced here in order to study the relative body behavior. Prior to docking, the faceplate can either be left free wheeling or be driven to synchronism with the target spin rate. After the impact transient, the plate will in both cases assume the spin rate of the target. Latching can then be performed and despin initiated. No hardware concept has been investigated, but the model remains sufficiently general to accommodate either kind of faceplate, whether on a shaft or on rollers.

The equations of the faceplate concept are presented in Appendix C.

A parametric study was performed with the double purpose of model validation and response analysis. One nominal case was first defined, then a sensitivity analysis was performed by variation of basic parameters around their nominal values.

Responses of the system as function of time can be seen in Section VII.

3.7 CONCLUSIONS

The following conclusions can be drawn from this analysis:

- The concept "capture-center" presented here is best suited for docking with spinning satellites.
- The same mechanism can be used for release and capture of different size targets on the same mission.
- The capture boundaries are mainly limited by the docking mechanism hardware.
- The rotating faceplate did not alter the stability characteristics of the scissoring motion.
- A rotating faceplate is justified if the friction between the docking rings cannot otherwise be reduced.

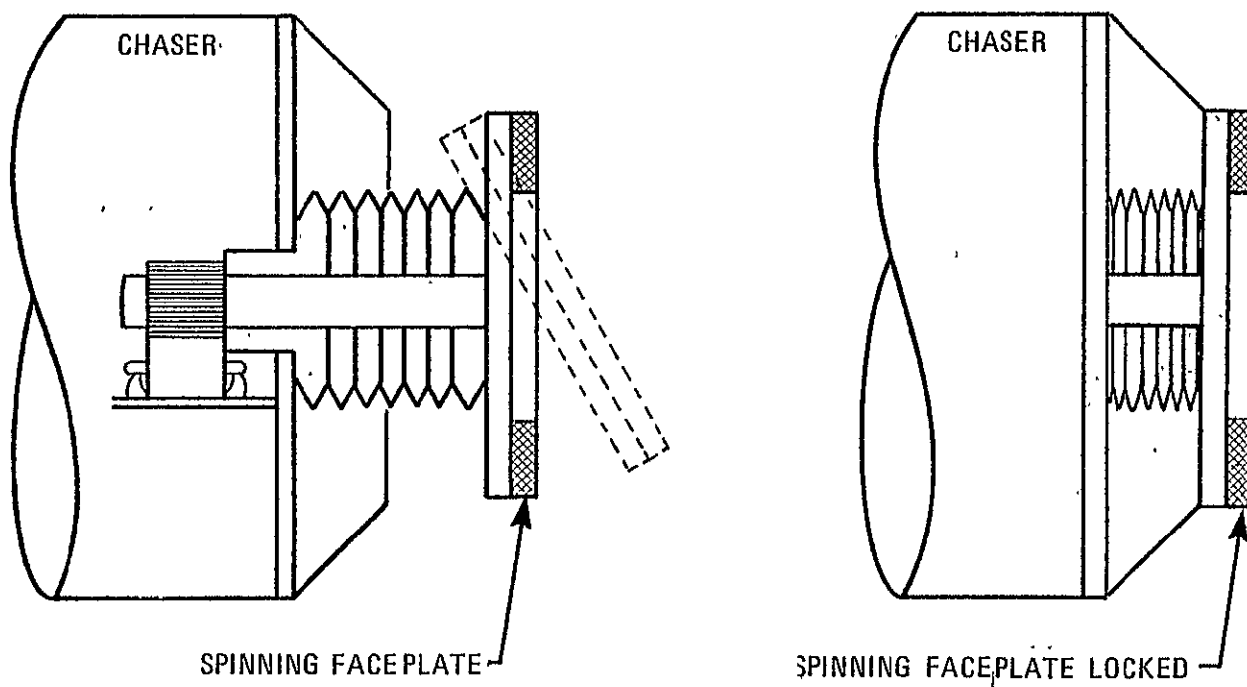


Figure 6. DOCKING INTERFACE OF SPINNING FACEPLATES

To be compatible with the docking mechanism investigated, the target should have the following characteristics:

- The angular rates and angular momentum of the target should be within given boundaries with the body spinning about the axis of maximum moment of inertia.
- The docking port must be located on the axis of maximum moment of inertia.
- The motion of the docking port axis relative to the principal axis must be within given boundaries. A nutation damper may be required to ensure this condition.
- The target should be capable of withstanding a given impact load applied through the docking port.

Section IV

PHASE C: PREDOCKING STUDY

4.1 METHODOLOGY

The purpose of conducting the system behavior analysis previous to the physical docking analysis was to determine the requirements necessary to ensure a safe and secure maneuvering of the chase vehicle toward the target docking port:

The requirement for a spin stabilization device located on the target itself was considered, and its effect during the docking transient as well as the case of a missed docking attempt was analyzed by a digital simulation.

The docking mission was defined as well as the successive phases of rendezvous, circling, positioning, and closing maneuvers. The performance of a laser-radar scanning system to be used with corner cube reflectors on the target was investigated for both long-range and short-range tracking with consideration of the effects created by the spinning of the target.

In the area of close vicinity maneuvering, the docking port recognition problem was investigated, and the methods to perform that task were outlined. An optical sensing system using reflective materials on the target was treated in detail.

For stabilization of the chase vehicle during the various phases of the mission, an attitude rate control system was considered. An attitude and attitude rate control system was also considered for guidance requirements of the chase vehicle. Both control systems were incorporated in the simulation to verify their performance in the overall docking mission with a spinning target.

Processing was performed on data obtained from the position and attitude sensing of the target.

Tests were performed to check the behavior and parameterize the gains of the control system.

The effect of liquid propellant slosh was assessed through a simulation of the motion within the tank of a "rubber ball" with characteristics similar to the liquid propellant. Observation of the system behavior for various initial conditions of the slosh mass was made for impacts before, during, and after the latching phase.

4.2 NUTATION DAMPING

A nutation damper was simulated as a mass-spring dashpot device judiciously placed on the spinning body as shown in Figure 7. The equations of motion are presented in Appendix D.

The nutation damper used in the simulation was tuned to be adapted to the GOMS satellite, spinning at 100 rpm with a coning angle of 5 degrees. Moments of inertia for the satellite were: $I_{xx} = 88.5 \text{ kg-m}^2$, $I_{yy} = I_{zz} = 80 \text{ kg-m}^2$.

The following values were selected for the nutation damper system: $m = 2.4 \text{ kg}$, $\mu = 0.01$, $k_p = 2.97 \text{ N/m}$, $C_p = 3.74 \text{ N/m/s}$, and $a = 0.13 \text{ m}$.

Since the equation of motion of the nutation damper has nonlinear coefficients, the solution for stability is a critical function of the fixed parameters. The solution is very sensitive to the location of the initiation damper from the vehicle c.g. (parameter a), and tuning was necessary to find the optimum damping.

The coning angle (also misalignment angle ν) of the satellite is shown in Figure 8a versus time. It can be seen that the satellite will tend toward the state of pure spin in a reasonably short time.

4.3 RESPONSE TO MISSED DOCKING

A docking condition was set up to simulate a missed docking attempt. The relative misalignment (ν) was set to 25 degrees and the closing velocity $v = 0.1 \text{ m/s}$. The target impacted with the chaser and was repelled without any latches being triggered. The succeeding motion is characterized by a nutation as shown in Figure 8b where no damper was activated. Figure 8c shows the same run with the nutation damper activated.

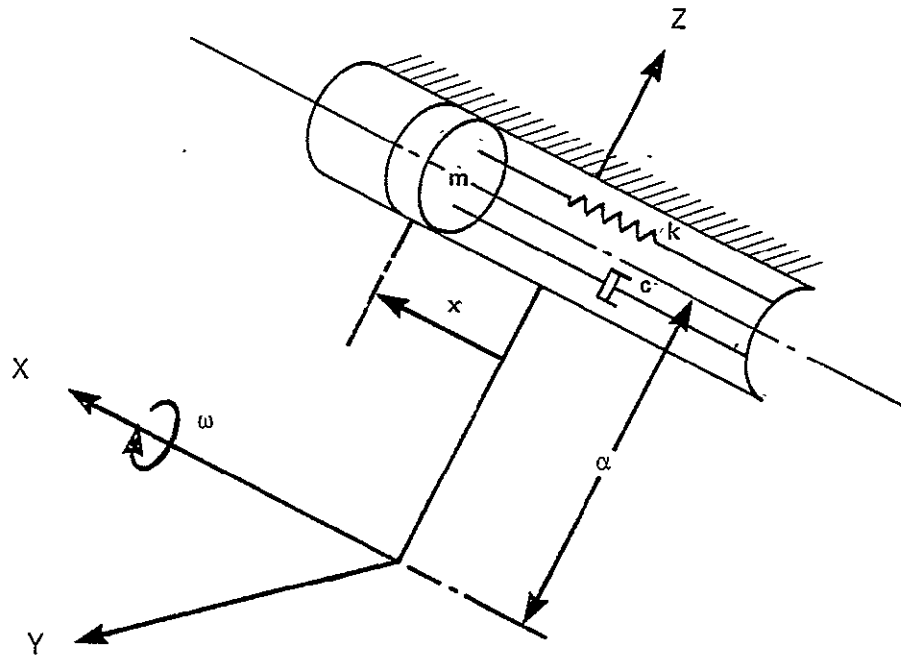


Figure 7. DAMPER CONFIGURATION

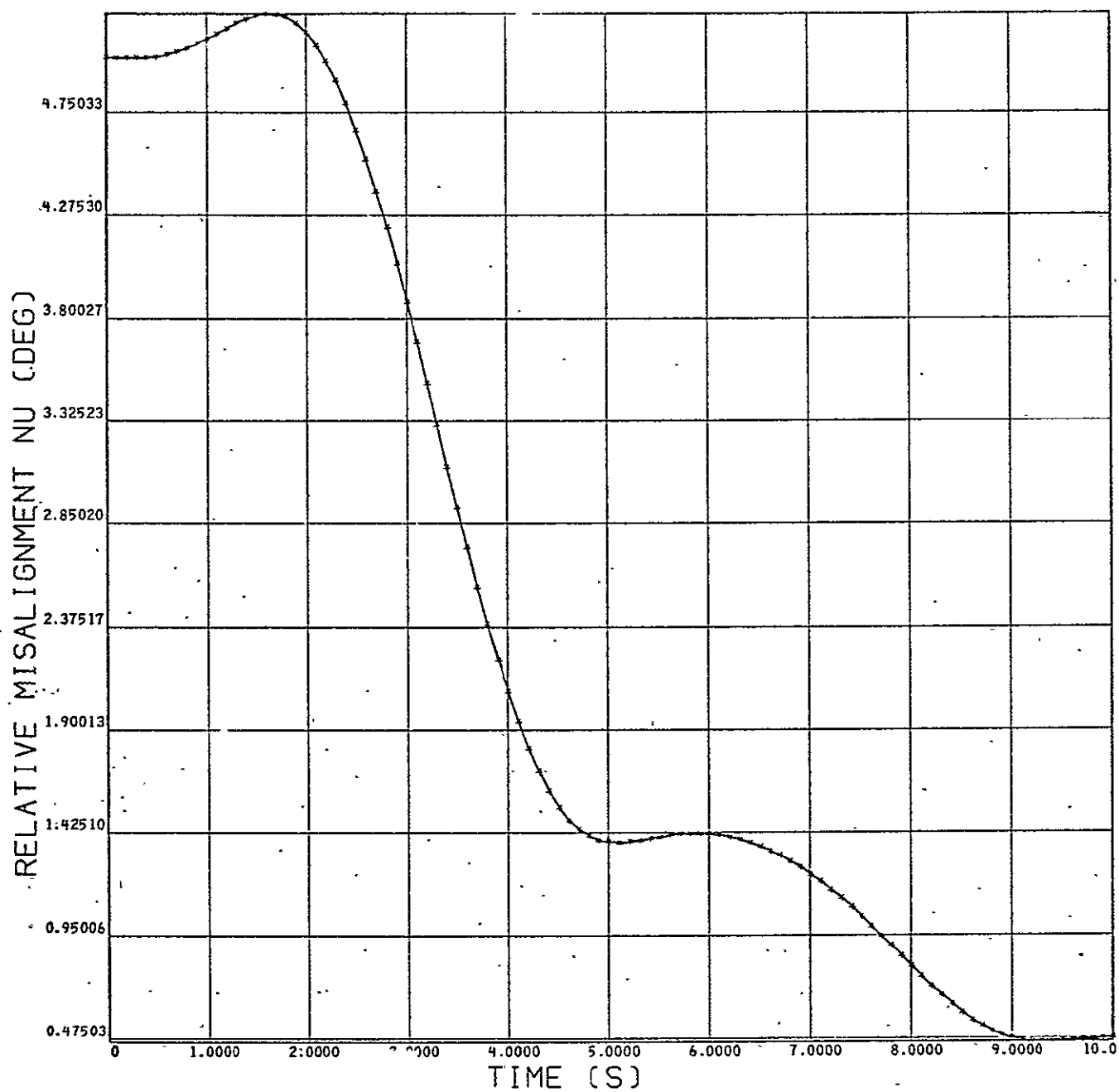


Figure 8a. SATELLITE CONING ANGLE VERSUS TIME WITH ACTIVE NUTATION DAMPER

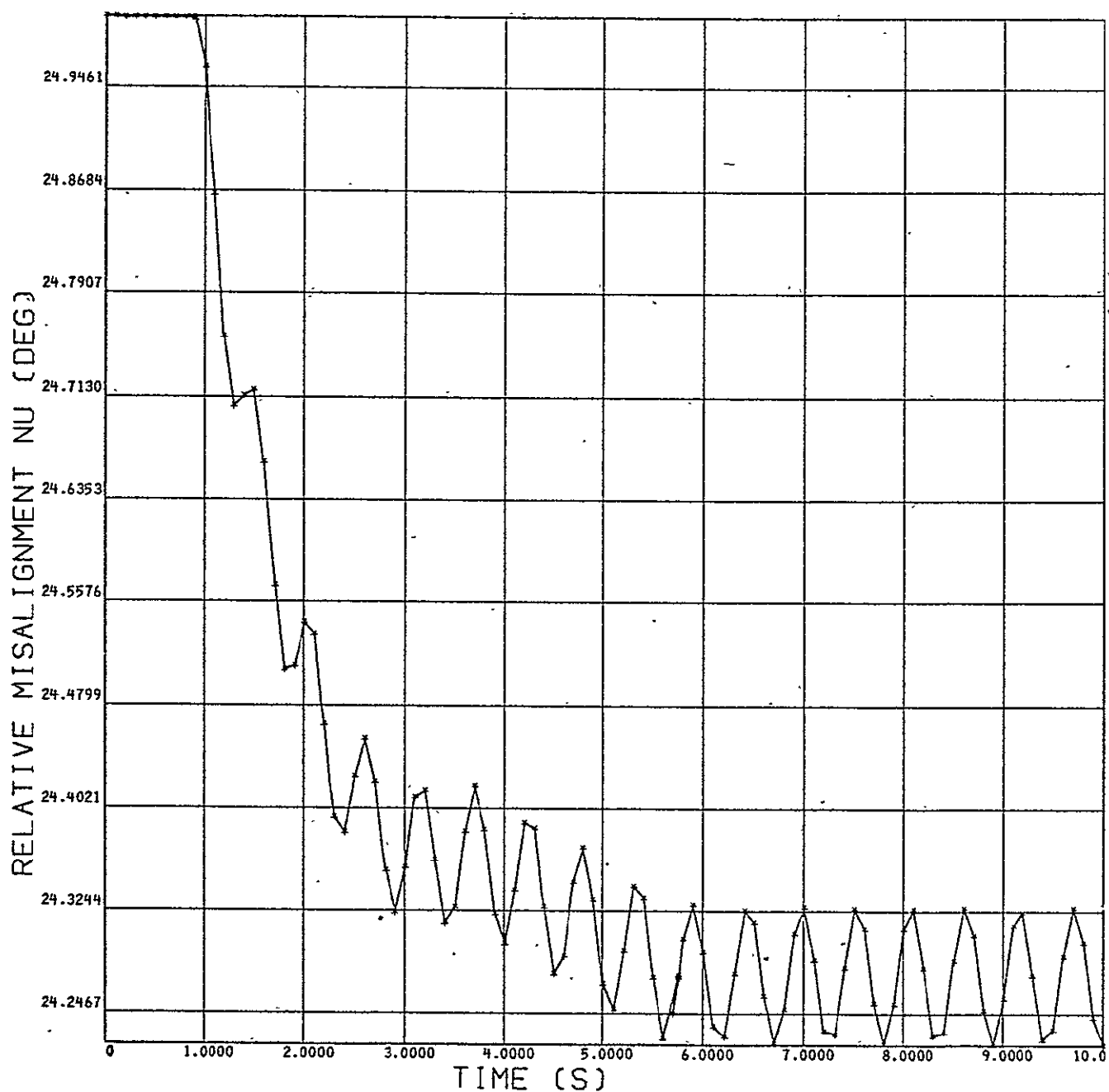


Figure 8b. MISALIGNMENT ANGLE VERSUS TIME FOR MISSED DOCKING ATTEMPT WITHOUT NUTATION DAMPER

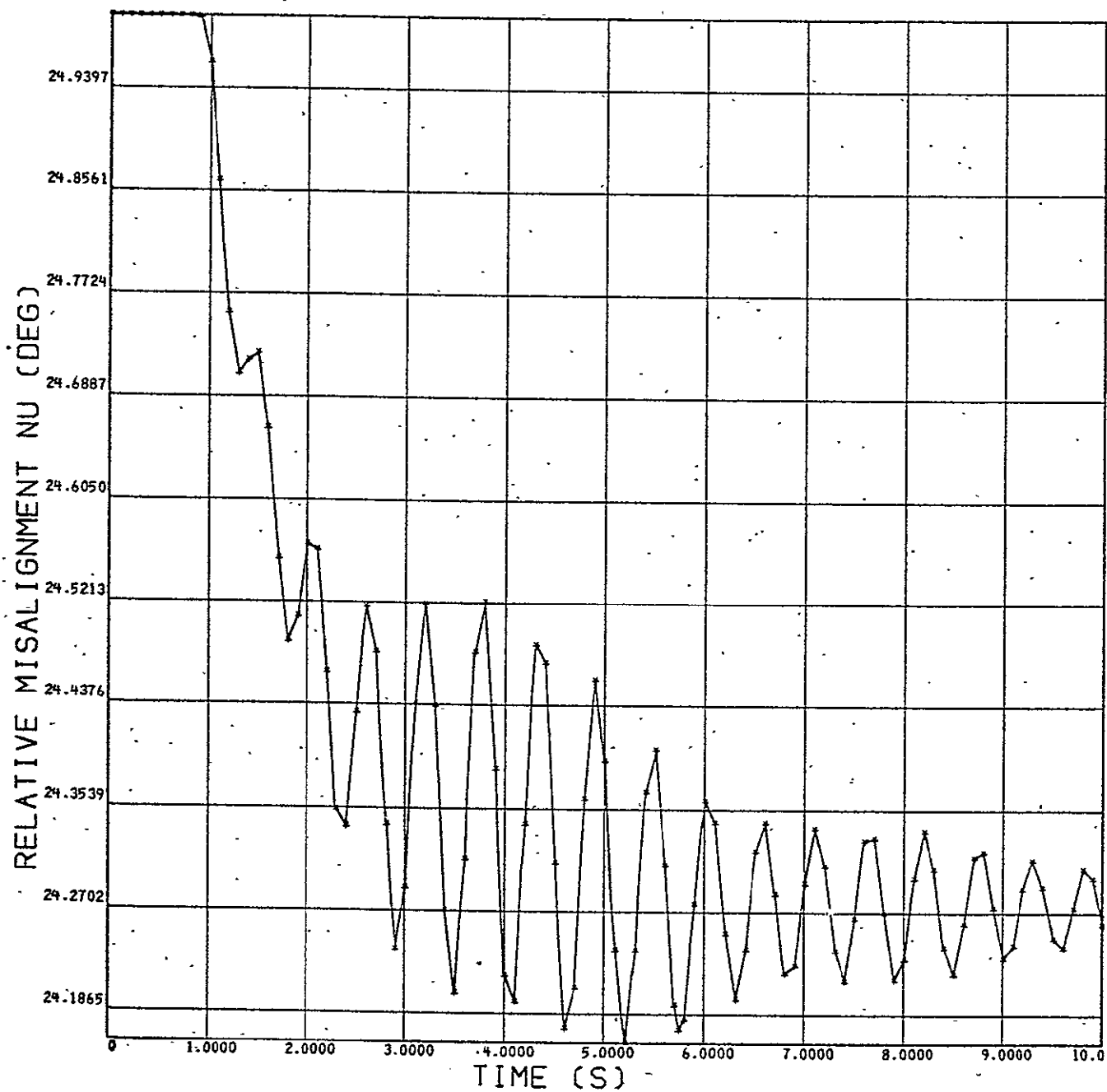


Figure 8c. MISALIGNMENT ANGLE VERSUS TIME FOR MISSED DOCKING ATTEMPT WITH NUTATION DAMPER

4.4 CONCLUSIONS

A nutation damper will induce large oscillations during the transitional phase of the docking, thus making it more difficult to ensure a safe and rapid latching. In the case of a missed attempt, the damper will be useful for stabilization purposes.

4.5 LIQUID PROPELLANT SLOSH

Investigation of the liquid propellant motion within the tank (Figure 9a) was performed.

The equations of motion for the liquid propellant are derived in Appendix E.

Simulation of the selected case (Table 4) was performed with an initial relative velocity for the propellant within the LOX tank of 0.1 m/s. Such an initial condition may occur during the docking sequence of the closing phase if the propellant was set in motion prior to or during the approach.

Figure 9b shows the motion of the slosh mass center - relative to the center of the tank. The largest force created by the slosh mass occurs at the time of impact as shown in Figures 9c and 9d along the x and y axes, respectively. The moment thus created is shown in Figure 9e. The magnitude will exceed the saturation level of the control system. The chase vehicle, therefore, will not be able to keep its attitude and will see a misalignment angle relative to its command attitude (that is, alignment with target) as shown in Figure 9f.

The propellant slosh effect can therefore be detrimental to the capture process if impact with the tank's wall occurs before the latching phase. Simulations of the dynamics of the bodies disturbed by a propellant impact after the bodies are latched showed no significant effect when the relative motion is damped out through axial and alignment dampers.

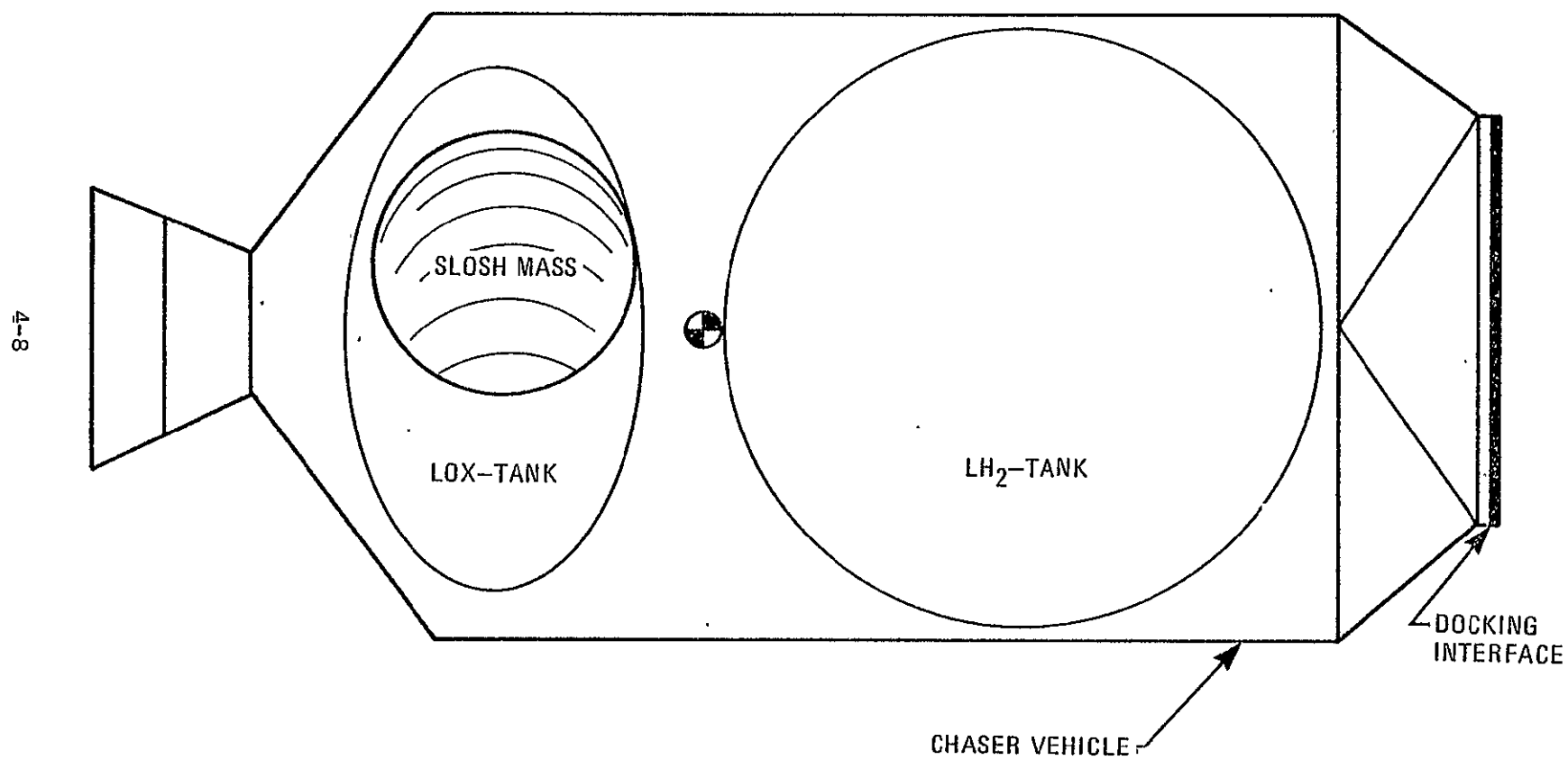


Figure 9a. PROPELLANT SLOSH MASS MODEL (LOX-Only)

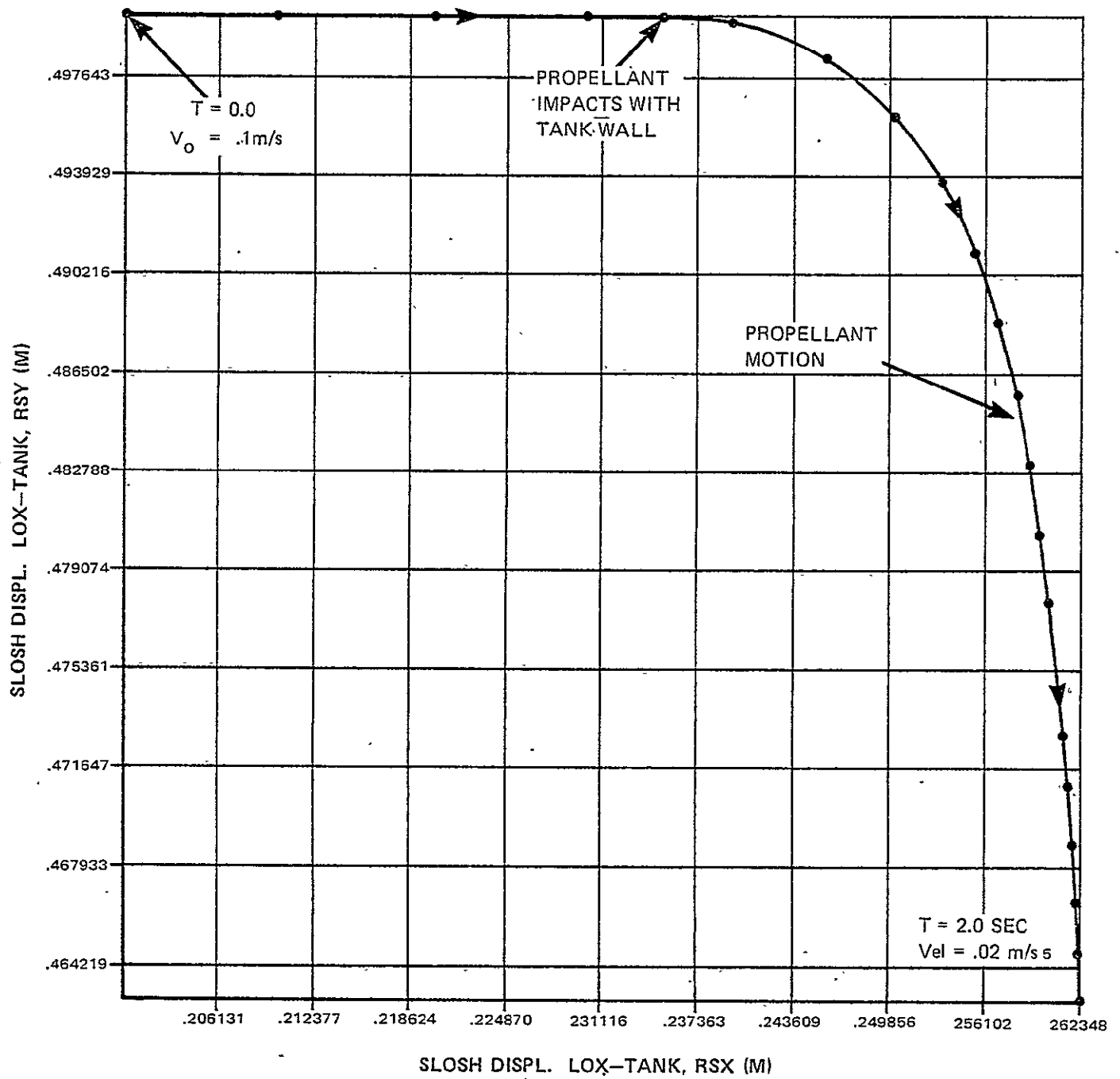


Figure 9b. PROPELLANT MOTION WITHIN THE LOX TANK ($V_0 = 0.1 \text{ m/s}$)

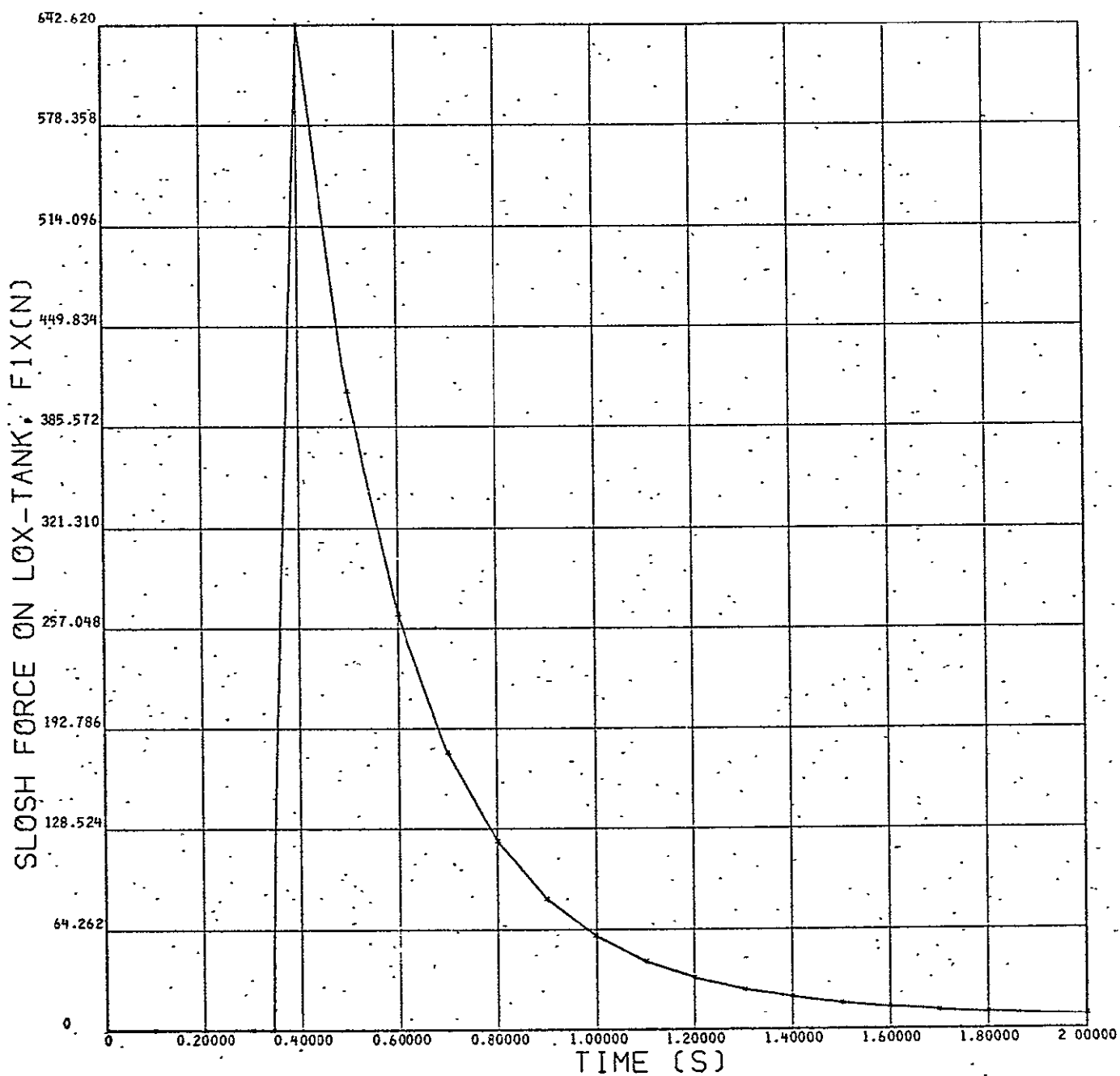


Figure 9c. SLOSH FORCE ON LOX TANK WALL, (X-AXIS) VERSUS TIME

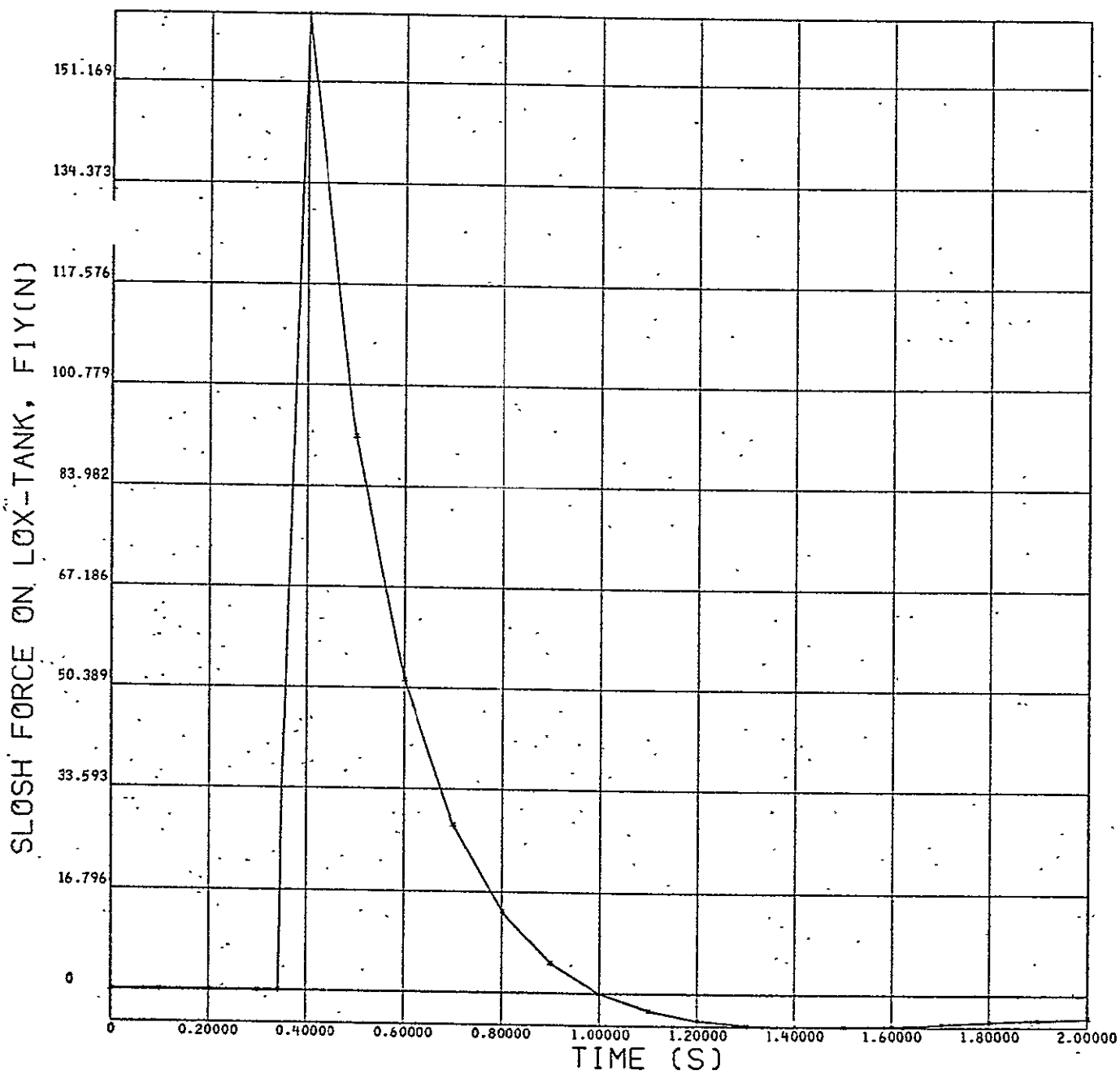


Figure 9d. SLOSH FORCE ON LOX TANK WALL, (Y-AXIS) VERSUS TIME

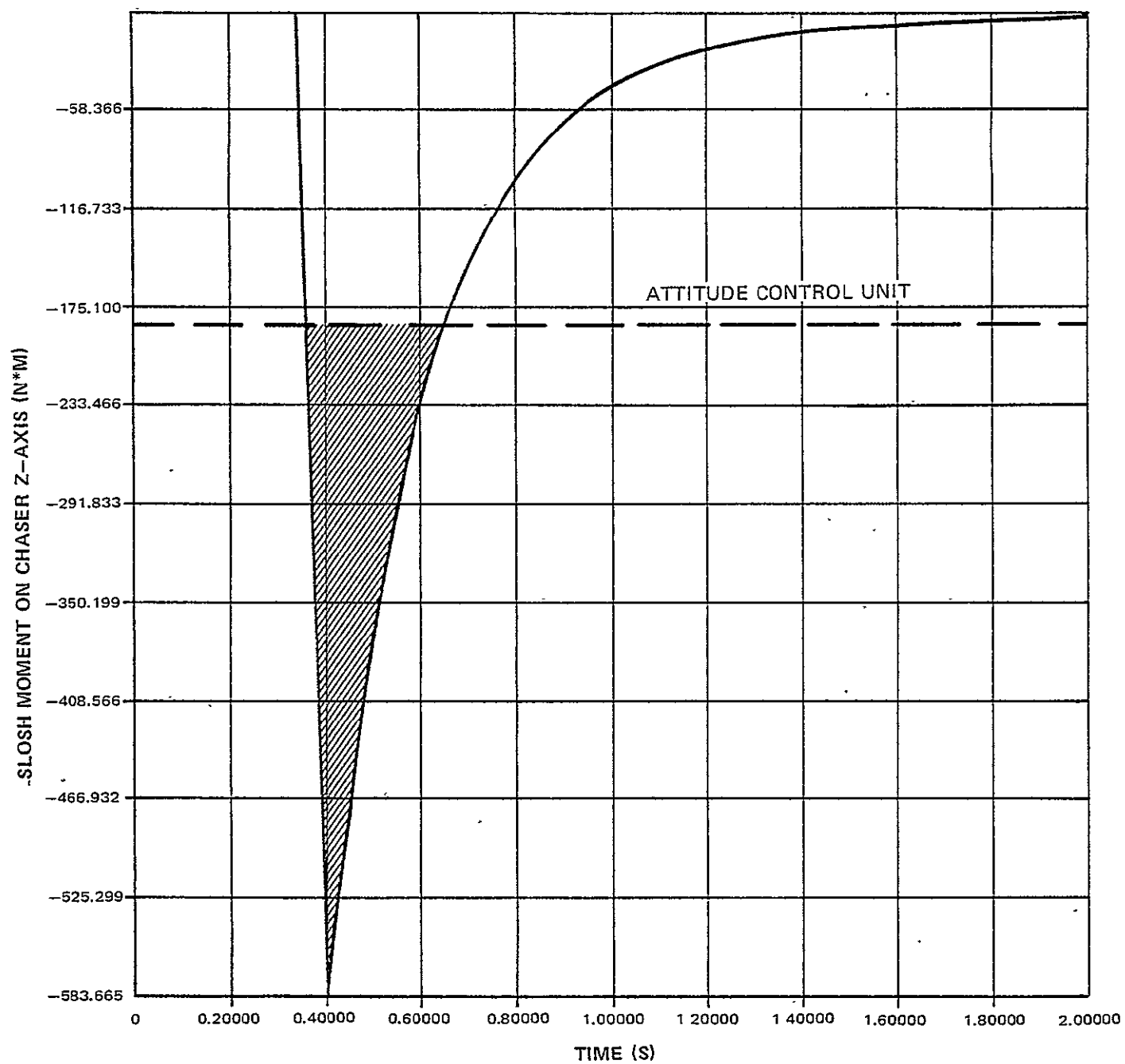


Figure 9e. SLOSH MOMENT ALONG Z-AXIS VERSUS TIME

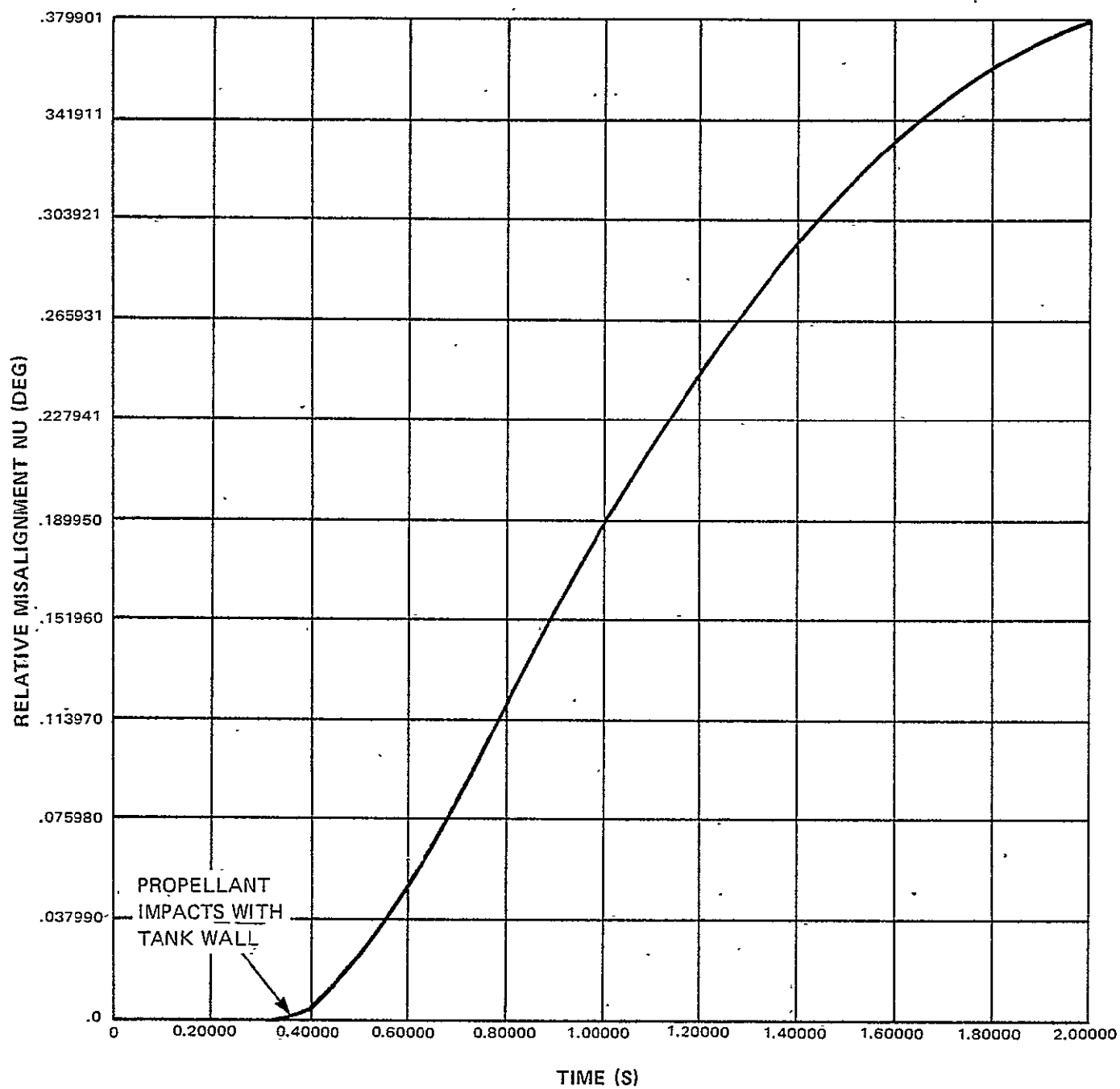


Figure 9f. MISALIGNMENT ANGLE OF CHASER DUE TO MOTION OF LOX PROPELLANT,
($V_o = 0.1$ m/s)

Table 4. DATA FOR SLOSH MODEL (LOX-MASS ONLY)

CHASE VEHICLE + LH ₂ MASS	3500 [KG]
LOX MASS	5200 [KG]
LOX MASS RADIUS	1 [m]
LOCATION OF TANK'S CENTER	-1.7 [m]
LOCUS OF SLOSH MASS C.G. AT IMPACT	.3, .8, .3 [m]
TANKS SPRING COEFFICIENT ($\tau = 5$ sec)	2000 [N/m]
NORMAL DAMPING CN ($\xi = .7$)	9150 [N/m/s]
PARALLEL DAMPING, C_p	915 [N/m/s]
PROPELLANT M.O. INERTIA	2080 [kg-m ²]

Section V

SENSING REQUIREMENTS

5.1 METHODOLOGY

To determine the sensing requirements for the capture of a spinning satellite, the system was partitioned into independent efforts, namely:

- The identification of the flight maneuvers that have to be performed during the mission.
- A discussion of the potential data required to perform those maneuvers.
- A brief presentation of the methods available for extraction of the data.
- The applicability of concepts which satisfy the mission requirements with a discussion of the advantages and disadvantages of those concepts.
- A selection of candidates most feasible for the recovery of a spinning satellite using the available steering laws.

5.2 RESULTS

5.2.1 Flight Maneuvers

Knowledge of the target's trajectory is the primary requirement for the rendezvous maneuver. After the trajectory of the target is known, the rendezvous maneuver is initiated to bring the chaser to the vicinity of the target.

Once the chaser has been brought into the vicinity of the target (100-200 m) a circling maneuver is initiated in order to locate the docking port. The circling maneuver is terminated when positive identification has taken place. Observation of the target for several cycles may be necessary to determine the standoff point. The chaser will then move to that location. A positive identification of the docking port will verify the stationary condition of the chase vehicle at the standoff point.

After reaching the standoff point and having determined the spin axis or the docking axis, the chase vehicle will initiate the final closure toward the target.

Attitude hold during the docking transient and orientation of the system to resume the flight are the last maneuvers of the recovery mission

5.2.2 Data Requirements

A go no-go decision is required as early as possible in the mission to decide whether or not the spinning target is recoverable, for example, is it spinning about the docking axis and is the lateral motion of the docking port within given boundaries?

Orbital parameters of the target must be determined to perform the rendezvous maneuver. The information required for that task includes range, azimuth angle, and elevation angle from which rates can be derived. This data is needed to compute the rendezvous trajectory and to update the navigation system.

The rendezvous maneuver as defined here is terminated when the chase vehicle reaches the standoff region. Distance to the target needs to be known at all times during the circling maneuver.

During the circling maneuver, the location of the target relative to the chase vehicle must be known in order to focus the Field of View (FOV) of the sensing system toward the target. Recognition of the docking port may require a standard pattern with which to compare received information.

The target relative motion is needed if the chase vehicle must remain stationary. Docking axis orientation, spin axis orientation, or momentum vector orientation may be required in order to compute the relative distance to the docking path.

5.3 SENSING CONCEPTS

5.3.1 Laser Radar

Laser radars have been successfully used in locating a target by sweeping the FOV with a pattern of light impulses. Corner cube reflectors (CCR) on the target reflect the signal when illuminated by the laser. The time lag permits the estimation of the range. Range rate is obtained from range

differentiation. Tracking distances up to 50 km are possible. For longer distances, an active target-mounted device (transponder) is required to intensify the reflected signal.

5.3.2 RF Radar

An RF Radar could be used as efficiently as the laser-radar for the acquisition and tracking modes. Attitude identification, however, would not be possible. Close range operations would then have to be monitored through an additional optical device.

5.3.3 Laser Beam Concept

A continuous laser beam could be used for close vicinity tracking. A design of reflective material would be placed on the target to form a recognizable pattern — a cross for example. The laser beam would then describe a circular motion and would be reflected when illuminating the reflective strips. Detection of the picture would allow for the determination of the docking port. The range and range rate can then be computed. The direction of the spin axis would be known after observation of the target for one whole period of its coning motion. The alignment angle of both bodies, necessary to determine the spin axis, can be obtained through the variable reflectivity of the laser beam on the target's reflective strips as a function of the incidence angle. The frequency of the laser beam coning motion would be selected as high as possible to obtain an "instant picture" of the docking port.

5.3.4 Video System

An optical system could be implemented to generate a video signal of the target in space when illuminated by the sun or to extract a video picture to determine patterns on the target when illuminated by a light source on the chase vehicle.

Processing of the image received will call for storage of the data, as well as extensive data processing for pattern recognition, range computation, and attitude determination.

5.3.5 Applicability

When tracking a spinning target with a laser radar, it is generally not possible to differentiate the various CCR's on the target. (The laser beam with a beamwidth of 0.1 degree will not discriminate two reflectors placed 1 meter apart at distances larger than 600 m). Also, CCR's need to be distributed around the periphery of the spacecraft in order to have at least one reflector visible at all times and thus avoid fictitious loss of track. If for any reason the target moves outside of the field of view, the system reverts to the acquisition mode and a new search is initiated.

It is therefore very difficult to determine through laser radar techniques the capturability of the spinning target defined by its damped wobbling motion.

A requirement for the laser-radar system is its capability to keep track of the target's motion by filtering out the motion of the CDR's relative to the target's center of mass (CM). This problem appears near the end of the RDV maneuver where individual reflectors will be discriminated (500 m through 50 m).

The use of a laser radar is also not indicated for close vicinity tracking. The minimum detectable range is around 20 meters. At that distance, the time lag of the reflected impulse from the emitted signal is no longer quantifiable. In the case of a fast spinning satellite, the sweep rate of the laser is inadequate. A reflector located at 1 m from the spin axis of a target spinning at 100 rpm would require a sweep rate of 12 deg/sec, a high rate compared to the 1 deg/sec available with the current technology.

The use of a conventional radar for tracking seems to be restricted to the range and range-rate computation. The consideration of the doppler effect however could be instrumental in the determination of the recoverability of the target, as well as to the identification of the momentum axis. No detailed research was made in this direction. Instead, investigation of a laser beam concept was performed to determine the docking axis.

A laser beam concept is shown in Figure 10 with a coning angle α for the laser beam. The light ray (0.1 deg) is illuminating the reflective strip at point X_1 , at a distance SX_1 from the line of sight incidence point S. The returned signal will be represented on the collector at location X'_1 . The distance to the incidence point S' will be $\overline{S'X'_1} = K \overline{SX_1}$ where K is a transformation constant of the optical system. A complete cycle of the laser beam will therefore determine points X'_1 through X'_4 . The intersection of $\overline{X'_1 X'_3}$ with $\overline{X'_2 X'_4}$ is at point O', the location of the docking port center point. The axis of the coning laser beam is subsequently centered on the target cross point O through a rotation in the direction of \vec{SO} by angle of $\frac{O'S'}{R}$ radians. The range (R) of the target is computed as

$$R = \frac{\overline{X'_1 X'_3}}{2K \tan \alpha}$$

The maximum error in range estimation ($\frac{\Delta R}{R}$) is computed in Appendix F as

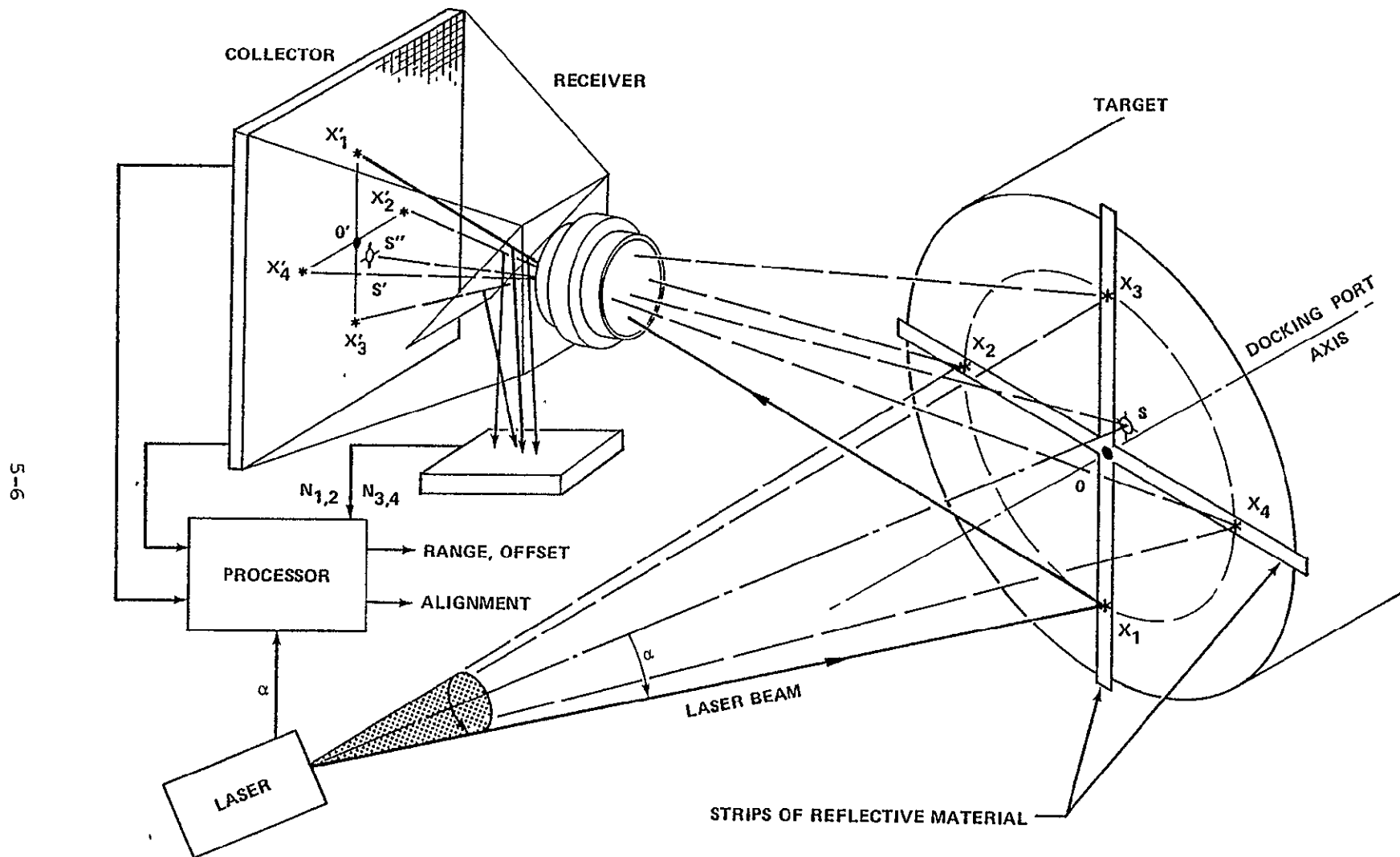
$$\frac{\Delta R}{R} = \frac{\frac{\Delta X}{X} + \frac{\Delta \alpha}{\alpha}}{1 - \frac{\Delta \alpha}{\alpha}}$$

It can be seen that the error will be minimum for a small error in the coning angle. Assuming a value of $\Delta \alpha$ constant over the range ($\Delta \alpha = 0.1$ degree beam-width), requirements will call for the largest α possible. This occurs when the diameter (D) of the painted circle on the target is equal to that of the docking port.

Thus:

$$\alpha = \tan^{-1} \frac{D}{2R} = \frac{D}{2R}, \text{ for } R \text{ large}$$

The error in range estimation is shown in Figure 11a as a function of the range R and diameter D as parameters. The error X was assumed to be negligible. Note that if $\frac{\Delta X}{X}$ is nonnegligible but assumes a value equal to $\frac{\Delta \alpha}{\alpha}$, the stand-off distance is reduced by one-half. Computation of the range through the sweeping laser beam reflection is therefore to be used only in close vicinity of the target with the largest painted circle possible.



5-6

Figure 10. LASER BEAM SENSING CONCEPT

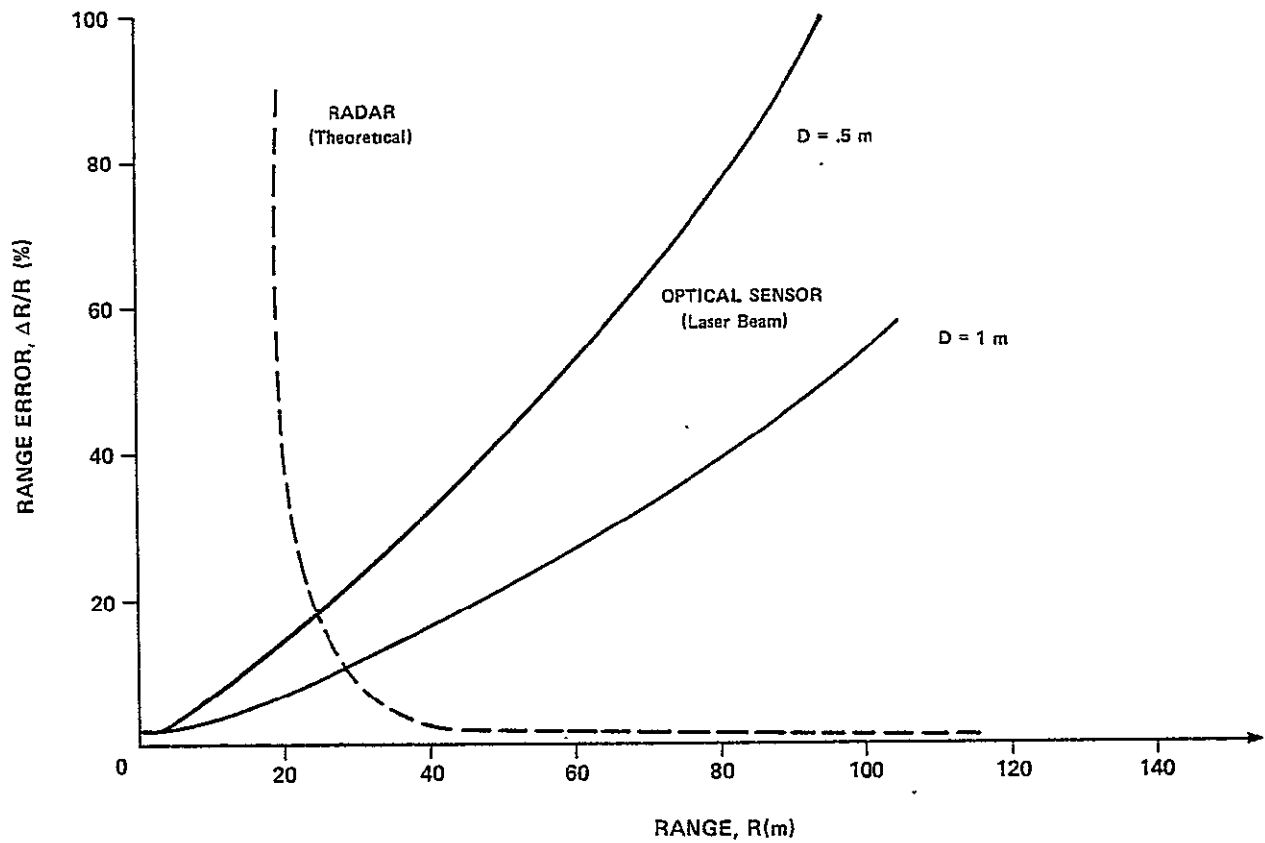


Figure 11a. ERROR ON RANGE ESTIMATION VERSUS RANGE FOR OPTICAL AND RADAR SENSORS

A reflective strip configuration is shown in Figure 11b. The returned signal (G) is a function of the laser beam incidence angle (γ) (Figure 11c).

The estimation of the docking port orientation can be determined through analysis of the magnitude of the reflected signals, (N_1 through N_4). The magnitude of the reflected signals will be a function of the incidence angle (γ) between plane A formed by the laser beam and the reflective strip and plane B formed by the reflective strip and the docking port axis (Figure 11d). The magnitude of the reflected signal should be the same for two opposite spots (X_1 and X_3). A zero incidence angle will occur when the laser beam is in the plane B where maximum reflectivity is obtained. This situation will be seen twice for each strip during one period of the target's spin. The larger signal will identify the plane (C) normal to the docking port and intersecting the laser source. The ratio of both signals will determine the magnitude of the misalignment angle (γ). The sign of that angle, however, is not known at this time; but its determination is necessary to initiate the alignment maneuver. This can be solved for large offsets by either observing the target or by initiating the move to see if the misalignment angle is converging. It is necessary to keep track of the relative position of both vehicles. This is very cumbersome in the case of a wobbling target or for a position near the nominal docking axis. The relative motion can be defined by using light detectors on the sides of the chaser. The sensor detecting the most light would determine the direction of the vector normal to the docking port. Further investigation is needed on the concept.

5.3.6 Advantages of the Laser-Beam Concept

An optical concept such as the one just described is easily implemented on the target. Reflective strips place no weight burden on the satellites and all sizes can be accommodated. The chaser will be able to track a wide range of targets with the same sensing apparatus.

The visual picture obtained can be remotely analyzed for the final docking or abort decision. Target spin rate can be determined when required for the docking with a prespun turntable.

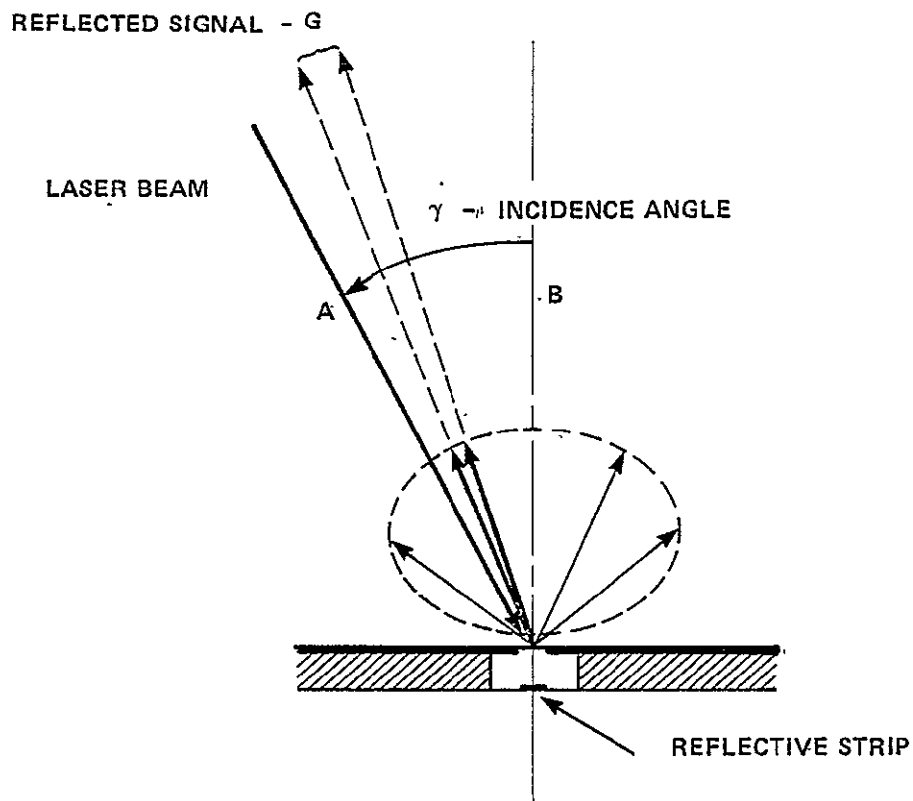


Figure 11b. REFLECTIVE STRIP CONFIGURATION

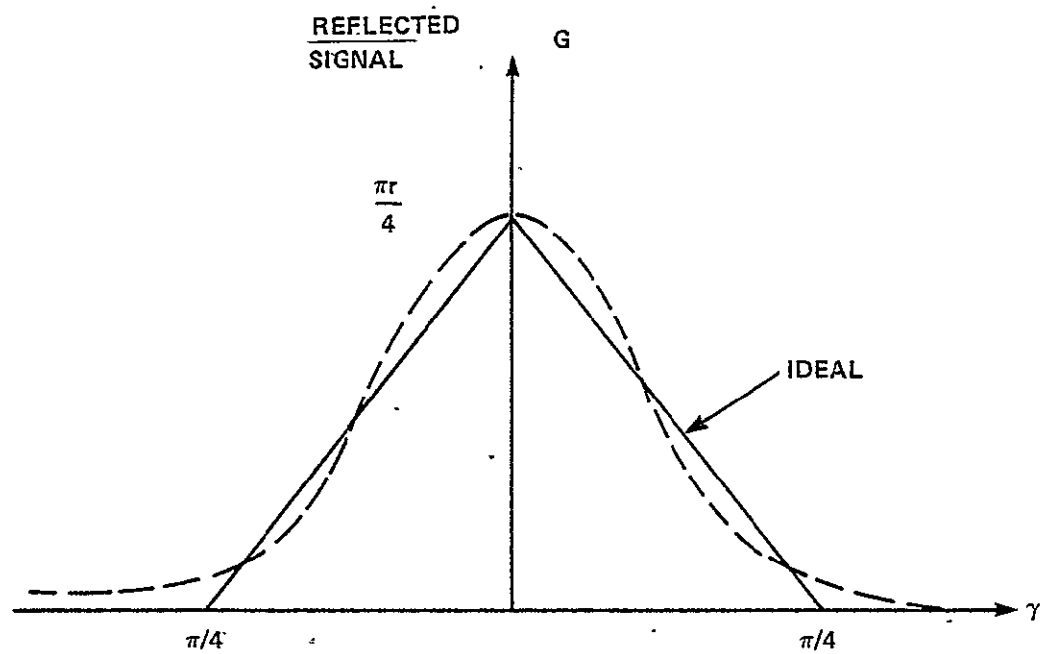


Figure 11c. REFLECTED SIGNAL VERSUS INCIDENCE ANGLE

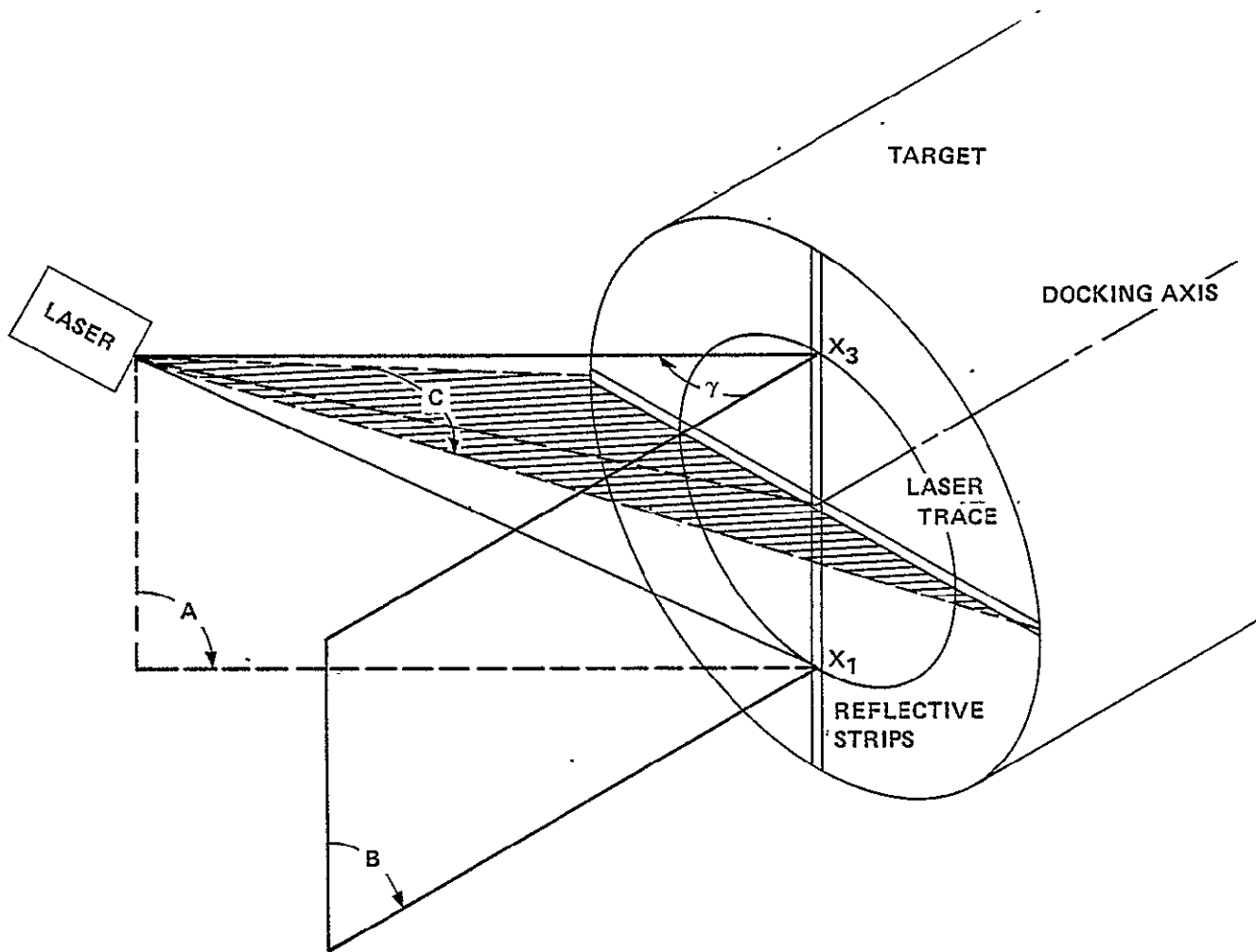


Figure 11d. DEFINITION OF INCIDENCE ANGLE γ

5.3.7 Disadvantages of the Laser-Beam Concept

The eventual decay of the reflective material can be a hindrance to the docking port sensing system. On the chaser, the complicated apparatus necessary to process the returned signals requires extensive data manipulation and storage space.

A video system should give the information necessary for the rendezvous maneuver to permit the transfer to the standoff region. It is implicitly assumed that the status determination is more accurate for close range sensing.

A video system where the laser beam is substituted by a spotlight and the reflective strips are substituted by a painted pattern on the docking face of the target could also be used.

Detailed investigation of the concept was not considered.

5.3.8 Preferred Candidate

Table 5 summarizes the special requirements needed for the sensing operation.

It can be seen that both laser radar and video systems are compatible with all maneuvers.

For the objective of cost minimization on the target, it is evident that the video system is preferable and should be investigated further.

For the time being, a selection of the docking maneuver must be made in order to assess the feasibility of a video system.

Table 5. SPECIFIC REQUIREMENTS FOR TARGET SENSING

MANEUVER	CHASER	TARGET
Tracking	Laser Radar Radar Video	Corner Cube Reflectors --- ---
Circling	Laser Radar Video	Reflective Strips Recognizable Pattern
Closing	Laser Radar Video	Reflective Strips Alignment Aid

Section VI

CONTROL REQUIREMENTS

6.1 METHODOLOGY

Assessment of control requirements for the docking mission with a spinning satellite was made by considering the following factors:

- The identification of the maneuvers applicable to the performance of the mission.
- The definition of the basic control commands necessary to maneuver the vehicle into a given configuration.
- The determination of the control commands required to perform the desired maneuvers.

6.2 RESULTS

The primary maneuver to the docking mission is the motion of the chase vehicle along the rendezvous trajectory. Navigation requirements are necessary along the path to ensure that the chase vehicle is on course. Corrections required must be performed at proper times.

A critical maneuver occurs when the approaching chase vehicle needs to be decelerated and must remain a safe distance from the target.

The flight pattern around the target characterizes the circling maneuver where the sensing system on the chase vehicle searches for the docking port. A maneuver is then performed to position the chase vehicle at the standoff point.

From the standoff point to the final docking, three approaches are analyzed: A feedback control, a trajectory approach, and an intercept control.

6.2.1 Feedback Control Approach

The feedback control approach is characterized by a continuous control system on the chase vehicle to correct the misalignment angles (ν) and (γ), (as identified in Figure 12) while the closing maneuver is being performed. A development of the control system is shown in Appendix F. The location of the

ν = MISALIGNMENT ANGLE OF TARGET

γ = MISALIGNMENT ANGLE OF CHASER

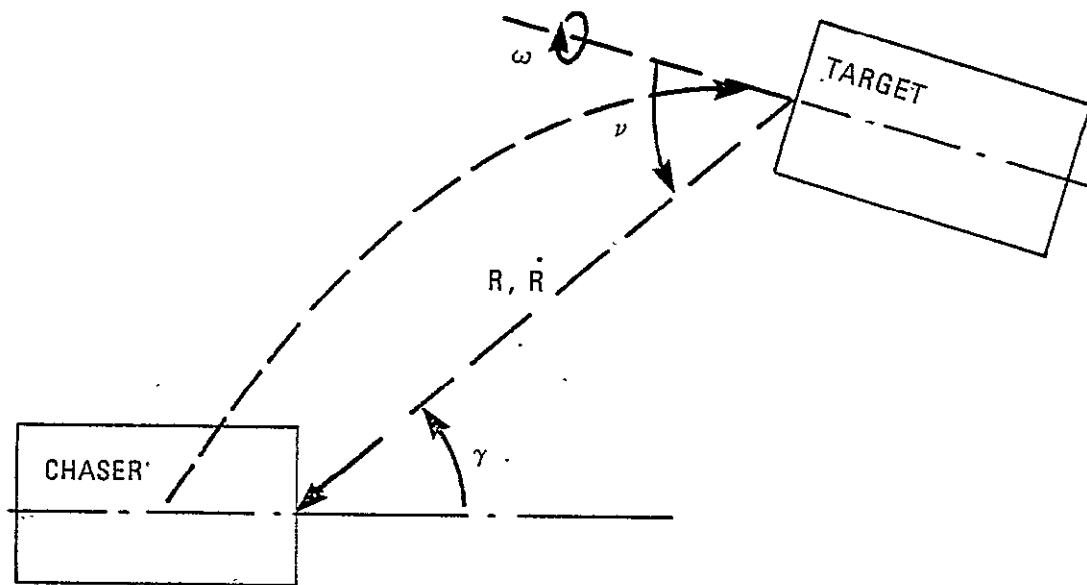


Figure 12. FEEDBACK CONTROL APPROACH

docking axis is supplied by the sensing system. The filtering of the data is performed to discriminate sensing errors and nutation motion from the target's coning and translation motion. It is important to observe the target from the standoff region for more than one coning period to determine the pure lateral motion. Once the closing motion is initiated, it is practically impossible to detect relative translation between the bodies.

A stationary positioning of the chase vehicle is required at the stand-off point. At the standoff point, the data processing of the sensor data cannot begin until enough data has been acquired to determine the docking vector. Then, the chase vehicle can initiate the closing maneuver and update its command from current sensor data.

The trajectory of the chase vehicle closing on a coning target and using the feedback control command is of helicoidal form with the magnitude of oscillation being a function of the cutoff frequency of the low-pass filter.

The major drawback of the feedback control approach is the necessity for tuning the filtering system to the particular satellites and the particular motion of the docking port. In this analysis, it was shown that the feedback control system would not be appropriate with a sensing device designed to follow the docking port motion. The tracking of the momentum axis of the target, characterized by a spot on the docking port with a minimum velocity relative to the chaser, could be of significant interest. Such tracking methods remain to be demonstrated.

6.2.2 Trajectory Approach

The basis of the trajectory approach is the identification of the target angular momentum axis prior to the closure maneuver. The most accurate position of the chaser to detect the momentum axis is believed to be in a plane normal to that axis.

A trajectory as shown in Figure 13 would allow the sensing system on the chase vehicle to identify that plane while crossing it at points A and B and to measure the vectors $\vec{\eta}_A$ and $\vec{\eta}_B$ necessary to compute $\vec{\eta}_C$ for the case of a stationary target. If the target is moving at a steady state, four points are necessary to determine the equations of motion of the target relative to the inertial reference.

The computation of the momentum vector for stationary and moving targets is described in Appendix G.

The approach considered is highly dependent upon the sensing system of the chase vehicle to supply the required data. A sensitivity analysis to determine the sensing requirements is recommended.

6.2.3 Intercept Control Approach

The idea of an intercept control approach was developed for docking with slowly coning satellites or with satellites whose docking port's motion is outside the permissible offset on the chaser's docking interface. The approach is initiated with a steady-state motion of the chaser along a predetermined path (Figure 14). The range and range-rate being known, the time of impact, as well as the location of the target at that time, can be estimated. A bang-bang system is turned on at the required times to bring the chaser's velocity to match the velocity of the target at the desired location. Controls can be set for lateral translation as well as for rotations in pitch and yaw of the chase vehicle. A more detailed discussion is presented in Appendix H.

6.3 BASIC CONTROL COMMANDS

For purpose of guidance of the chase vehicle, two types of thrusters are generally used: a primary system of forward thrusters which are used mainly for boosting of the vehicle, and a secondary system of attitude thrusters used for control of pitch, yaw, and roll motions. The boosting thrusters can be fired for deceleration if a rotation of the vehicle is possible.

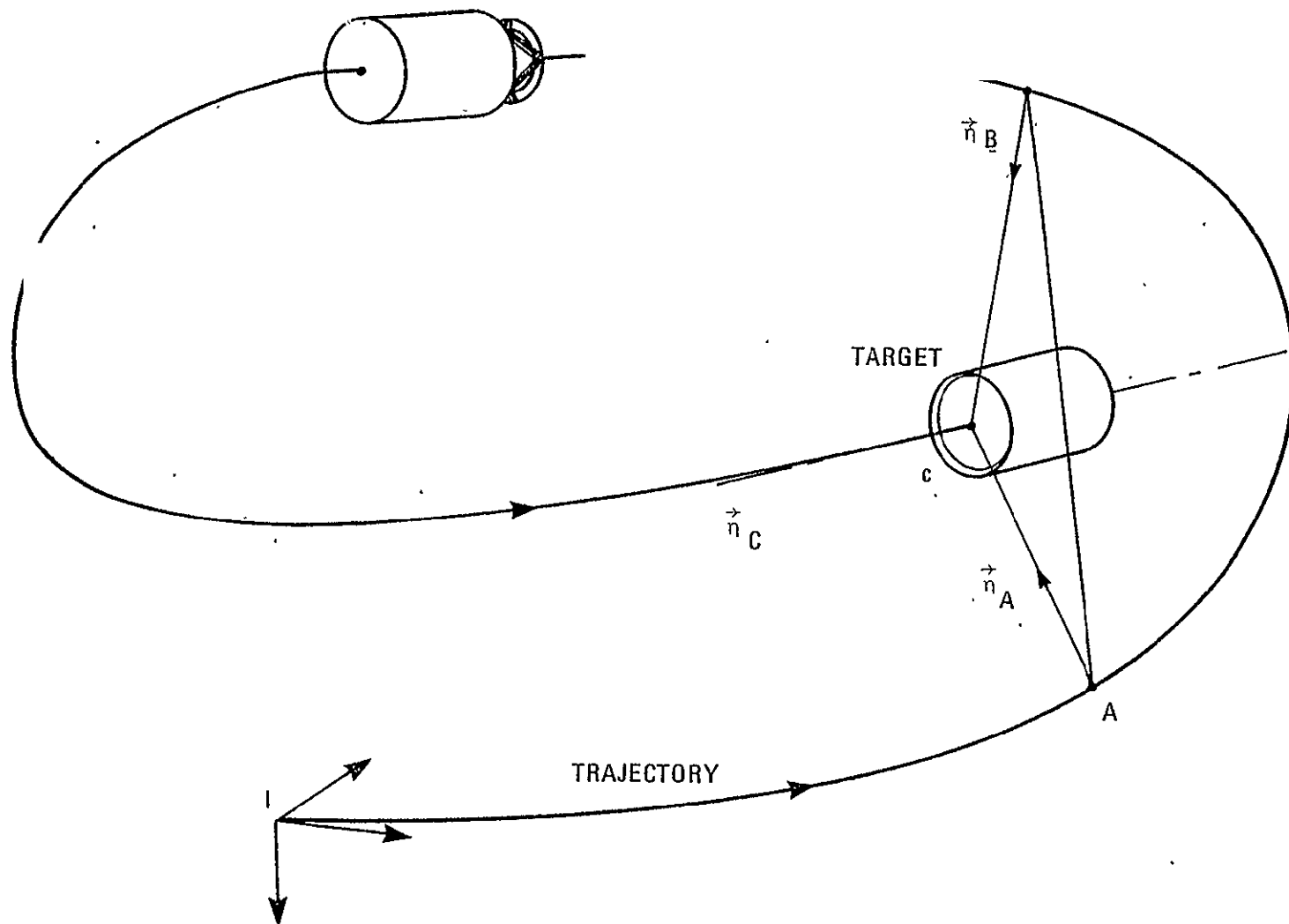


Figure 13. TRAJECTORY APPROACH

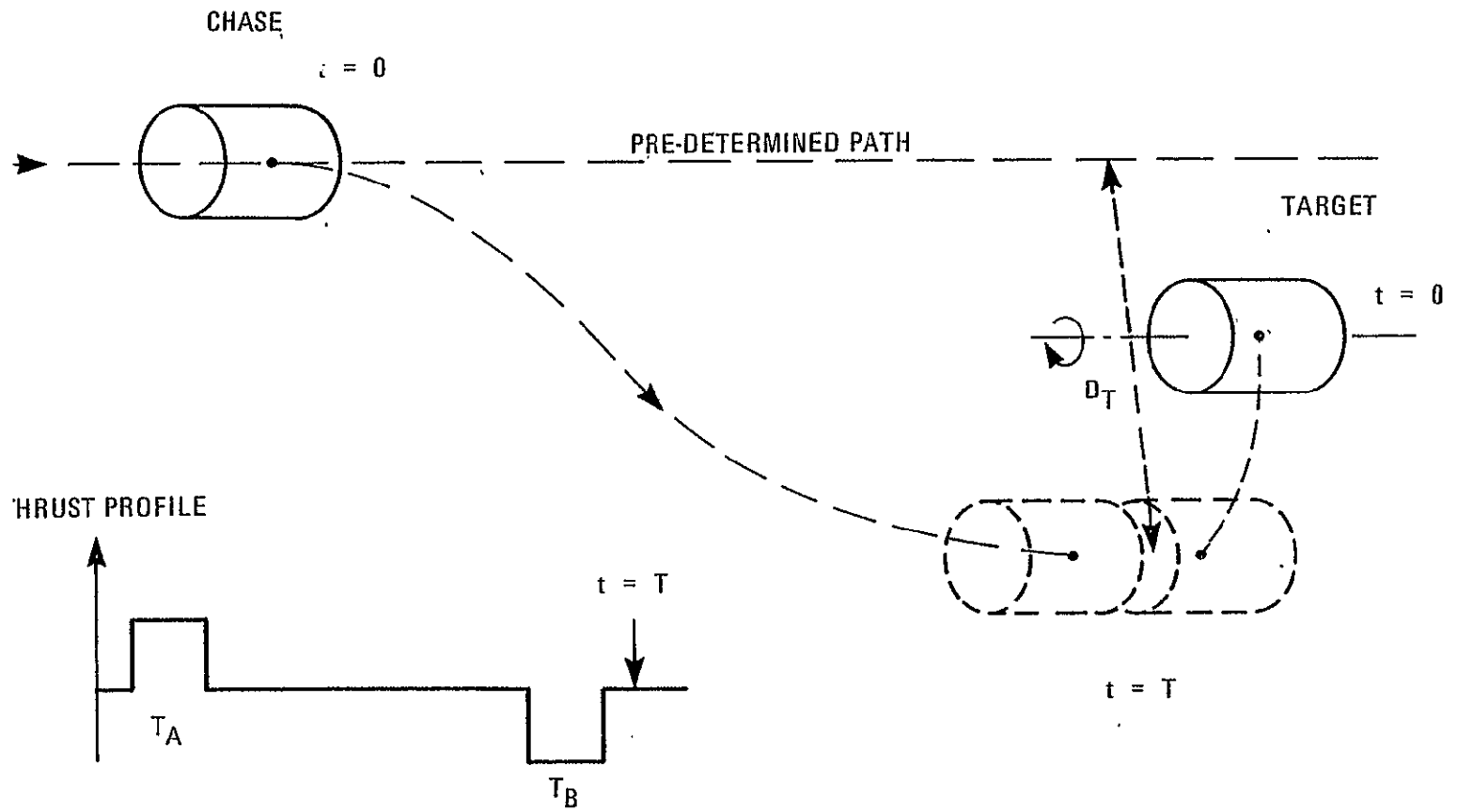


Figure 14. INTERCEPT CONTROL

The sensor's field of view requirements or restrictions due to plume impingement may not allow operation of the thrusters.

The thrusters are expected to give a constant thrust when operating. The duration of the impulses, subject to a minimum firing time, is therefore the input to the thrust command and is determined by the selected guidance system.

6.3.1 Control Commands

Distinct maneuvers must be performed during the rendezvous phase by the chase vehicle, during the circling phase, and during the closure maneuver itself. A common task, however, exists in the requirement for the chase vehicle to face the target at all times. The chase vehicle must be able to react and to align itself to have the target in its field of view.

A control system may be designed to use the gimbal on the forward thruster or thrusters and thus avoid unnecessary firing of the secondary thrusters. The attitude control thrusters could then be used for supplementary control as well as for deceleration of the chase vehicle, when required. Two concepts of chase vehicle deceleration at the end of the rendezvous maneuver in the vicinity of the target are presented.

The first concept consists of directing the rendezvous path toward the target. Two possibilities to decelerate the chase vehicle using primary and secondary thrusters then exist. Use of the primary thruster requires rotation of the vehicle and would therefore require a sensing device to scan the entire space. Plume impingement effects may be unfavorable in the vicinity of the target, particularly for primary thruster firing. Also, fuel consumption when using secondary firing may be too high.

A second concept as shown in Figure 15 and described here depicts the circling maneuvers integrated with the last phase of the rendezvous maneuver. The rendezvous trajectory is computed to "miss" the target by distance (m). The

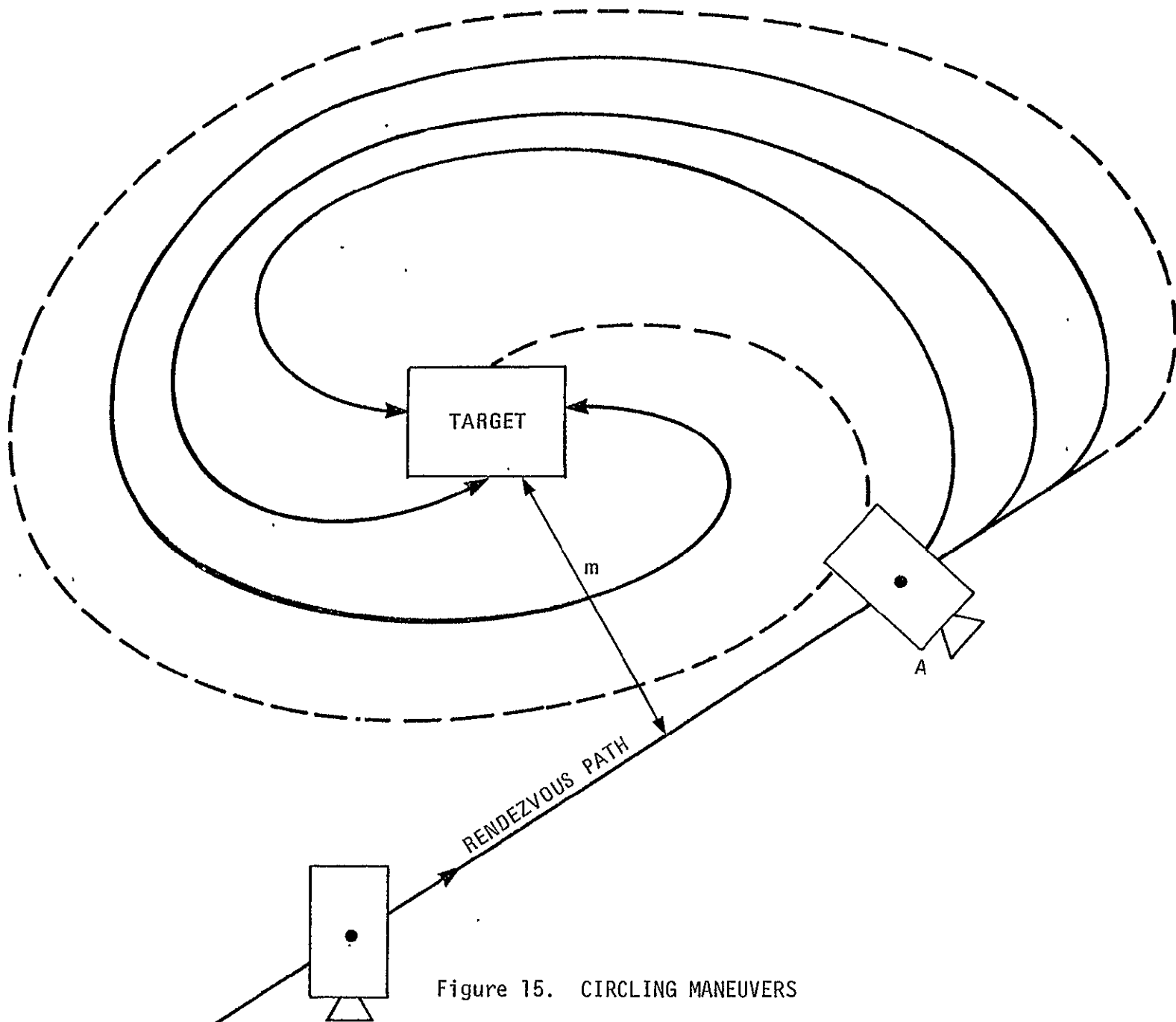


Figure 15. CIRCLING MANEUVERS

chase vehicle is moving along at a steady state and is slowly rotating to face the target while passing, thus keeping the target in its field of view. At location A, which remains to be determined, the primary thrusters are operating while the chase vehicle is being rotated. During the circling maneuver, the sensing system is operating and will identify the location of the docking port. That will determine the number of revolutions necessary to perform the required maneuver to bring the target within the vicinity of the standoff point with a low velocity relative to the target.

A forward thrust to satisfy the minimum velocity requirement is supplied by the main thrusters while attitude thrusters fire according to the approach requirements.

6.3.2 Simulation Response

Docking was simulated using the data described in Table 3a for the satellites GOMS and HEAO and Table 3b for the chase vehicle. The closing velocity was selected to be high (1m/s) in order to accelerate the docking process.

6.3.3 GOMS

The satellite was given an inertial spin rate of 100 rpm and a coning motion of 5 degrees. The chase vehicle was aligned along the coning axis. A nutation damper activated at initiation time reduces the coning motion as shown in Figure 16a. After 10 sec, the docking takes place resulting in a different frequency of oscillation, as shown in Figure 16b. The nutation damper reacts as shown in Figure 16c. Note the large displacement of the damper mass (not optimum). Figure 16d, shows the alignment rate can be seen before, during, and after docking.

The propellant slosh force on the chase vehicle is shown in Figure 17a. The propellant mass (Table 4) was initiated at 0.05 m/s. The motion is illustrated in Figure 17b.

A prespin torque was applied to the rotating faceplate before impact. A despin torque was applied after 20 seconds angular rate as shown in Figure 17c. The axial force seen by the chaser is shown in Figure 17d.

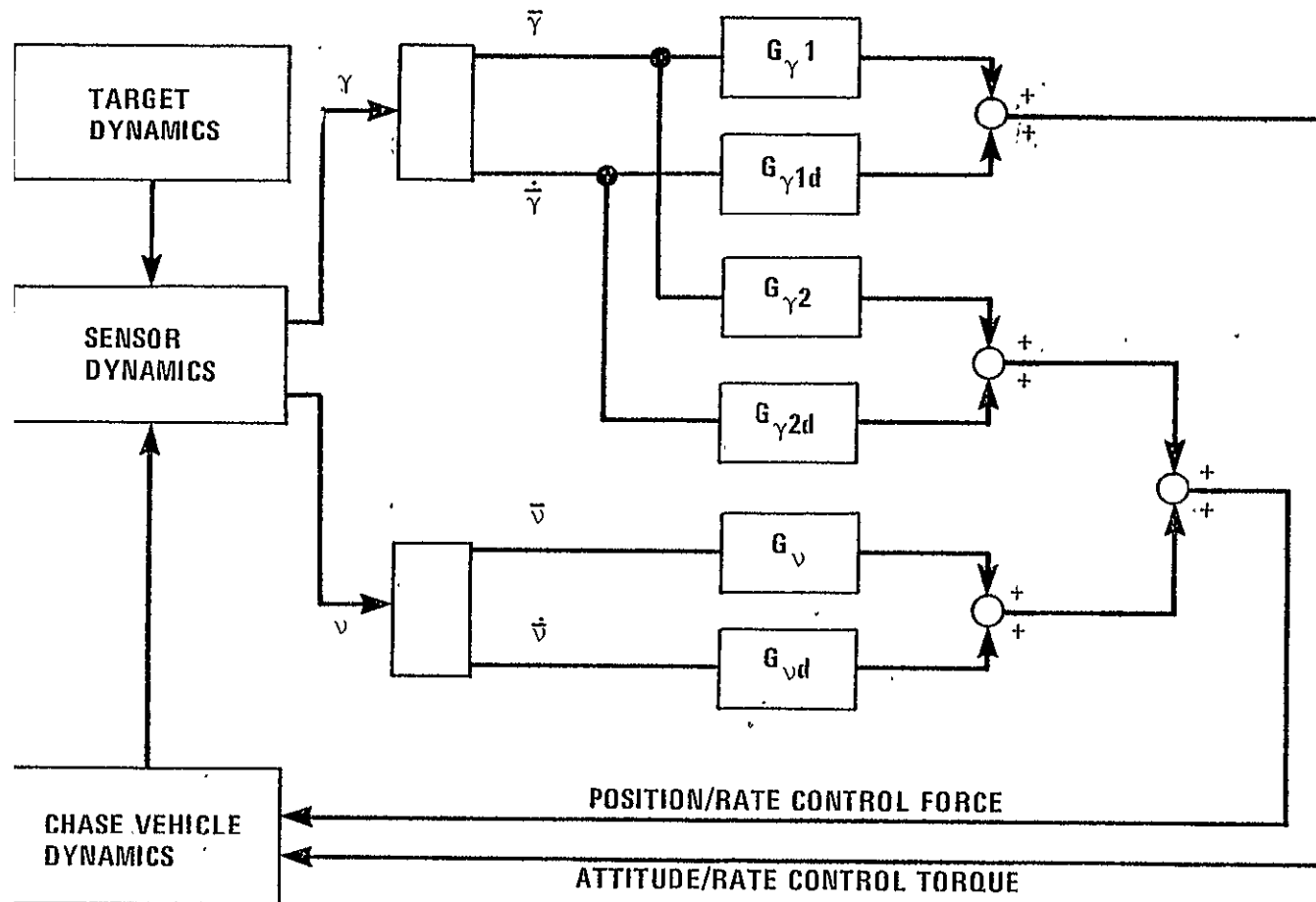


Figure 16a. FEEDBACK CONTROL COMMAND

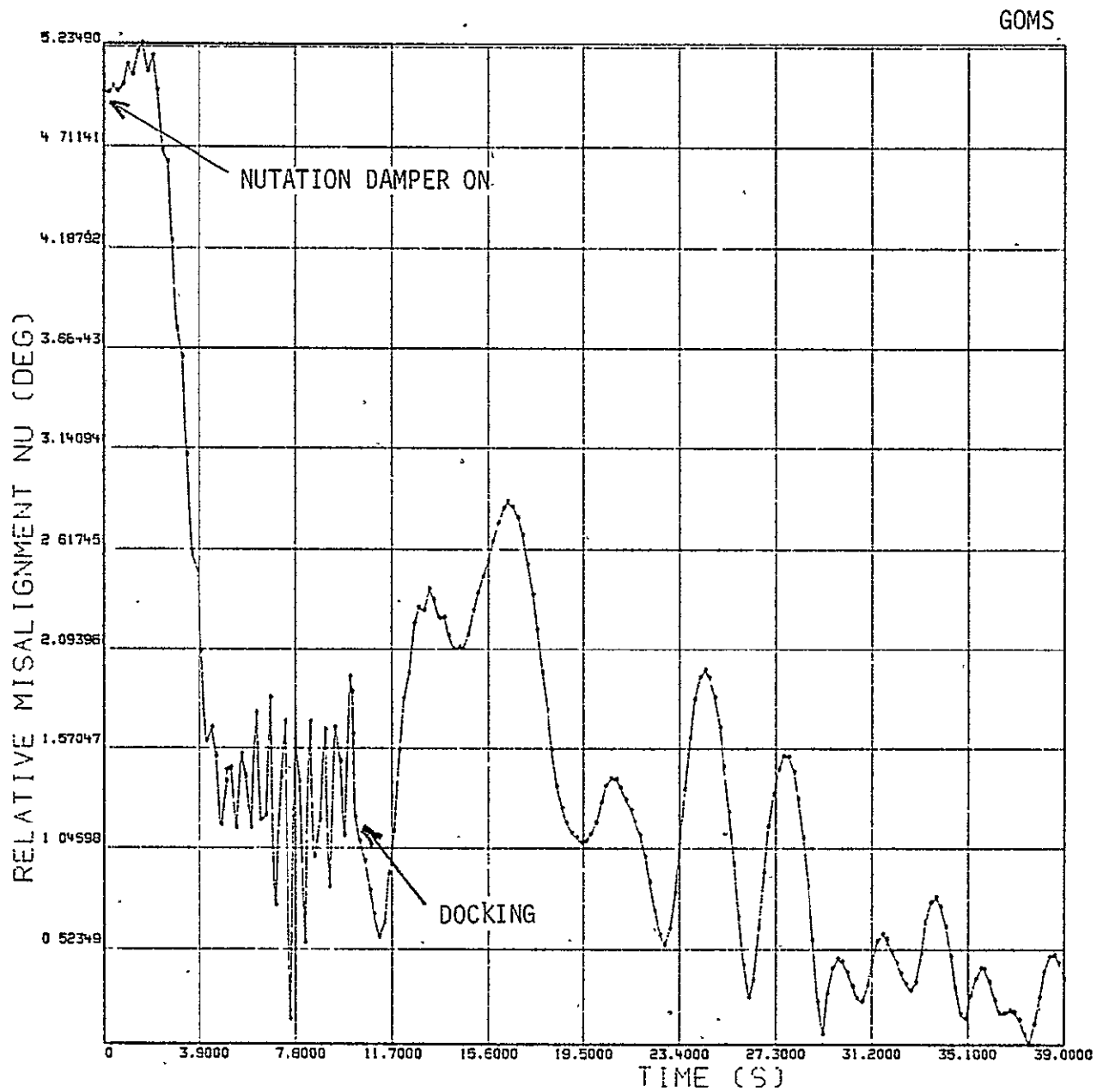


Figure 16b. MISALIGNMENT ANGLE VERSUS TIME

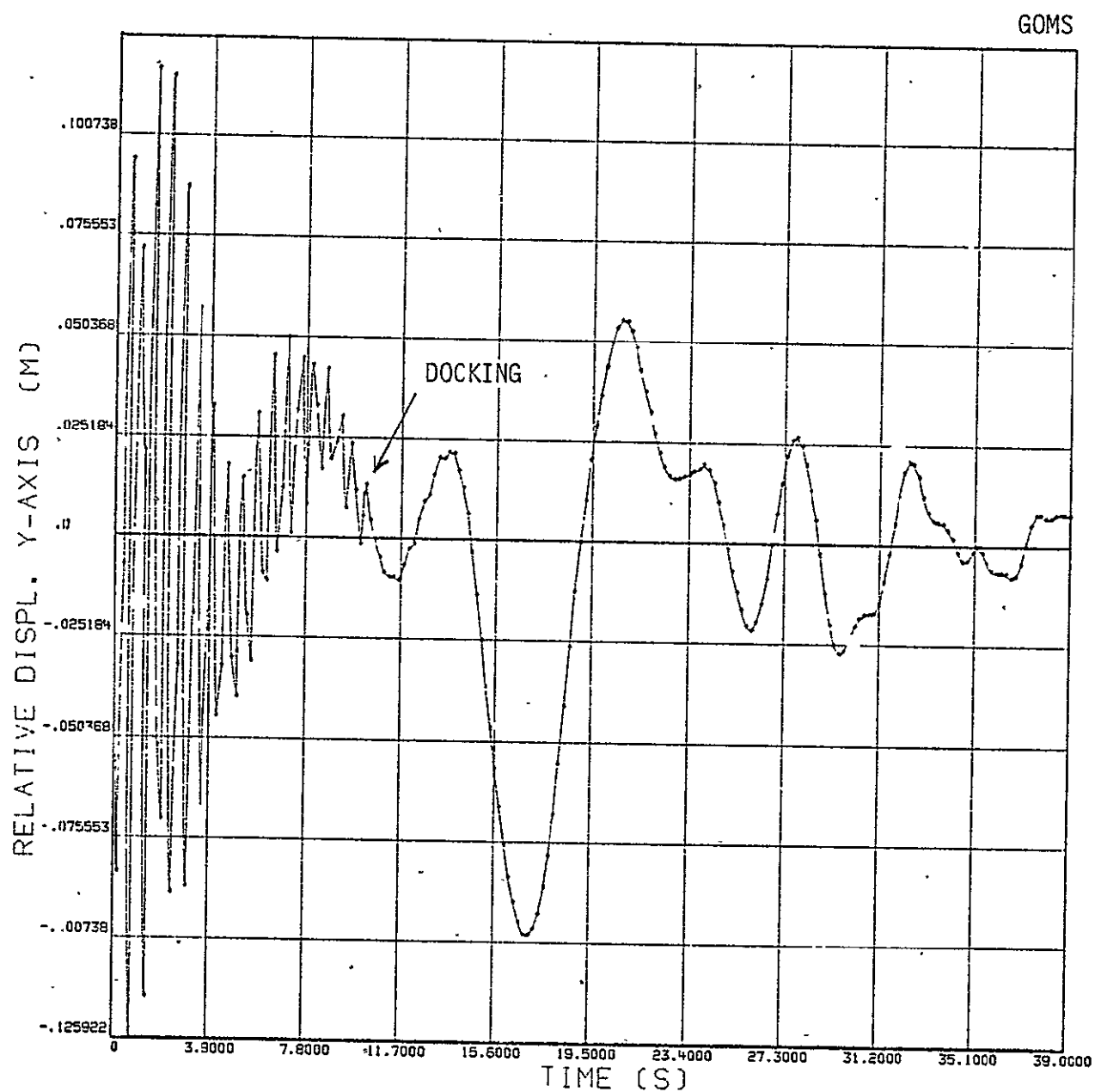


Figure 16c. LATERAL DISPLACEMENT VERSUS TIME

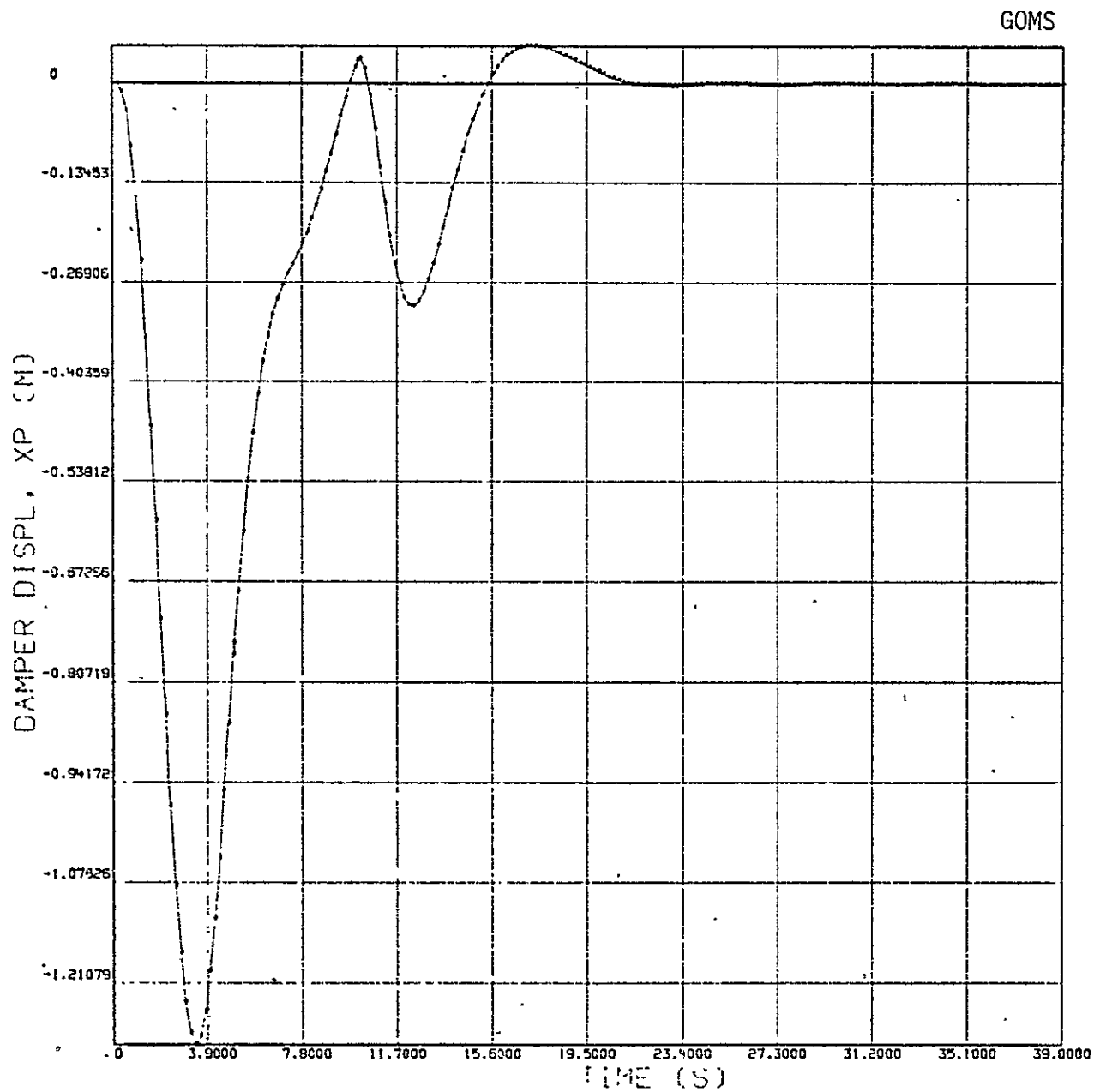


Figure 16d. NUTATION DAMPER DISPLACEMENT VERSUS TIME

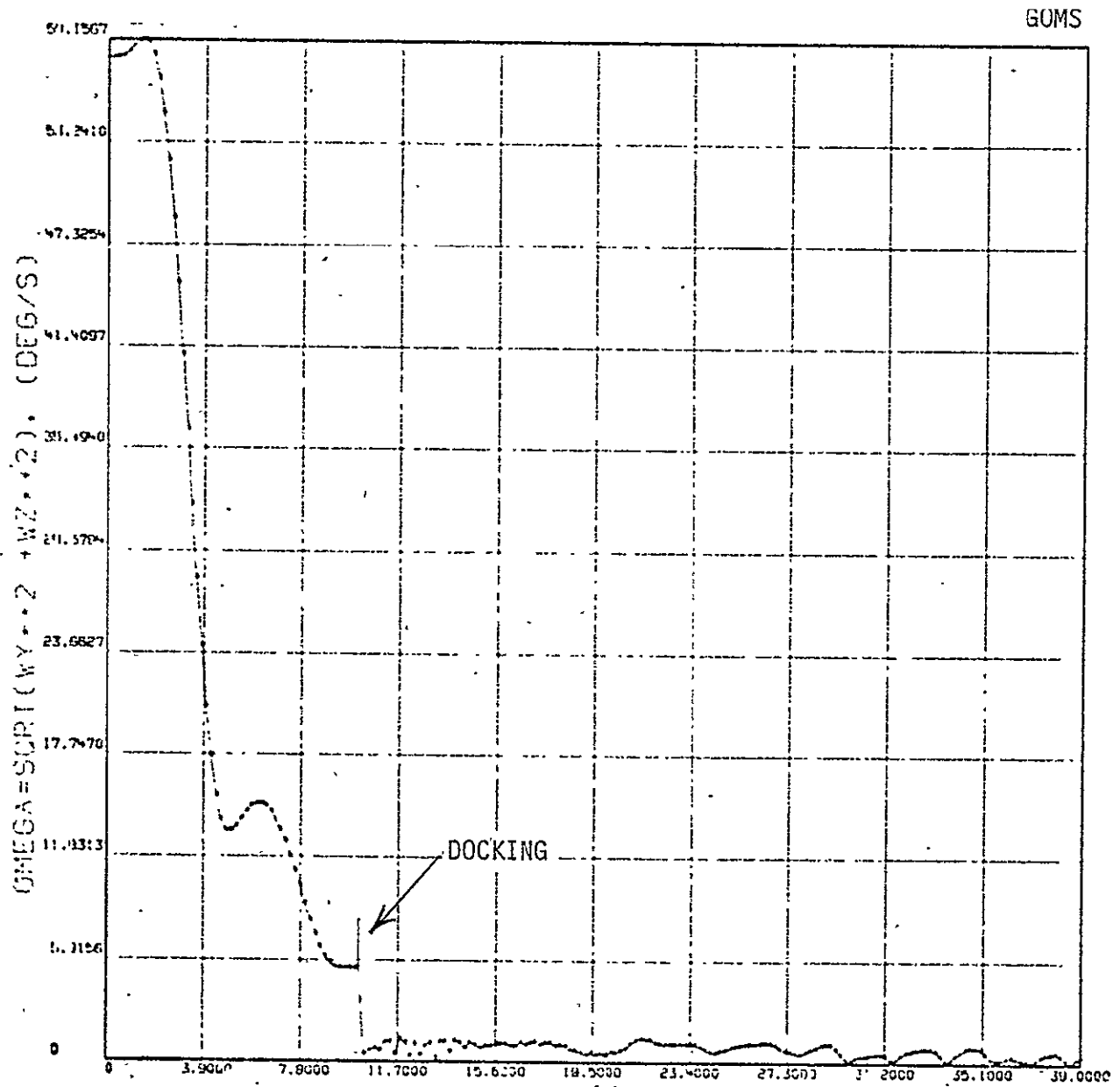


Figure 16e. ALIGNMENT RATE VERSUS TIME

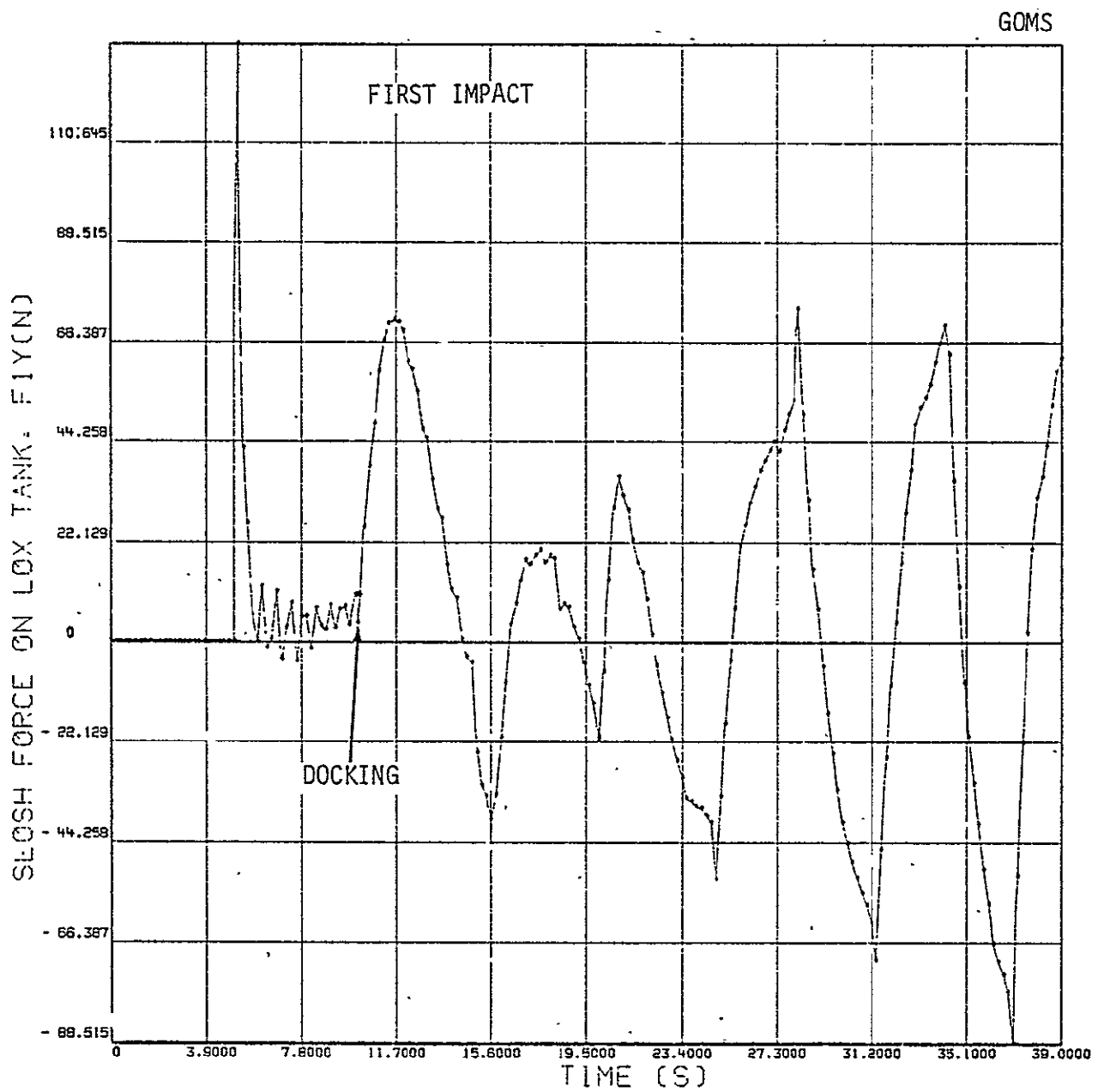


Figure 17a. SLOSH FORCE VERSUS TIME

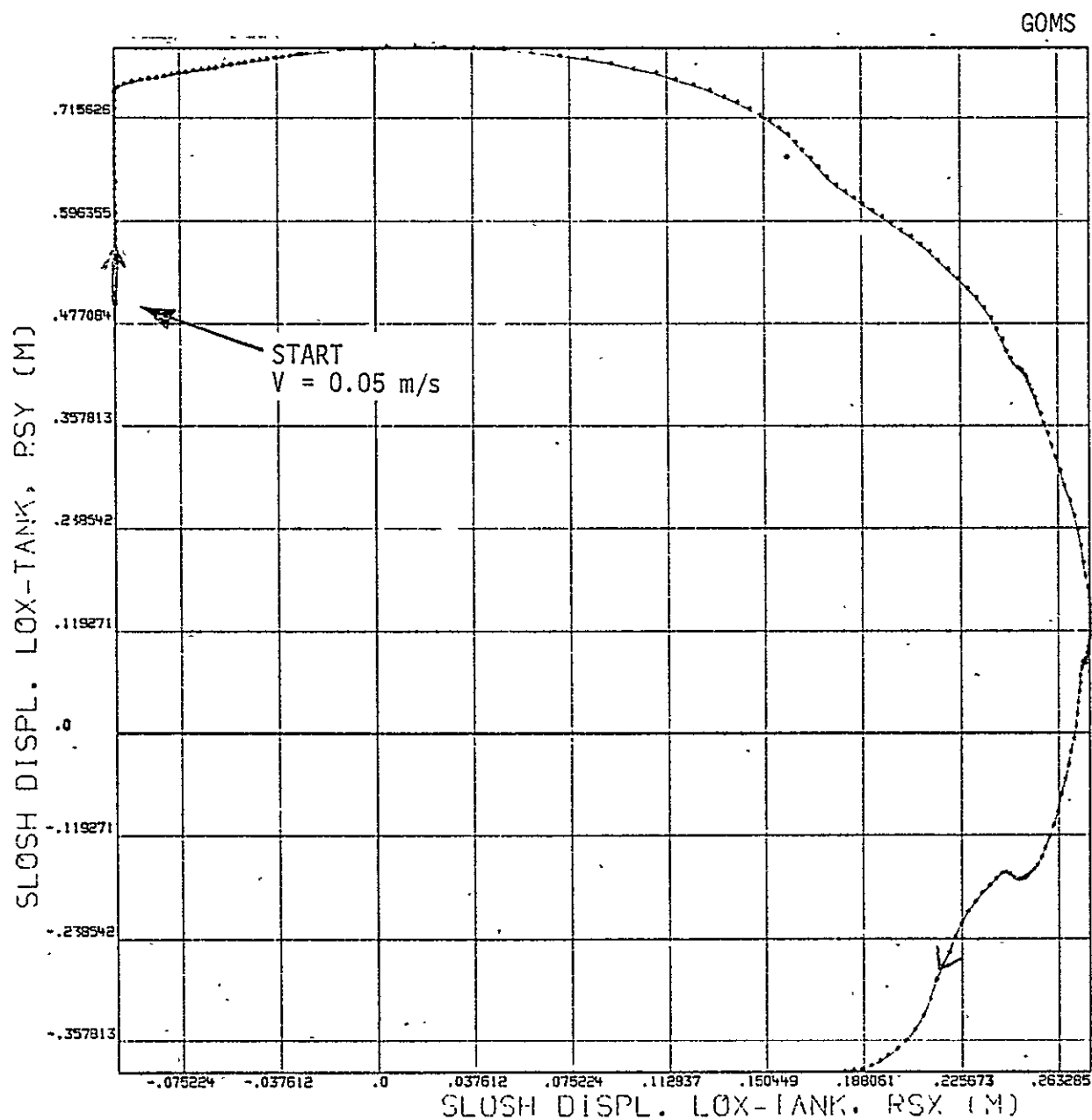


Figure 17b. SLOSH MOTION

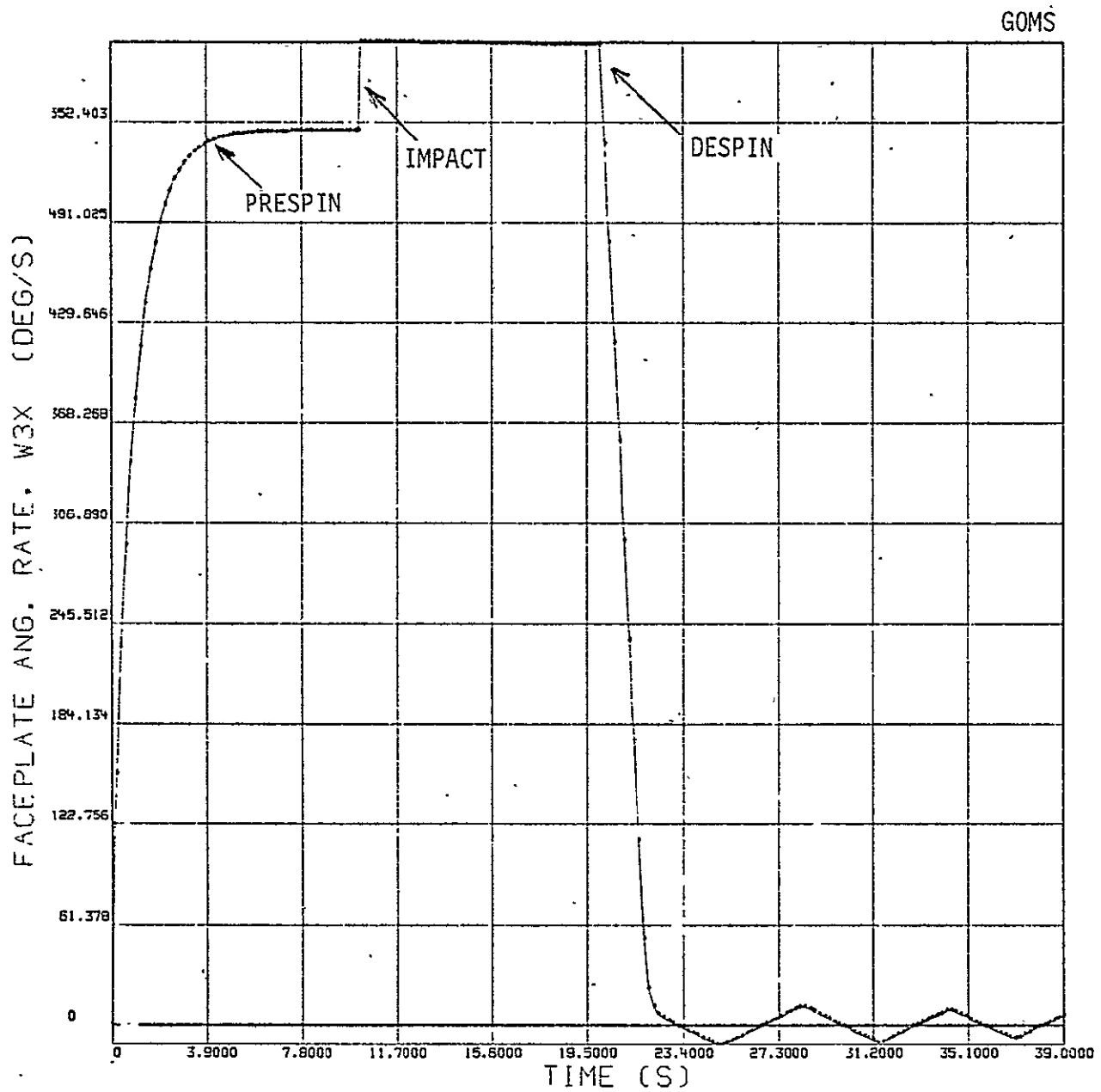


Figure 17c. FACEPLATE ANGLE RATE VERSUS TIME

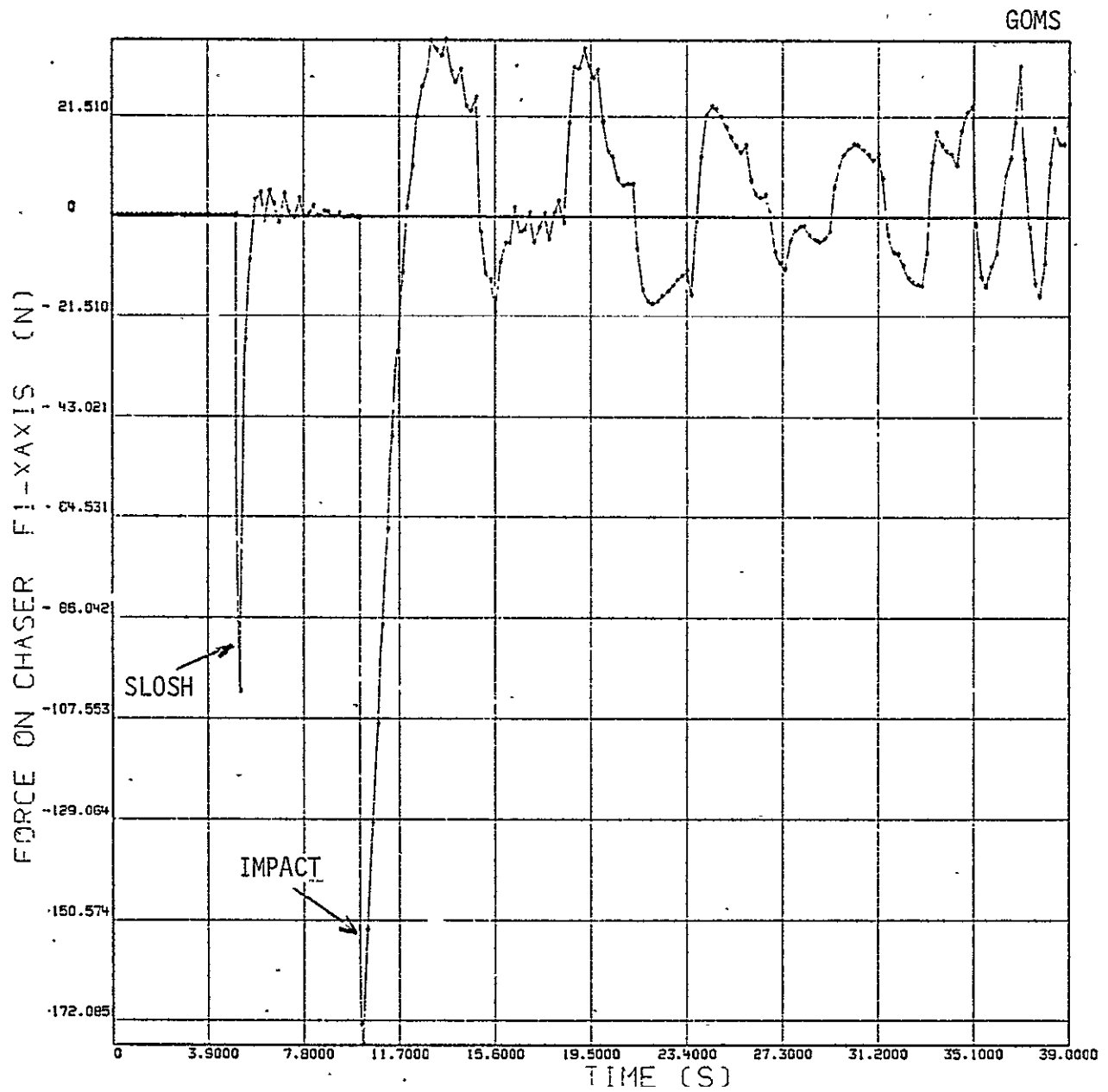


Figure 17d. FORCE ON CHASER VERSUS TIME

6.3.4 HEAO

Different responses obtained while docking with HEAO are shown in Figures 18a through 18d. Here, the HEAO was not coning, but had a 5 degree misalignment with the chase vehicle and was spinning at 2 rpm. A large penetration (Figure 18b) and a large radial motion of the docking ports (Figure 18c) can be noticed. Those are mainly caused by the slosh effect.

Alignment of the bodies in this particular case was hard to achieve. As shown in Figure 19a, the control torques necessary to perform a stabilization reached the level values of saturation as shown in Figures 19c and 19d. Attitude control after docking requires special attention.

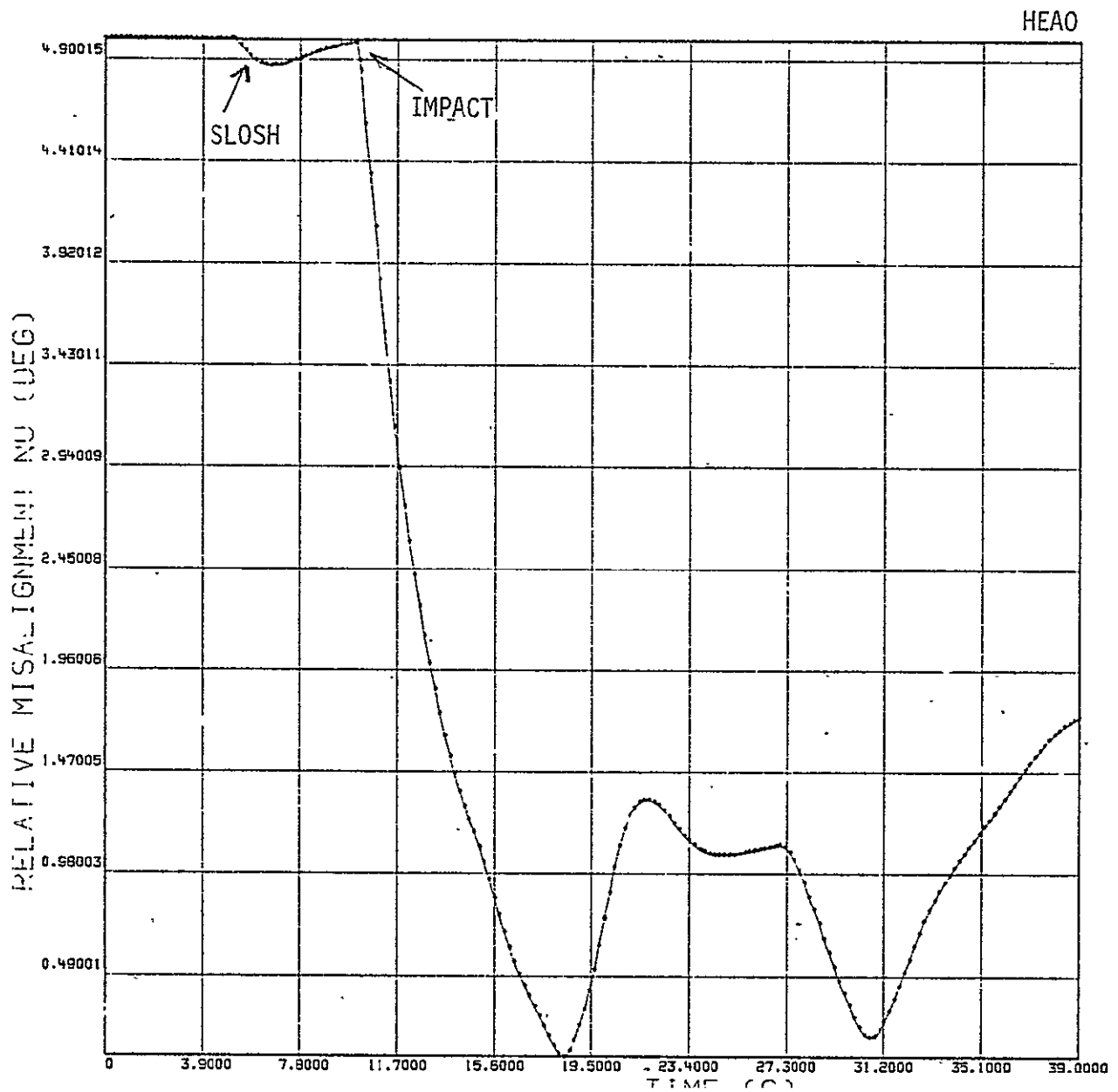


Figure 18a. MISALIGNMENT VERSUS TIME

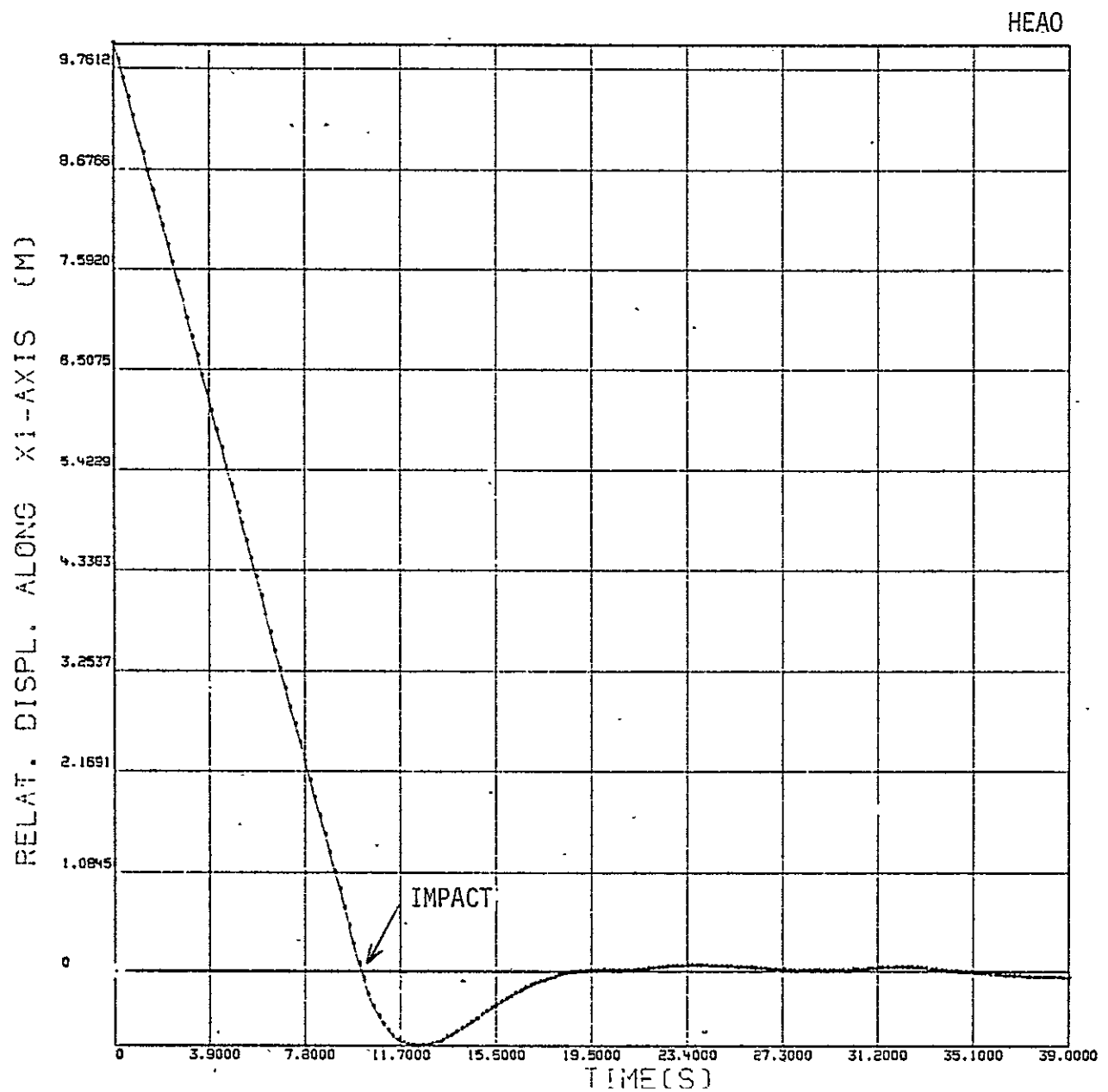


Figure 18b. AXIAL DISPLACEMENT VERSUS TIM

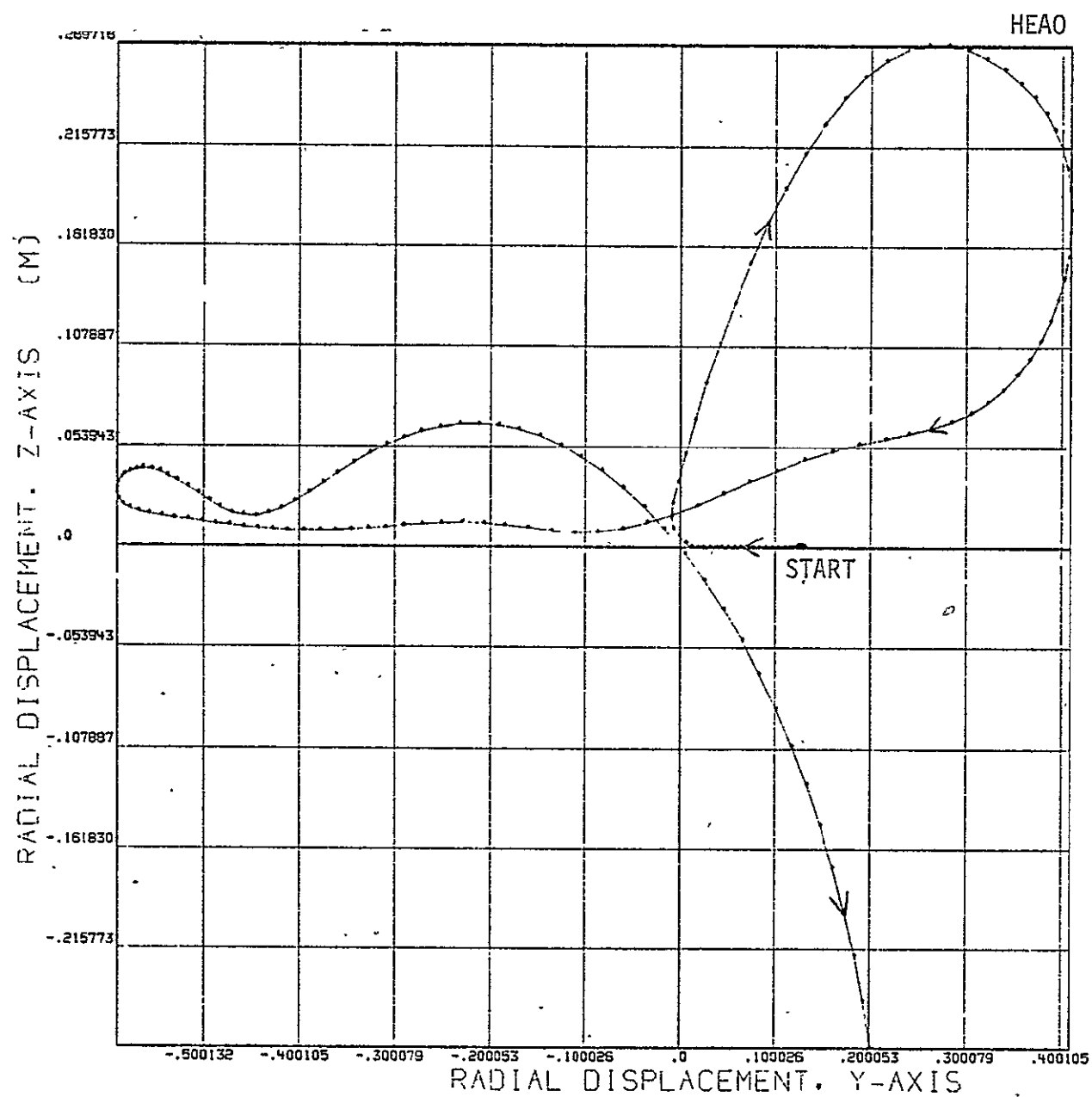


Figure 18c. RELATIVE RADIAL MOTION OF DOCKING PORTS

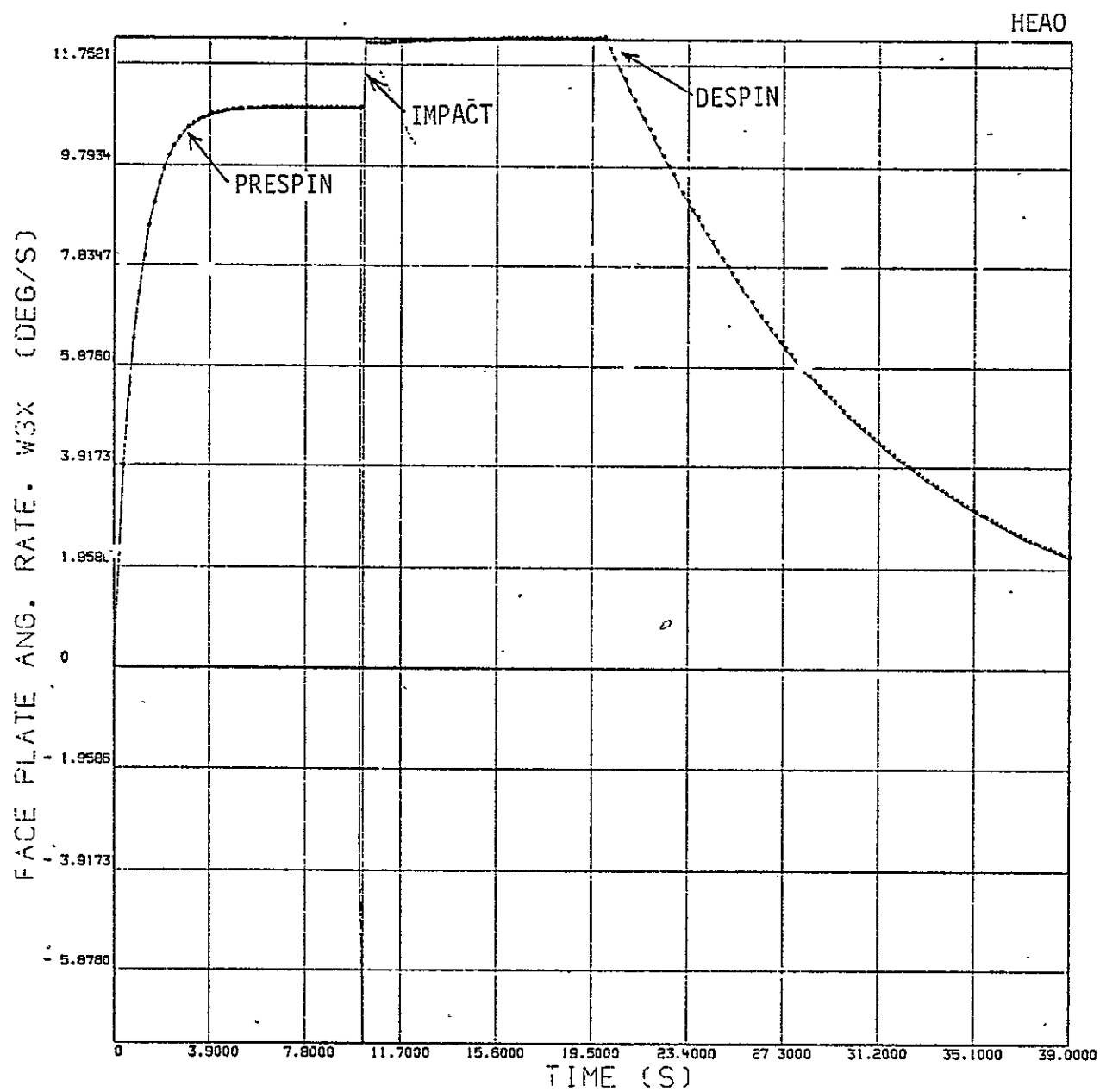


Figure 18d. FACEPLATE ANGLE RATE VERSUS TIME

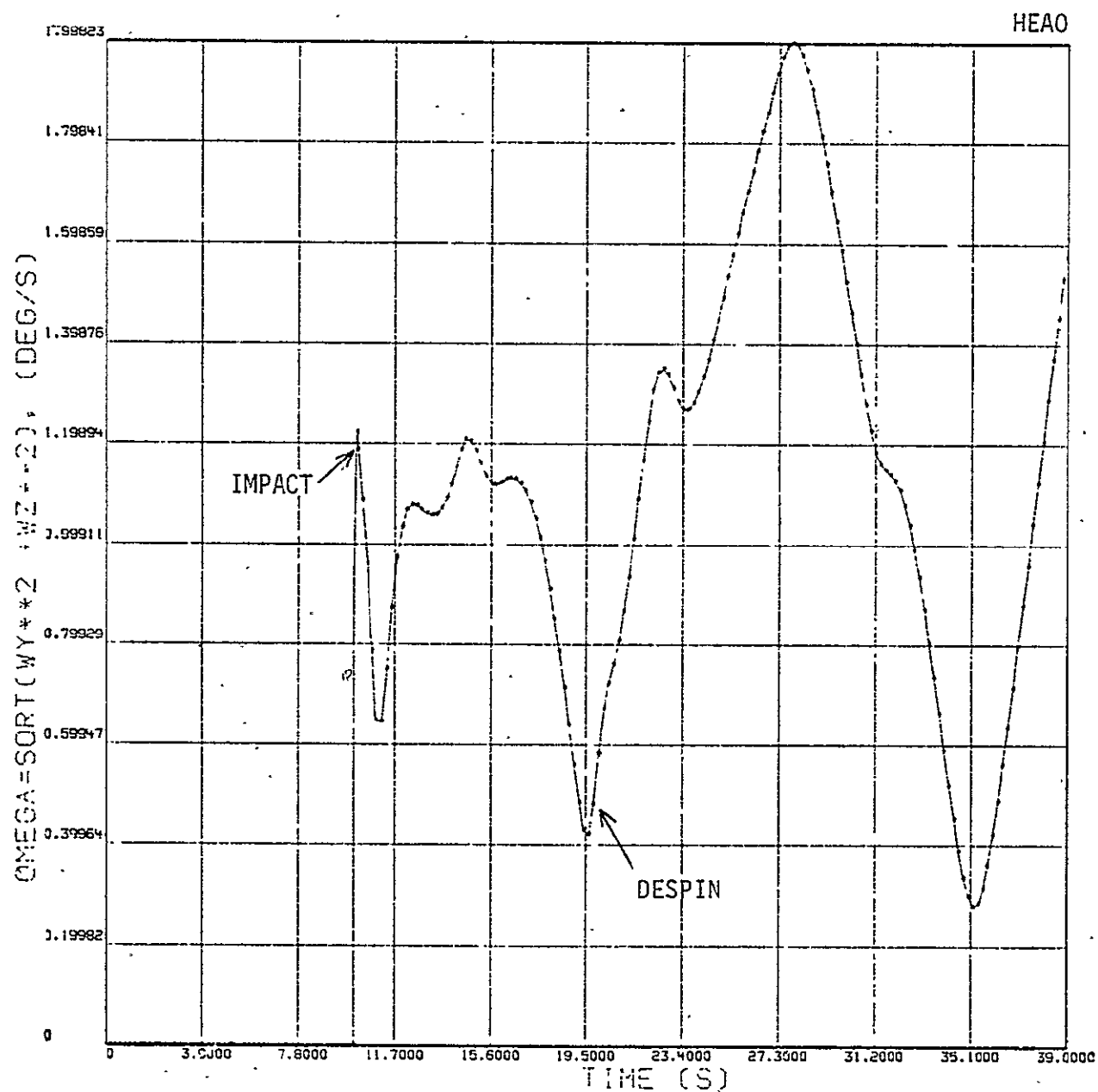


Figure 19a. ALIGNMENT RATE VERSUS TIME

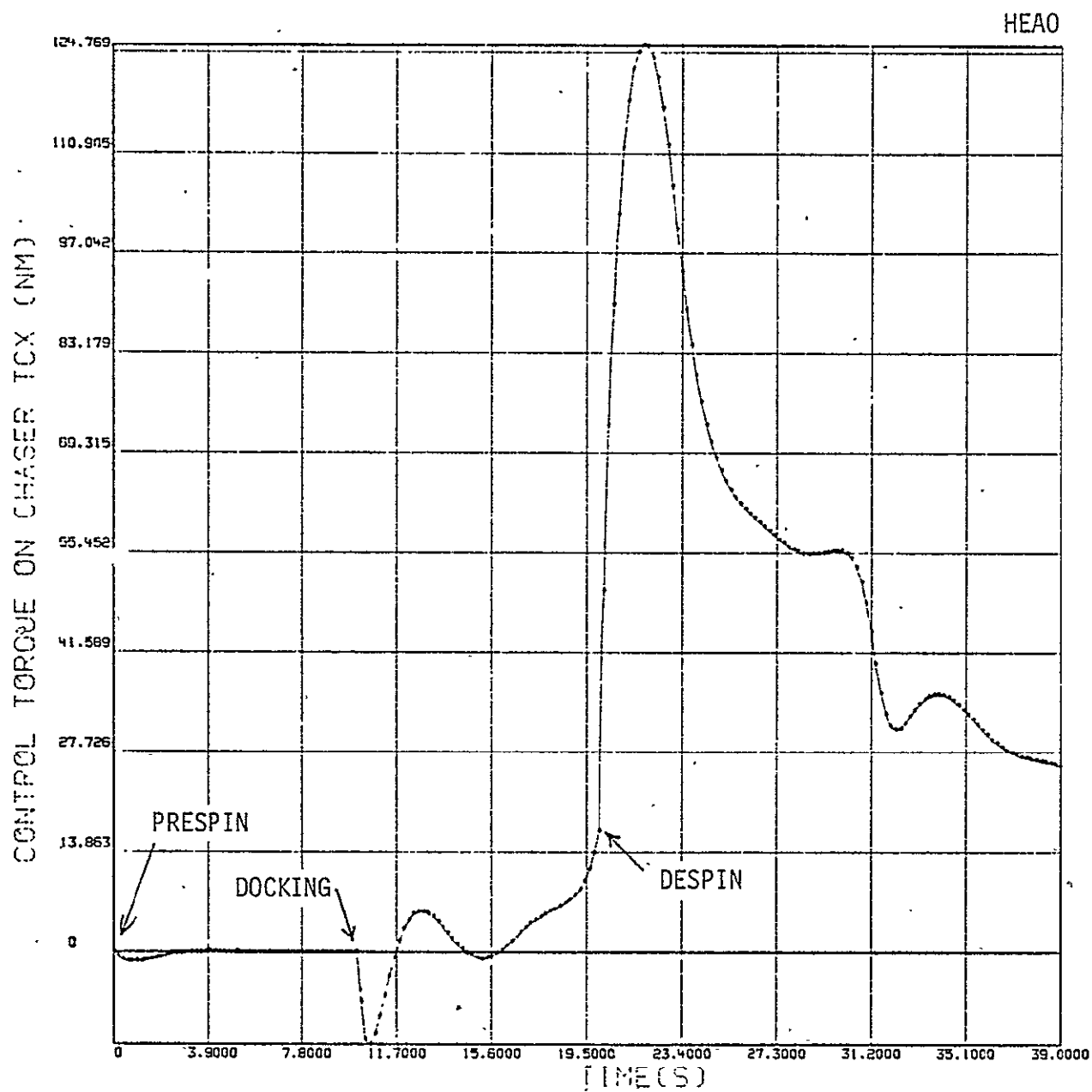


Figure 19b. CONTROL TORQUE ON CHASER VERSUS TIME

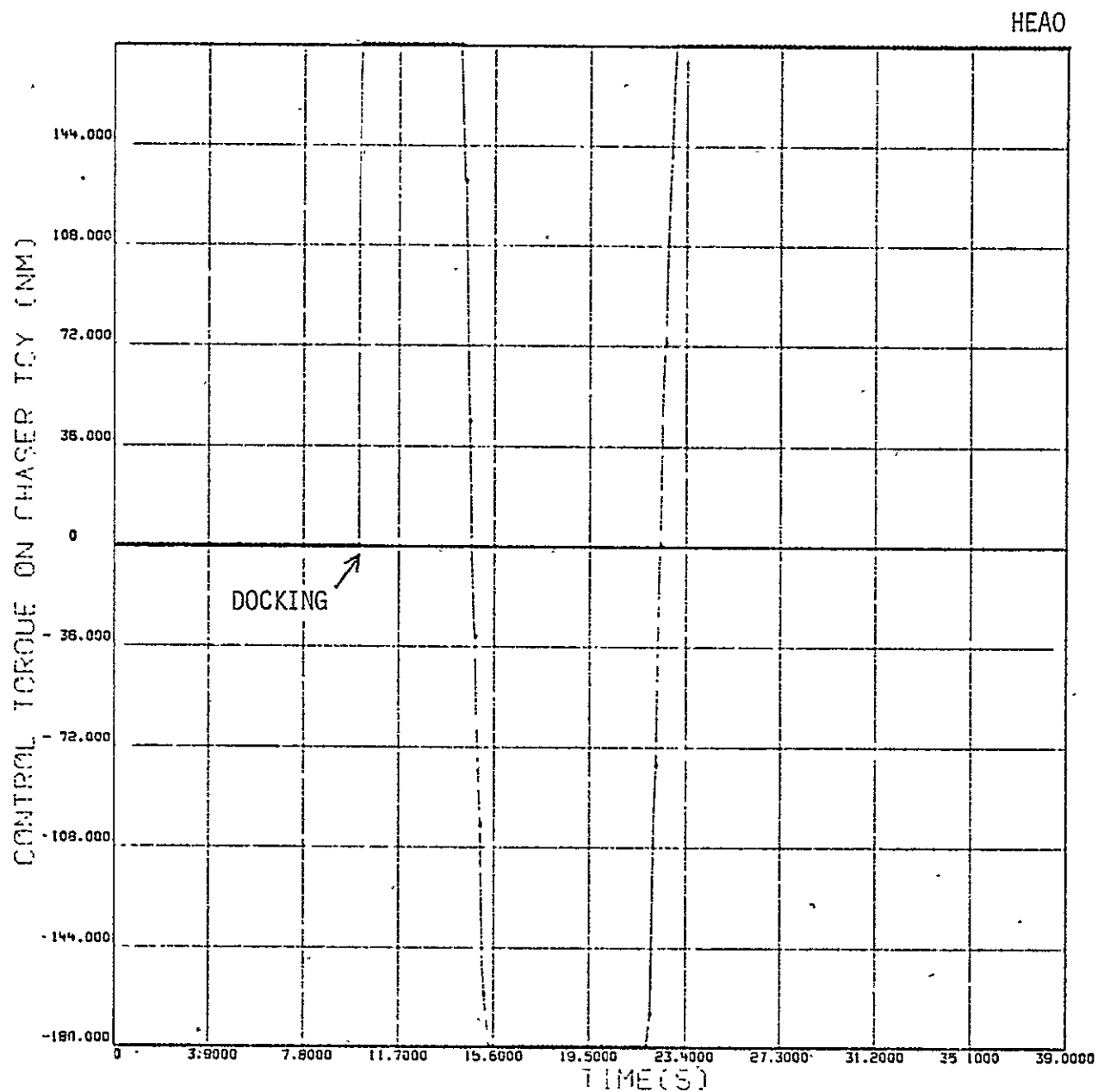


Figure 19c. CONTROL TORQUE ON CHASER VERSUS TIME

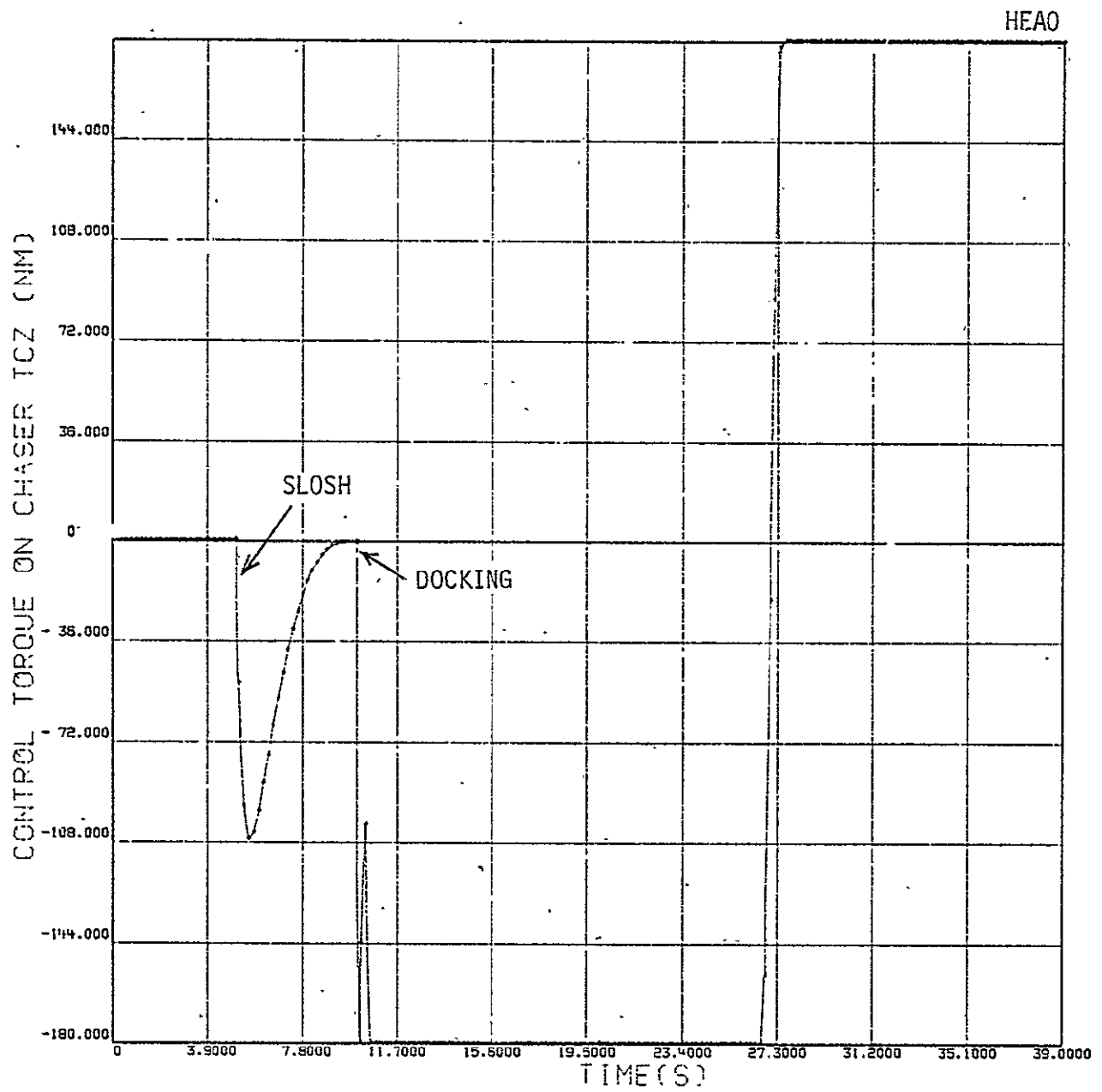


Figure 19d. CONTROL TORQUE ON CHASER VERSUS TIME

Section VII

CONCLUSIONS

An investigation of recovery techniques for capture of spinning satellites leads to the following conclusions:

7.1 POST-DOCK STUDY

- A two-body coupled system where one body is spinning is stable as long as some dissipative and energy storage (spring and damper) alignment torque exists.

7.2 SOFT-DOCK STUDY

- A capture-center approach for the recovery of a spinning satellite is conceivable. Convergence toward the docking port center is ensured if latches close properly and the oscillation is not too large.

7.3 PREDOCK STUDY

- A nutation-precession damper on the target does not significantly affect the docking transient. However, it greatly facilitates the recapture in the case of a missed docking attempt.
- A spinning faceplate is a very effective interface for the capture of a spinning target when the friction coefficient of the docking surfaces is too large to permit direct contact.
- The liquid propellant slosh effect must be avoided during the closing maneuver. Impact on the tank wall can occur after the latching is completed.
- The closing maneuver aligned with the momentum axis of a nutating target will follow the docking port with a phase lag depending upon the characteristics of the sensing data filter.
- An interception type docking where the chaser moves along the pre-determined momentum axis and ultimately moves to intercept the docking port is possible for slowly nutating targets.
- A trajectory approach is possible if a sensing system can be used to determine the momentum axis. The chase vehicle in this case must be equipped with a sophisticated navigational system.
- The sensing system should be mounted on a gimbal and be constantly searching for the docking port in order to avoid loss of target track.

- The closing velocity must be controlled for synchronization in the interception concept presented above.

7.4 RECOMMENDED CONCEPT

On the basis of the studies made in the analysis of docking techniques, the following concept is recommended.

The concept uses a single component on the target vehicle -- a docking ring. Other devices are used by the chase vehicle as shown in Table 6. The docking ring is detected by the video system. The approach procedure recommended is the trajectory approach discussed earlier. The docking interface on the chase vehicle should have axial and alignment dampers. Mechanical or electromagnetic latches could be used to secure the target ring.

Summarized, the recommendations for further studies are to:

- Develop sensing devices (pattern recognition)
- Integrate recognizable pattern with docking interface
- Expand trajectory and intercept concepts
- Develop docking mechanism hardware.

Table 6. REQUIREMENTS FOR RECOMMENDED CONCEPT

REQUIREMENTS OPERATIONS	ON CHASE VEHICLE	ON TARGET
	VIDEO SYSTEM	DOCKING RING
SENSING		
NAVIGATION & GUIDANCE	PLATFORM GIROS COMPUTER	--
FLIGHT MANEUVERS	FORWARD THRUST REACTION JETS	--
DOCKING	AXIAL DAMPER ALIGNMENT TORQUE LATCHES DESPIN TORQUE	DOCKING RING

Section VIII

REFERENCES

1. Roberts, James R. and Todd, Robert S., "Digital Simulation For Post-Docking Response," Technical Report TR-250-1378, Northrop Services, Inc., Huntsville, Alabama, December 1974.
2. Tao, Kuoting M. and Roberts, James R., "Analytical Stability and Simulation Response Study For A Coupled Two-Body System," Technical Report TR-250-1400, Northrop Services, Inc., Huntsville, Alabama, January 1975.
3. Coppey, Jean M., "A Study of The Capture of Cooperative Spinning Satellites," Technical Report TR-250-1559, Northrop Services, Inc., Huntsville, Alabama, January 1976.
4. Coppey, Jean M., "SPNDOK - A Digital Simulation of Docking With A Spinning Satellite," Technical Report TR-250-1555, Northrop Services, Inc., Huntsville, Alabama, January 1976.
5. Mahaffey, W. R., "SPNDOK II - A Digital Simulation of Docking With A Spinning Satellite (A Users Manual)," Technical Report TR-224-1779, Northrop Services, Inc., Huntsville, Alabama, March 1977.

Appendix A

BODY EQUATIONS OF MOTION

The two bodies, chaser and target ($i = 1, 2$ respectively) are modeled as two separate rigid bodies connected (after contact) by a massless pattern of springs and dampers. The center of mass (CM) of each body is located relative to an inertial coordinate system by $\underline{R}_1, \underline{R}_2$.

The relationship between the inertial and body coordinate frames is as follows:

$$\{X\}_I = T_1 \{X\}_1$$

$$\{X\}_I = T_2 \{X\}_2$$

$$\{X\}_1 = T_1^{-1} T_2 \{X\}_2 = T_1^T T_2 \{X\}_2 = T' \{X\}_2$$

The transformation T_i , ($i = 1, 2$), is developed from 3-2-1 Euler angle sequence going from the inertial to the body reference frame.

The translational and rotational equations of motion are given by

$$\left. \begin{aligned} \ddot{\underline{R}}_i &= \underline{F}_i / m_i \\ \text{and} \quad \dot{\underline{I}}_i + \underline{\omega}_i \times \underline{I}_i + \underline{I}_i \cdot \underline{\omega}_i &= \underline{L}_i \end{aligned} \right\} \quad i = 1, 2$$

Appendix B

ALIGNMENT TORQUER CONCEPT

B.1 ALIGNMENT TORQUE

To damp the scissoring type angular motion between the vehicles, an optional alignment torque is provided, that is,

$$\underline{L}_A = K_A \underline{v} + C_A \dot{\underline{v}}$$

where K_A and C_A are the spring and damper coefficients and \underline{v} is an error vector based on the amount of angular misalignment between the docking port axes.

The system assumes the x-axes of the vehicles are to be aligned. Thus

$$\underline{v} = \hat{i}_1 \times \hat{i}_2$$

where \hat{i}_j is the x-axis unit vector of body j , $j = 1, 2$. Since

$$\underline{T}' = [\hat{i}_2 | \hat{j}_2 | \hat{k}_2] = [\underline{T}'_{j1} | \underline{T}'_{j2} | \underline{T}'_{j3}]$$

then \underline{v} and $\dot{\underline{v}}$ referenced to the body 1 coordinate frame is

$$\underline{v} = \hat{i}_1 \cdot \underline{T}'_{j1} = \begin{Bmatrix} 0 \\ -\underline{T}'_{31} \\ \underline{T}'_{21} \end{Bmatrix}, \quad \dot{\underline{v}} = \begin{Bmatrix} 0 \\ -\dot{\underline{T}}'_{31} \\ \dot{\underline{T}}'_{21} \end{Bmatrix}$$

B.2 CHASER ATTITUDE CONTROL

An attitude and attitude rate feedback control system was used for preliminary studies, with given values for time constant (τ) and damping ratio (ζ). The control torque is computed as

$$\underline{T}_c = 2 \operatorname{sgn}(Q_4) [K_O] \begin{Bmatrix} Q_1 \\ Q_2 \\ Q_3 \end{Bmatrix} + [K_1] (\omega_1 - \omega_R)$$

where the gain matrices are defined respectively in terms of the estimated vehicle inertia matrix \underline{I}

$$[K_O] = \frac{4\pi^2}{\tau^2} \underline{I} \qquad [K_1] = \frac{4\pi\zeta}{\tau_1} \underline{I}$$

ω_R is the angular rate of the reference system.

B.3 CONSTRAINT FORCES

Physical constraint forces and torques are calculated using the general equations

$$\underline{F}_C = K \underline{d} + C \dot{\underline{d}}$$

and

$$\underline{L}_C = \underline{d} \times \underline{F}_C$$

where K and C represent the structural flexibility and damping coefficients, \underline{d} being the connecting vector between the two bodies, and $\dot{\underline{d}}$ the time rate of change of \underline{d} . These forces are used in the simulation of the docking mechanism.

B.4 DESPIN TORQUE

When one body is spinning, a torquer is available for despinning. The despin torque can be applied from either body (reflecting actual hardware considerations), but such application is only on the x-axis. For high relative spin rates, the despin torque is limited, providing a constant output, whereas for low relative spin rates the torquer output is linear as seen by the following equations:

$$L_{DX} = \text{sgn}(\omega_{2x} - \omega_{1x}) T_{LIM}, \quad -\Delta\omega > \omega_{2x} - \omega_{1x} > \Delta\omega$$

$$L_{DX} = G(\omega_{2x} - \omega_{1x}), \quad -\Delta\omega < \omega_{2x} - \omega_{1x} < \Delta\omega$$

Appendix C

ROTATING FACEPLATE EQUATIONS

A torquer is assumed to be on the chaser to spin up the faceplate and to despin the whole target once it is latched. The spin rate of the target (ω_2) is estimated by the sensing device located on the chaser. The equation of motion of the faceplate along its spin axis is:

$$\ddot{\theta}_3 I_3 = T_{QT} + T_{RQ} + T_{Q2}$$

with

$$T_{QT} = G_{PL}(\omega_2 - \omega_3) \quad -470. < T_{QT} < 470 \text{ Nm},$$

$$T_{RQ} = -C_{PL}(\omega_3 - \omega_1)$$

where G_{PL} is the gain of the torquer, and C_{PL} is the friction coefficient of the face plate. $T_{Q2} = \mu c N$, where c is the location of impact point, N is the normal force of impact, and μ is the coefficient of friction at the point of impact defined as:

$$\mu = \mu_o - \alpha V_s + \beta V_s^2$$

and

$$\mu_o = \text{dry friction coefficient}$$

$$\alpha, \beta = \text{dynamic friction coefficients}$$

with

$$V_s = \text{sliding velocity}$$

A schematic diagram of the faceplate simulation model is shown in Figure C-1.

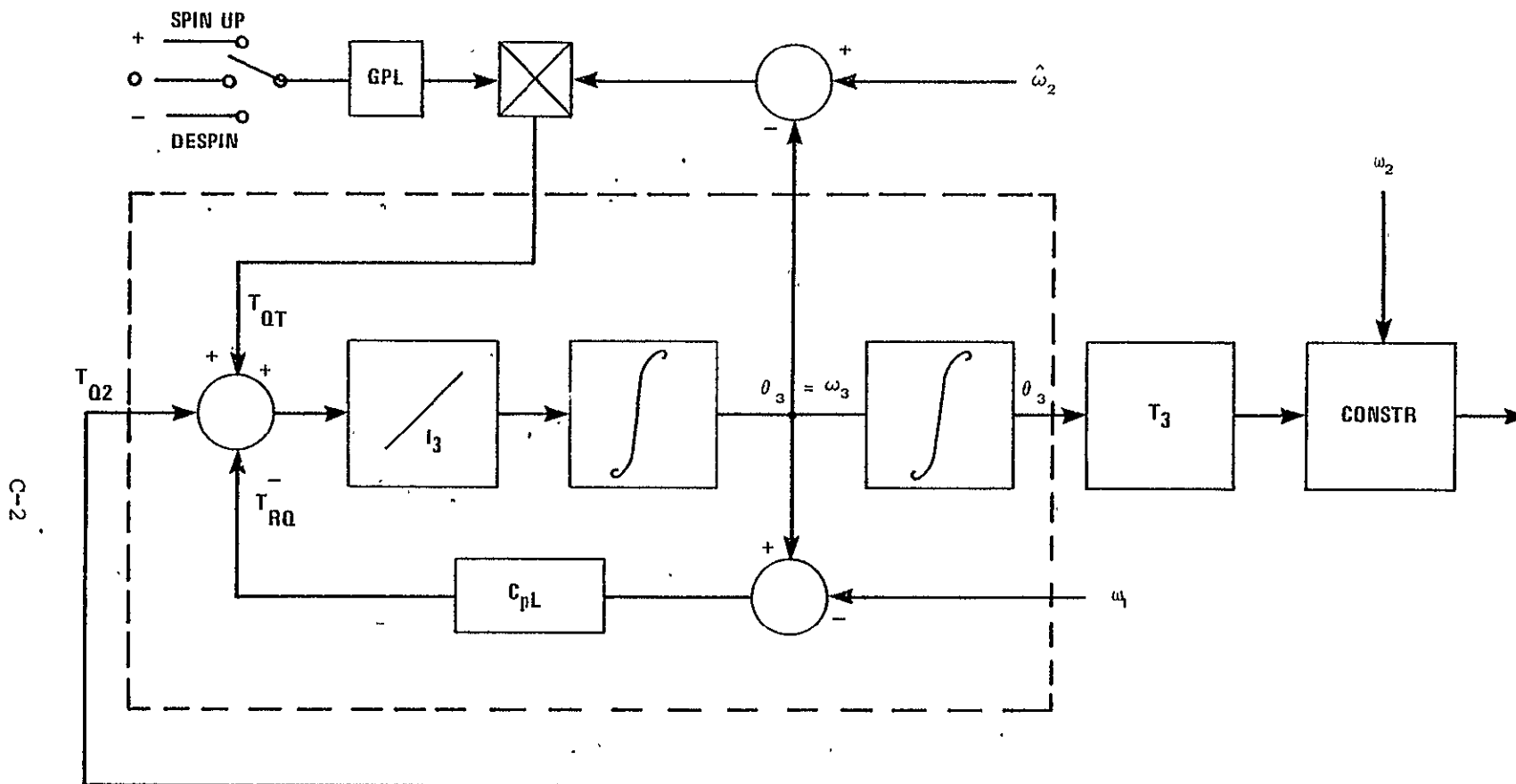


Figure C-1. FACEPLATE SIMULATION MODEL

Appendix D

PRECESSION DAMPING EQUATIONS

A nutation damper was simulated as a mass-spring-dashpot device judiciously placed on the spinning body as shown in Figure 7. The damper is set parallel to the spin axis at a distance (a) from that axis. The equation of motion of the damper mass was derived as:

$$m^* \ddot{X}_P + C_P \dot{X}_P + K'_P X_P = -ma (\omega_1 \omega_3 + \dot{\omega}_2) - m^* \ddot{X}_2$$

with

$$m^* = m(1-\mu) \text{ and}$$

$$K'_P = K_P - m(1-\mu) (\omega_2^2 + \omega_3^2)$$

where m is the damping mass, μ the ratio of damping mass to total mass, C_P the dashpot constant and K'_P the spring constant, \ddot{X}_2 being the main body acceleration. The damper is tuned to the precession frequency, that is its natural frequency of vibration matches the frequency of precession of its support. Therefore:

$$K_P = m\omega_P^2 \quad \text{and}$$

$$C_P = 2\xi\omega_P$$

The nutation frequency is determined as $\omega_P = \frac{A-C}{C} \omega_1$, where A , B and C are the moments of inertia of the spinning body with $A > B$ and $B = C$ assumed for this preliminary design.

The force generated by the motion of the damping mass will be transmitted to the main body as torques:

$$T_{q1} = am[2\omega_3 \dot{x}_p + (\omega_3 + \omega_1 \omega_2)x_p]$$

$$T_{q2} = -am[\ddot{x}_p + x_p(\omega_1^2 - \omega_3^2)]$$

$$- m^* [(\dot{\omega}_2 - \omega_1 \omega_3)x_p^2 + 2\omega_2 x_p \dot{x}_p]$$

$$T_{q3} = am[x_p(\dot{\omega}_1 - \omega_2 \omega_3)]$$

$$- m^* [(\dot{\omega}_3 + \omega_1 \omega_2)x_p^2 + 2\omega_3 x_p \dot{x}_p]$$

The nutation damping system is simulated independent of the spinning spacecraft to keep the same order in the system and to make it readily adaptable to any spinning body. A fourth-order Runge-Kutta integration method with fixed step size is used for the damping system. The spinning body equations are integrated with a variable time step.

Appendix E

PROPELLANT SLOSH MODEL

The propellant is modelled as a "sticky rubber ball", a spherical mass, with adhesive, compressive and damping properties. The fuel tank is assumed to be of an elliptical form, see Figure E-1. A resulting force and torque are computed and applied to the carrying body. The slosh mass equations of motions are solved independently in order to limit the order of the system. A Runge Kutta integration method is used for solving the differential equations. A fixed time step is assumed. The forces acting on the liquid mass are decomposed in aerodynamic drag, forces normal to the impact surface and parallel to it. The slosh mass also has a rotational motion and can be initiated in any state within the tank.

The equations of motion for the slosh mass are:

$$\begin{aligned}\vec{F}_s &= m_s \ddot{\vec{R}}_s \\ \vec{L} &= \vec{I}_s \dot{\vec{\omega}}_s\end{aligned}$$

where

m_s is the slosh mass,

\vec{I}_s is the slosh inertia tensor

$\vec{\omega}_s$ the slosh body rate vector

\vec{R}_s the position of m_s relative to the center of the tank

The general equation for the force is given as:

$$\vec{F}_s = -U(\delta) [(K\delta + C_\perp \dot{\delta})\vec{n} - C_\parallel V_\parallel] - C_d \dot{\rho}$$

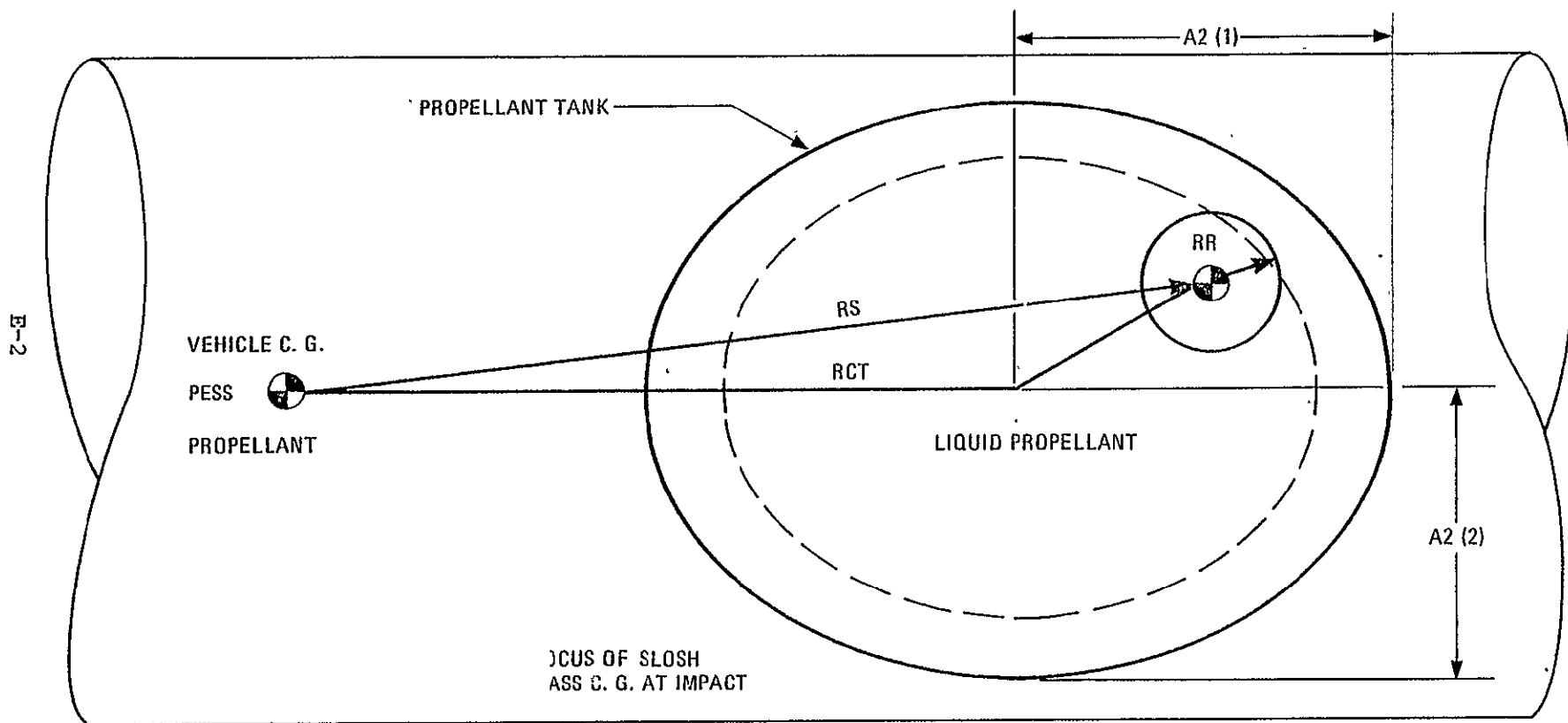


Figure E-1. PROPELLANT SLOSH MODEL COORDINATES

where δ is the distance to the tank's wall and $U(\delta)$ a switching function for determination of contact conditions. K is the tank's wall spring constant; the values C_{\perp} and C_{\parallel} are respectively normal and parallel damping coefficients on the tank's wall and C_d is the drag coefficient inside the tank. The simulation of a realistic case is essential to obtain the degree of significance of the slosh effect.

Data were obtained from the Tug's configuration and estimated as follows. With an assumed weight of 3200 kg for the liquid hydrogen, the mass radius with a density of $\rho_{LH_2} = 0.71 \times 10^3 \text{ kg/m}^3$, becomes $R = \sqrt[3]{\frac{3m/1000}{4\pi \rho_{LH_2}}} = 2.2 \text{ m}$. For pur-

pose of the simulation, the LH_2 -Tank is assumed to be spherical with a radius $R_{LH_2} = 2.25 \text{ m}$. The liquid oxygen tank with a full weight of 19,000 kg has an analogous radius of 1.58 m ($\rho_{LOX} = 1.141 \times 10^3 \text{ kg/m}^3$). An ellipsoid with axis $R_x = 1.3$, $R_y = 1.8 \text{ m}$ was selected. See Figure 9a. For a preliminary study, the motion of the hydrogen mass was not considered, the liquid being fixed within the tank. Data for the slosh model are shown in Table 4.

Appendix F

FEEDBACK CONTROL SYSTEM

As shown in Figure 18 the feedback control command consists of a closed loop system on the alignment angles of both bodies. The data supplied by the sensor is filtered and fed to a position and an attitude/rate controller.

A moving average computation (\bar{v}) was performed using the iterative method

$$\bar{v}_t = (1 - \alpha) \bar{v}_{t-1} + \alpha v_t$$

where α is the smoothing factor.

An attitude/rate control system was developed to maintain the chase vehicle aligned with the vector joining both vehicles; angle γ in Figure 12. Such as

$$T_Q = G_{\gamma 1} \quad \bar{\gamma}_t = G_{\gamma 1d} (\bar{\gamma}_t - \bar{\gamma}_{t-1}) / \Delta t$$

$$\text{with } |T_Q| \leq T_{Q \max}.$$

A position/rate control system was developed to maneuver the chase vehicle toward the docking axis of the target. The misalignment angle v in Figure 12 was used as a steering variable for the control system. Similarly:

$$F_Q = G_v \bar{v}_t + G_{vd} (\bar{v}_t - \bar{v}_{t-1}) \Delta t \\ + G_{\gamma 2} \bar{\gamma}_t + G_{\gamma 2d} (\bar{\gamma}_t - \bar{\gamma}_{t-1}) \Delta t$$

with

$$|F_Q| \leq F_{\max}.$$

C.2

Appendix G

TRAJECTORY APPROACH

The trajectory approach is characterized by the identification of the momentum vector in inertial space and a reference platform with a navigation system on the chase vehicle. The stationary target is considered first.

The key in the identification of the momentum vector is to position the chase vehicle at two positions which satisfy the requirements of being located in a plane normal to the momentum vector (points A and B in Figure 13). Once both points have been located in inertial space, (selected before circling maneuver) the direction of the vectors $\vec{\eta}_A$ and $\vec{\eta}_B$ will give enough information to solve the system and determine the inertial position of (C) and the momentum vector $\vec{\eta}_C$. The position of the chase vehicle (F) then can be used to compute the error vector \vec{E} and the misalignment angles ν and γ . In inertial space \vec{A} , \vec{B} , and unit vector $\vec{\eta}_A$ and $\vec{\eta}_B$ allow the following to be determined,

$$\vec{C} = \vec{A} + \vec{\eta}_A \lambda_A = \vec{B} + \vec{\eta}_B \lambda_B$$

$$\vec{\eta} = \vec{\eta}_A \times \vec{\eta}_B$$

$$\vec{D} = \vec{B} - \vec{A} = \lambda_D \vec{\eta}_D \quad \lambda_D \text{ Known:}$$

$$\lambda_A \underbrace{(\vec{\eta}_A \cdot \vec{\eta}_D)}_{\cos \alpha_A} + \lambda_B \underbrace{(\vec{\eta}_B \cdot \vec{\eta}_D)}_{\cos \alpha_B} = \lambda_D$$

$$\vec{B} - \vec{A} = \lambda_A \vec{\eta}_A - \lambda_B \vec{\eta}_B = \lambda_D \vec{\eta}_D$$

$$\lambda_A \underbrace{(\vec{\eta}_A \cdot \vec{\eta}_A)}_1 = \lambda_B (\vec{\eta}_A \cdot \vec{\eta}_B) + \lambda_D (\vec{\eta}_D \cdot \vec{\eta}_A)$$

1

$$\lambda_A = \lambda_B (\vec{n}_A \cdot \vec{n}_B) + \lambda_D (\vec{n}_D \cdot \vec{n}_A)$$

$$[\lambda_B (\vec{n}_A \cdot \vec{n}_B) + \lambda_D (\vec{n}_D \cdot \vec{n}_A)] (\vec{n}_A \cdot \vec{n}_D) + \lambda_B (\vec{n}_B \cdot \vec{n}_D) = \lambda_D$$

$$\lambda_B ((\vec{n}_A \cdot \vec{n}_B) (\vec{n}_A \cdot \vec{n}_D) + (\vec{n}_B \cdot \vec{n}_D)) = \lambda_D (1 - (\vec{n}_A \cdot \vec{n}_D)^2)$$

$$\lambda_B = \lambda_D \frac{[1 - (\vec{n}_A \cdot \vec{n}_D)^2]}{[(\vec{n}_A \cdot \vec{n}_B) (\vec{n}_A \cdot \vec{n}_D) + (\vec{n}_B \cdot \vec{n}_D)]}$$

The error vector $\vec{E} = \vec{C} - \vec{F}$ transformed into chaser coordinates gives attitude command.

The misalignment angle $D = \cos^{-1} (\vec{n}_c \cdot \vec{n}_e)$ gives translation information commands.

Appendix H

INTERCEPT CONTROL

Controls on the chase vehicle are based on a bang-bang system turned on before impact with the target. The magnitude of the impulse is fixed (thrusters on); the firing time is variable. The typical thrust profile for each of the position and attitude controllers is shown in Figure 14. The values for T_A and T_B can be seen from the following derivation,

Assumptions

$$x_1(0) = 0$$

$$\dot{x}_1(0) = 0$$

Then,

Desired Status

$$x_1(t_i) = x_2(t_i)$$

$$\dot{x}_1(t_i) = \dot{x}_2(t_i)$$

$$\dot{x}_1(t_i) = a[T_A - T_B] \quad (1)$$

$$x_1(t_i) = \frac{a T_B^2}{2} + a T_A T_C + \frac{a T_B^2}{2}$$

$$x_1(t_i) = \frac{a}{2} [T_A^2 + 2T_A T_C + T_C^2] \quad (2)$$

$$T = T_A + T_B + T_C \quad (3)$$

and T_A, T_B are shown.

$$\text{From (1) - (2), } T_B = T_A - \frac{\dot{x}_1(t_i)}{a}$$

$$\text{and in (3) - (2) } T_C = T - T_A - T_B \quad (4)$$

$$\text{Then, } x_1(t_i) = \frac{a}{2} [T_A^2 + 2T_A (T - T_A - T_A + \frac{\dot{x}_1(t_i)}{a}) + (T_A - \frac{\dot{x}_2}{a})^2]$$

$$x_2(t_i) = \frac{a}{2} [\frac{\dot{x}_2^2}{a} + T_A (2T + \frac{2\dot{x}_2}{a} - \frac{2\dot{x}_2}{a}) - 2T_A^2] ;$$

or

$$x_2(t) = \frac{x_2^2}{2} + a[T - T_A] T_A$$

with

$$T_A = \frac{x_2(t) - x_2^2/2}{a(T - T_A)}$$

This is a quadratic equation

$$-aT_A^2 + aTT_A - x_2(t) + \frac{x_2^2}{2} = 0$$

$$T_A^2 - TT_A + \frac{x_2(t) + x_2^2(t)}{a} = 0$$

Let $C = \frac{x_2(t) + x_2^2(t)}{a}$, then

$$T_A^2 - TT_A + C = 0$$

and

$$T_A = \frac{T - \sqrt{T^2 - 4C}}{2}$$

Substituting, we obtain

$$T_B = T_A - \frac{x_2^2(t)}{a}$$

with the condition $T^2 > 4C$

for a given maximum acceleration (a),

$$T^2 > \frac{4}{a} [x_2 + x_2^2/2]$$

Consider the following example,

$$\dot{x}_2 = 0 \quad T > 2 \frac{\bar{x}_2}{a}$$

$$a = \frac{F}{N} = \frac{300 \text{ N}}{3000 \text{ KS}} = .1$$

$$T > 2 \sqrt{10 x_2}$$

$$x_2 = 1\text{m} \quad T > 6.4 \text{ Sec.}$$

Let $T = 10 \text{ sec}$

then

$$T_A = \frac{10 - \sqrt{100-4}}{2} = .1 \text{ Sec}$$

and

$$T_B = .1 \text{ Sec}$$

Appendix I

COMPUTATION OF RANGE ERROR

The range R computed from the data supplied by the sensor can be written as:

$$R = \frac{X}{2K \tan \alpha} \sim \frac{X}{2K} \quad (\text{for small } \alpha)$$

and $\frac{X'_1}{X'_3} \equiv X.$

The error on the range ΔR can be estimated as:

$$\begin{aligned} \Delta R &= \frac{X + \Delta X}{2K(\alpha - \Delta\alpha)} - \frac{X}{2K\alpha} \\ &= \frac{(X + \Delta X)\alpha - X(\alpha - \Delta\alpha)}{2K(\alpha - \Delta\alpha)\alpha} \\ &= \frac{\Delta X\alpha + X\Delta\alpha}{2K(\alpha - \Delta\alpha)\alpha} \\ &= \frac{\Delta X + X \frac{\Delta\alpha}{\alpha}}{2K(1 - \frac{\Delta\alpha}{\alpha})\alpha} = \frac{X}{2K\alpha} \cdot \frac{\frac{\Delta X}{X} + \frac{\Delta\alpha}{\alpha}}{1 - \frac{\Delta\alpha}{\alpha}} \\ \frac{\Delta R}{R} &= \frac{\frac{\Delta X}{X} + \frac{\Delta\alpha}{\alpha}}{1 - \frac{\Delta\alpha}{\alpha}} \end{aligned}$$

A minimum error in the range estimation would require $\frac{\Delta X}{X} \ll \frac{\Delta\alpha}{\alpha}$.

Thus:

$$\begin{aligned} \frac{\Delta R}{R} &= \frac{\frac{\Delta\alpha}{\alpha}}{1 - \frac{\Delta\alpha}{\alpha}}, \quad \text{Substituting } \alpha = \frac{D}{2R}, \text{ where } D \text{ is the diameter} \\ &\quad \text{of the pointed diameter} \\ &= \frac{\frac{\Delta\alpha}{D} \cdot 2R}{1 - \frac{\Delta\alpha}{D} \cdot 2R} = \frac{2\Delta\alpha R}{D - 2\Delta\alpha R} \end{aligned}$$